Dissertation

submitted to the
Combined Faculties for the Natural Sciences and for Mathematics of
the Ruperto-Carola University of Heidelberg, Germany
for the degree of Doctor of Natural Sciences

presented by

M.Sc. Myriam Friedel
born in Heidelberg

Date of oral examination: 23.09.2014

The Impact of Galectin-8 on Interactions of Multiple Myeloma Cells with Endothelial Cells

Referees:
Prof. Dr. Rainer Zawatzky
PD. Dr. Reinhard Schwartz-Albiez

Declaration

I hereby declare that I have written the submitted dissertation myself and in this process have used no other sources or materials than those expressly indicated.

Heidelberg, June 26, 2014

Myriam Friedel

Contents

Zusammenfassung

Das multiple Myelom (MM) ist eine maligne Erkrankung, die durch die Entartung reifer Plasmazellen im Knochenmark charakterisiert ist. Im Krankheitsverlauf kommt es zu einer verstärkten Proliferation und Expansion von MM Zellen im Knochenmark. In einigen Fällen tritt eine übermäßige Produktion von Proteinen (Immunglobulinen), die im Blut oder Urin nachgewiesen werden können, auf. Bei vielen Patienten kommt es zudem zu einem Abbau des Knochengewebes durch eine vermehrte Aktivierung von Osteoclasten (Knochen-abbauende Zellen). Ohne Therapie überleben Betroffene ca. 3-6 Monate, mit den momentan gegebenen Therapiemöglichkeiten erhöht sich die Überlebenserwartung auf ca. 3-6 Jahre. Die Krankheitsentwicklung wird im Wesentlichen vom Mikromilieu im Knochenmark bestimmt, da die MM-Zellen gezielt ins Knochenmark einwandern können (Homing) und dort angiogene Prozesse auslösen, was zur Vaskularisierung des Tumorgewebes führt.

Die vorliegende Arbeit beschäftigt sich mit dem Einfluss von Galektin-8 (Gal-8), einem zuckerbindenden Protein (Lektin), welches zwei Kohlenhydrat-Binderegionen besitzt die durch eine Peptid Linker-Region miteinander verbunden sind, auf den Verlauf des MM. Ich konnte nachweisen, das Gal-8 im Serum vom MM Patienten im Vergleich zu gesunden Probanden erhöht ist und das eine hohe Gal-8 Expression auf mRNA Ebene mit einer schlechteren Überlebensprognose korreliert. Durch *in vitro* Experimente konnte ich zeigen, dass Gal-8 sowohl an MM als auch an Endothelzellen bindet und keinen Effekt auf die Angiogenese hat, dafür jedoch auf das Homing von MM Zellen an das Gefäßendothel. Die erhöhte Bindung durch die Gabe von rekombinantem Gal-8 von MM Zellen an Endothelzellen konnte sowohl statisch, als auch dynamisch während einer Simulation des Blutflusses, nachgewiesen werden. Auch durch Zugabe von Gal-8 aus konditionierten MM Überständen ist eine Erhöhung der Adhäsion nachweisbar. Es gibt zwei verschiedene Isoformen des Proteins, die sich in der Länge des Polypeptid-Linkers unterscheiden (S-kurz; L-lang), der pro-adhäsive Effekt tritt vor allem bei Zugabe der Gal-8L Isoform auf. Dass vor allem die Isoform mit dem langen Peptid-Linker die Adhäsion stark erhöht, lässt sich eventuell mit der Bildung von Gal-8 Komplexen erklären. Obwohl seit langem von solchen extrazellulären Galektin-Komplexen hypothetisch ausgegangen wird, konnten diese bisher noch nicht eindeutig nachgewiesen werden. Ich konnte mit Hilfe der Thermophorese zeigen, dass Gal-8L in der Lage ist in einen multimeren Zustand überzugehen. Interessanterweise geschieht dies ohne die Interaktion mit einem Zuckerliganden. Die Tatsache, dass sich Gal-8S und Gal-8L in Lösung unterschiedlich verhalten, kann wiederum Auswirkungen auf die unterschiedliche biologische Aktivität der zwei Isoformen haben.

Summary

Multiple myeloma (MM) is a hematological malignancy characterized by the clonal proliferation of mature plasma cells in the bone marrow. During the progression of the disease, post-germinal B-cells proliferate and expand rapidly. In some cases, high amounts of proteins (immunoglobulins) can be detected in blood or urine. Additionally, many patients suffer from an activation of osteoclasts (cells that resorb bone). Without therapy, patients survive 3-6 months, treatment with state-of-the-art therapy prolongs the life expectation to 3-6 years. The progression of the disease depends on the microenvironment in the bone marrow, since MM cells migrate into the bone marrow (homing) leading to increased tumorangiogenesis promoting the vascularization of the tumor.

My thesis is about the influence of Galectin-8 (Gal-8) on the interaction of MM with endothelial cells (EC). Gal-8 is a carbohydrate binding protein (lectin) that consists of two carbohydrate recognition domains (CRD) connected by a peptide linker. I was able to show that the content of the Gal-8 protein in the serum of MM patients is higher compared to healthy donors and that high expression of Gal-8 on mRNA level correlates with a poor prognosis. Using several *in vitro* approaches, I showed that Gal-8 binds both, MM and EC and has no effect on angiogenesis, but on homing of MM to EC. Recombinant Gal-8 enhances the binding of MM cells to EC is in static, as well as in shear stress conditions during the simulation of blood flow. Gal-8 conditioned MM supernatants were also capable of promoting adhesion. Gal-8 appears in two isoforms differing in the length of the linker peptide (S-short; L-long), the pro-adhesive effect is particularly stronger by the addition of the Gal-8L isoform. This effect might be explained by the formation of Gal-8 complexes. Although these processes have been assumed hypothetically, no experimental evidence exists. Using thermophoresis, I was now able to show that Gal-8L can form multimers. Interestingly, this happens without the addition of a carbohydrate ligand. These findings are in contrast to the existing interaction-models. The measurements show that Gal-8S and Gal-8L act differently in solution, this could have an impact on the biological activity of both isoforms.

List of abbreviations

APC	allophycocyanin
BAEC	bovine aortic endothelial cell
BJ	Bence Jones
BM	bone marrow
BMSC	bone marrow stromal cell
CD	cluster of differentiation
CRD	carbohydrate recognition domain
DNA	desoxyribonucleic acid
EC	endothelial cell
EC_{50}	half maximal effective concentration
ECM	extra-cellular matrix
EFS	event-free survival
ELISA	enzyme linked immunosorbent assay
FACS	fluorescence activated cell sorting
FITC	fluoresceinisothiocyanat
FRET	fluorescence resonance energy transfer
fwd	forward
Gal	galectin
GEP	gene expression profiling
HBMEC-60	human bone marrow endothelial cells 60
HD	healthy donor
HLA	human leukocyte antigen
HMVEC-L	human micro-vascular lung endothelial cell
HUVEC	human umbilical vein endothelial cells
ICAM1	inter-cellular adhesion molecule 1
MAA	Maackia amurensis lectin II
MFI	median fluorescence intensity
MGUS	monoclonal gammopathy of undetermined significance
MM	multiple myeloma
MST	microscale thermophoresis
Mut	mutant
NHDF	normal human dermal fibroblasts
OAS	over-all survival
PBS	phosphate buffered saline
PCR	polymerase chain reaction

PE	phycoerythrin
PNA	arachis hypogaea peanut agglutinin
POX	horseradish peroxidase
qRT-PCR	quantiative real-time polymerase chain reaction
rev	reverse
RT	room temperature
SEM	standard error of the mean
SLS	static light scattering
SMM	smoldering multiple myeloma
SNA	sambucus nigra (elderberry) bark lectin
TNF-α	tumor necrosis factor α
TT2	total therapy 2
TT3	total therapy 3
VEGF	vascular endothelial growth factor

1

Introduction

1.1 Clinical aspects on Multiple Myeloma

Multiple myeloma (MM) is a hematologic malignancy characterized by the transformation and clonal proliferation of mature plasma cells in the bone marrow (BM) [1]. According to the "Surveillance, Epidemiology, and End Results Program" (SEER) statistic in 2012, the median age at diagnosis is 69. In between 2003-2009, the 5 year survival rate was 43.2%, the median age at death is 75 years. In 2013, the number of estimated new cases was 22,350 which is 1.3% of all cancer cases in the USA [2].

MM evolves from a monoclonal gammopathy of undetermined significance (MGUS) that progresses from asymtomatical myeloma (smoldering myeloma, SMM) to the symptomatic MM [3]. Diagnostic criteria for the staging of the disease are summarized in Table 1.1.

	MGUS	**SMM**	**MM**
Serum M protein	3g per 100ml	$\geq$3g per 10ml	3g per 100ml
Bone marrow plasma cells	$<$10%	$\geq$10%	$>$10%
Urine light chain protein	none	none	$>$1g per day

Table 1.1: Staging criteria of MM (according to Anderson *et al.* [3])
MGUS: monoclonal gammopathy of undetermined significance; SMM: smoldering myeloma; MM: multiple myeloma.

The prevalence of MGUS is 3.2% in persons older than 50 years, 0.5%-3% of people having MGUS progress to MM per year [3, 4]. Not much is known about the process that drives the development from MGUS to MM. Active MM is defined by the occurrence of CRAB criteria (Hyper**C**alcemia (serum calcein $>$11.5mg/dl), **R**enal insufficiency (serum creatinine $>$2mg/dl), **A**nemia (hemoglobin $>$10g/dl or

>2g/dl below the lower limit of the normal range) and **B**one disease such as lytic lesions, osteopenia or pathologic fracture [1]. Patients present usually with unspecific pain in their back and a general lethargy which makes MM difficult to diagnose [5].

In the course from MGUS to MM, several genetic aberrations occur leading to the manifestation of the disease (Figure 1.1) [6]. MM cells are very heterogenous caused by their origin from long-lived plasma cells, which are already highly diverse, and many different genetic alterations appear during the progression of the disease (chromosomal translocations or the loss or gain of chromosomes).

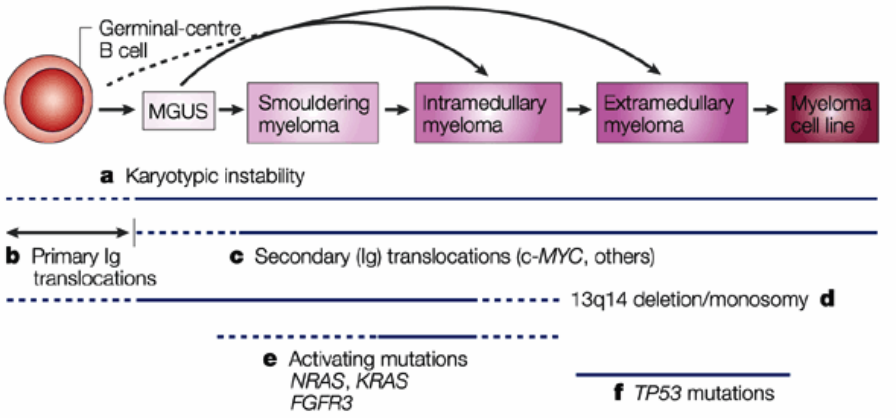

Figure 1.1: Oncogenic events during MM progression
In the progression from MGUS to MM, several genetic lesions occur. The figure was taken and modified from Kuehl and Bergsagel [7].

Using the mSMART (Mayo Stratification of Myeloma and Risk-Adapted Therapy) classification, patients are classified according to their genetic abnormalities in high-, intermediate- and standard-risk (Table 1.2) [8].

High risk	Intermediate risk	Standard risk
del 17p	t(4;14)	t(11;14)
t(14;16)	cytogenic del 13	t(6;14)
t(14;20)	hypodiploidy	all others
GEP: high risk signature	PCLI≥3%	

Table 1.2: Risk stratification
Frequent genetic alterations are used to classify patients according to the "Mayo Stratification of Myeloma and Risk-Adapted Therapy" (mSMART) [8]. GEP=gene expression profiling; PCLI=plasma cell labeling index

Treatment is not curative at the moment, but can prolong the life expectation of patients. Currently, five different classes of therapeutics are available: alkylating agents such as melphalan, anthracyclines like adriamycin and liposomal doxorubicin, corticosteroids (dexamethasone and prednisone), immunomodulatory drugs (thalidomide and lenalidomide), and proteasome inhibitors, e.g. bortezomib and carfilzomib [8]. Additionally, there is the possibility of autologous stem cell transplantation, which improves progression-free survival as well as over-all survival of patients [9]. Treatment options have to be optimized for each patient after diagnosis and staging of the disease.

1.2 Biology of MM in the BM

Understanding MM progression on a molecular level is crucial in order to find new treatment options and to understand why MGUS develops to MM. During the progression of the disease, MM cells home into the BM and are able to modify stromal cells in their host according to their requirements, promote the vascularization of the neoplasm (tumor angiogenesis) and cause bone resorption (osteolysis) as a consequence of activation of osteoclasts [10].

The BM microenvironment consists of several components like the extracellular matrix (ECM), bone marrow stromal cells (BMSC), fibroblasts, osteoblasts, osteoclasts, adipocytes and endothelial cells (EC) [11]. ECM and bone marrow cells are all in close contact and being altered by the invading MM cells. Since MM cells depend on the BM microenvironment for their growth and viability, they induce many signaling pathways to ensure their survival. This leads to a highly complex and interactive signaling network within the BM (Figure 1.2).

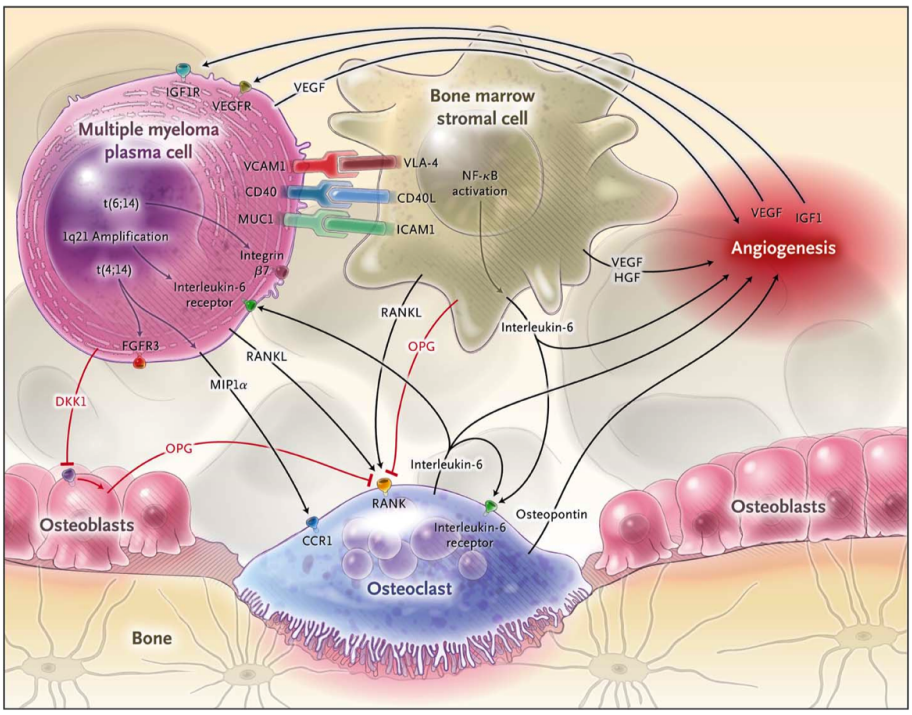

Figure 1.2: Interactions of MM cells with the BM microenvironment
Binding of the MM cells to BMSC triggers the transcription and expression of many factors, like IL-6, VEGF, TNFa, IGF1, SDF-1a, IL-1beta and MIP-1a. Those are able to mediate MM cell survival and proliferation in the BM [11, 12]. Many characteristics of the disease are due to those factors remodeling the BM. MM cells are able to induce osteolytic bone lesions by stimulating osteoclasts. They produce RANK-ligand (RANKL) which can bind to osteoclasts, leading to their activation and the downregulation of OPG expression, which is an inhibitor of RANKL. Another example is the expression of macrophage inhibitory protein alpha (MIP-1a) which is another activator of osteoclasts. After activation by MM cells, osteoclasts themselves produce IL-6 and osteopontin. Those factors stimulate the growing and survival of MM cells in the BM [7]. Another hallmark of MM progression is the induction of bone marrow angiogenesis. Either the direct production of pro-angiogenic molecules by MM cells or their induction in stromal cells or EC lead to the formation of tumor blood vessels in the BM. Adhesion molecules like VLA-4, VCAM or ICAM induce the adhesion of MM cells to the BM microenvironment. (The figure was taken from Palumbo and Anderson [1])

Complex interactions between MM cells and EC in the BM influence the processes of MM development. They are on the one hand involved in tumor-angiogenesis and on the other hand in the homing of the malignant cells into the BM. Further investigations are necessary in order to obtain deeper insights into the complex interplay between MM and EC in the context of the BM microenvironment.

1.2.1 Angiogenesis

Angiogenesis is a process leading to the formation of a new blood vessel network. The vasculature is important for the supply of all organs with oxygen and nutrients but also the disposal of cellular waste and immune cell trafficking into inflamed tissues [13]. All mammalian cells must be located within 100-200µm of a blood vessel in order to ensure their survival, since the diffusion limit of oxygen lies within

that distance. Organs growing beyond this size need to induce the formation of a blood vessel system to guarantee their survival [14]. After building a vessel network during embryogenesis *de novo*, EC usually remain quiescent and are able to survive for years. In healthy adults, active angiogenesis only occurs after injuries, when wounds have to be repaired or in female reproductive organs during menstruation [15, 16, 17]. Three distinct modes of vessel formation have been described so far (Figure 1.3). Vasculogenesis is the differentiation of endothelial precursor cells (angioblasts) into EC and their *de novo* assemble to a vasculature. This process occurs during embryogenesis. Sprouting angiogenesis describes the expansion of a preexisting network, intussuseption is the split of one vessel into two new vessels [13, 18]. During these processes, complex and dynamic interactions between EC and extracellular microenvironment occur [18].

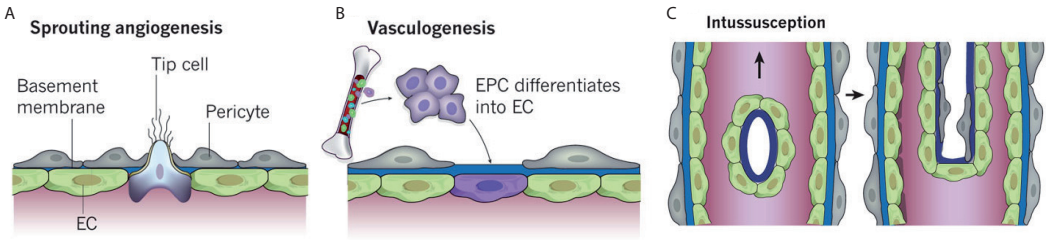

Figure 1.3: New blood vessel formation
The formation of new blood vessels can occur by several distinct mechanisms. A: Sprouting angiogenesis extends an already existing network B: Vasculogenesis occurs during embryogenesis to built the vasculature *de novo* C: Splitting of a pre-existing vessel by intussuseption. (The figure was taken and modified from Carmeliet and Jain [13])

Vessel formation is a tightly regulated process driven by several pro-and anti-angiogenic factors [14]. Members of the vascular endothelial growth factor (VEGF) family are the predominant signaling molecules for the induction of angiogenesis. The family consists of only a few members, VEGF-A being the most important one signaling by binding to VEGF receptor 2 (VEGF-R2) [13, 19]. Neuropilins (NRP1 and NRP2) are co-receptors that are on the one hand able to enhance VEGF-R2 activity or, on the other hand, signal independently [13, 20]. Many other factors are also involved in angiogenesis, e.g. fibroblast growth factors (FGF), platelet-derived growth factors (PDGF) angiopoietins (ANG) and several integrins and proteases[13, 19]. Since in adults EC are mostly quiescent and the vasculature remains stable, these growth factors need to be tightly balanced [13].

As Hanahan and Weinberg described the six hallmarks of cancer in 2000, angiogenesis was one among them, highlighting the importance of this process in tumor biology [21, 22]. Like all other organs, tumors are dependent on the constant supply with oxygen and nutrients [15]. If tumors grow beyond sizes of 100-200µm, a blood

vessel system is needed to enable further cell growth and metastasizing (Figure 1.4) [14]

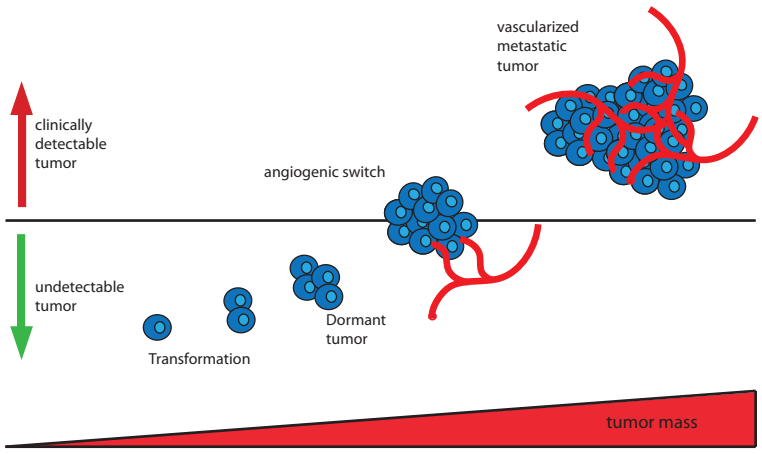

Figure 1.4: Angiogenic switch
Small, clinically undetectable tumors do not need blood vessels for growing. If the tumor mass reaches a certain size (100-200µm), the cells need blood vessels for the supply with nutrients and oxygen and for metastasizing. (The figure was taken and modified from Albini *et al.* [23])

Even though hematologic tumors, like MM, do not consist of a solid tumor mass, they depend on the vasculature and promote tumor angiogenesis. A high micro vessel density in the BM of MM patients has been observed already in studies from 1994 by Vacca *et al.* [24]. Several studies have shown that the occurrence of a higher micro vessel density in MM is a marker for faster progression [25, 26]. Additionally, several pro-angiogenic factors, like FGF-2 or VEGF are upregulated during the progression of the disease leading to the vascularization of the tumor in the BM [25, 26, 27]. These findings lead to a hypothetical model by Vacca and Ribatti [26] (Figure 1.5). They proposed that MGUS, the preliminary stage of MM, is the avascular phase not depending on tumor angiogenesis. After certain transformation events (activation of oncogenes, inactivation of tumor-suppressor genes) cells start to proliferate and secrete chemokines and cytokines leading to the angiogenic switch. Fully established MM is in a vascular phase where many proliferating clones are located in the BM and in the blood stream [26, 27]. The mechanisms why MGUS progresses to MM and how this angiogenic switch occurs are still unknown [26].

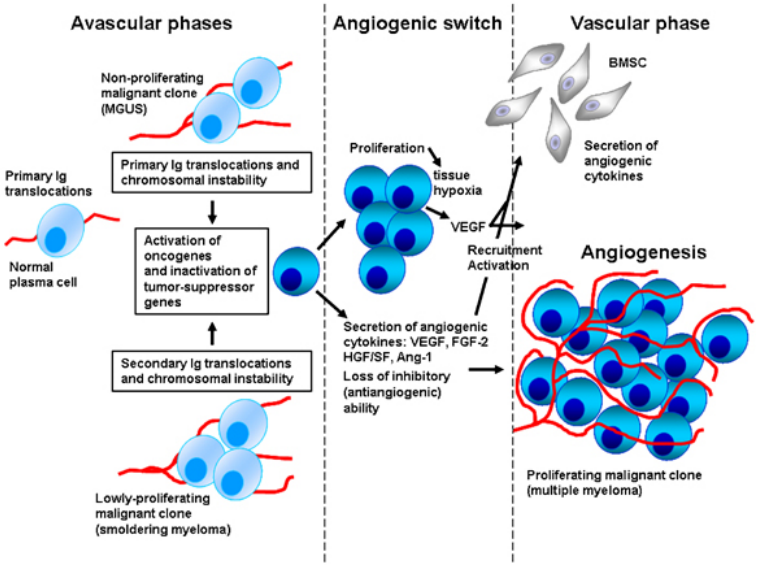

Figure 1.5: Angiogenesis and the angiogenic switch in MM
Hypothesis on the progression of MM in the BM. During the early avascular phase, MM cells do not need a tumor vasculature. Normal plasma cells transform due to certain genetic alterations to non-proliferating malignant clones (MGUS). After massive proliferation and reaching a certain size, tumor cells start to induce tumor angiogenesis by secreting pro-angiogenic molecules, e.g. VEGF. This leads to an establishment of the disease. (The figure was taken from Vacca and Ribatti [26])

1.2.2 Homing

Besides angiogenesis, the invasion and homing of MM cells into the BM is a hallmark of the disease. Although MM cells in the BM represent most of the tumor mass, a small number of cells is able to circulate in the blood vessel system [28]. These cells most likely represent the tumor-spreading component of the disease. These findings show that MM cells have capacity to (re)circulate, extravasate and migrate back into the BM showing how important homing mechanisms are for the progression of the disease [10]. In later stages of the disease, MM cells are able to become BM independent, meaning they are able to survive without BM stroma, leading to an increased number of circulating cells in the blood stream [29, 30].

The leucocyte adhesion cascade was described in 1990 by Butcher and Picker [31] and in extended form in 2007 by Ley *et al.* [32]. The adhesion of leucocytes to EC can be separated into several distinct steps all needing to be highly specific in order to only allow the immune cells to bind (Figure 1.6).

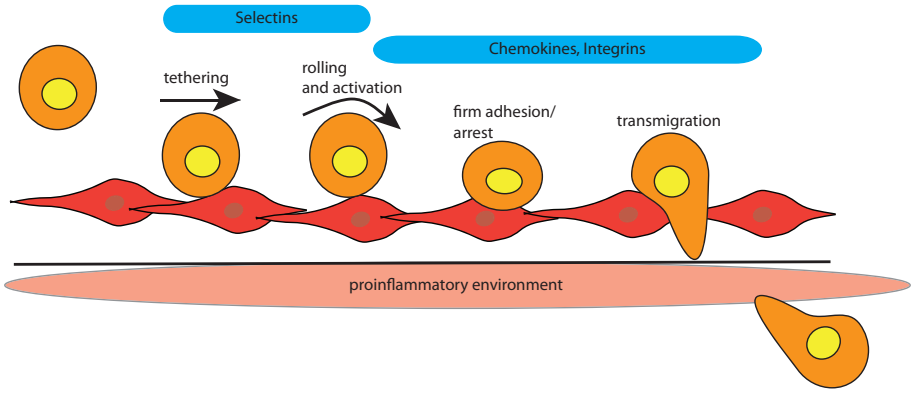

Figure 1.6: The leucocyte adhesion cascade
Leucocyte adhesion is a stepwise process. First, cells loosely attach to the endothelium (tethering) and start rolling on the EC. These first interactions are mainly mediated by selectins. By binding of integrins, the cells firmly adhere and are able to transmigrate through the vessel wall into inflamed tissues.

For the specific interactions between leucocytes and activated EC, many adhesion molecules need to be expressed. The most important ones on both cell types are listed in table 1.3 and further described in the following paragraph.

EC	Leucocyte	Process
E-selectin	PSGL1, CD44, ESL1	rolling
PSGL1	L-selectin	rolling
VCAM1	VLA4 (β_1-integrin)	firm adhesion
ICAM1	LFA1 (β_2-integrin)	firm adhesion

Table 1.3: Adhesion molecules and ligands on EC and leucocytes

At first, the leucocytes loosely attach to the EC (tethering) and start rolling on the EC layer. These initial steps are predominantly mediated by a set of specific selectins. Selectins are type I membrane glycoproteins, binding to these receptors is dependent on the glycosylation of the ligand [33]. Three different selectins are important for leucocyte adhesion: L-selectin which is expressed by leucocytes, P-selectin and E-selectin which are expressed by inflamed EC. The dominant interaction partner of all three selectins is the P-selectin ligand 1 (PSGL1), but this is only functionally when it is glycosylated correctly. Other known glycosylated ligands for

E-selectin are CD44 and E-selectin ligand 1 (ESL1) [32, 33]. It has been shown that L-Selectin and P-selectin require shear stress for binding as the rolling cells detach when the flow is stopped [34, 35, 36]. The binding of selectins to their ligands induces downstream signaling on both sides, but these signaling pathways are not well understood yet [32].

After being activated, the immune cells adhere firmly and are able to transmigrate through the vessel wall into the surrounding tissue. The transmigration can occur by two distinct mechanisms, the cells enter either via para- or transcellular routes. The paracellular route is described as the migration of leucocytes between two EC through endothelial junctions, the transcellular route is through one cell by intracellular channels [32]. These leucocyte - EC interactions during the adhesion cascade are mainly driven by binding to integrins and by the signaling through several chemokines. Integrins are heterodimeric glycoprotein receptors that consist of two non-covalently bound α and β subunits [37]. There are 18 α and 10 β subunits known so far, which can combine to 24 distinct integrins [38]. One example expressed by leucocytes is **V**ery **L**ate **A**ntigen 4 (VLA4), an $\alpha_4\beta_1$-integrin that is able to bind to **V**ascular **C**ell **A**dhesion-**M**olecule 1 (VCAM1) on EC. Another β_2-integrin expressed on leucocytes, **L**ymphocyte-**F**unction associated **A**ntigen 1 (LFA1) binds to **I**nter-**C**ellular **A**dhesion **M**olecule1 (ICAM1), mediating the firm adhesion of leucocytes [32]. It is important to note that the glycosylation of the integrin receptor plays an essential role in the function of the protein. In many tumors integrin glycosylation can be altered, leading to changes in adhesion and migration properties [39].

There are some molecules that have been shown to be of particular interest in MM homing. MM cells express CD44 and VLA4, which are both known receptors involved in leucocyte homing (see above) [11]. VLA4 is able to bind fibronectin in the BM ECM and VCAM-1 on BMSC. The binding of BMSC can trigger IL-6 secretion, a factor promoting MM cell survival and proliferation [10, 12]. The highly expressed surface proteoglycan Syndecan-1 (CD138), which is a marker for plasma cells and at the same time is used as a marker for MM, binds also to the ECM. This transmembrane heparan sulfate bearing proteoglycan is expressed in most MM cells and able to bind to type I collagen [11]. BMSC express stromal-cell derived factor-1 (SDF1), which is the ligand for CXCR4 expressed on the MM cells. Besides its role in B-cell migration and proliferation, CXCR4 plays also an important role in MM homing. SDF-1/CXCR4 mediated adhesion promotes transendothelial migration of MM cells by upregulation of VLA-4/VCAM-1 [40, 41].

In addition to the expression of several adhesion molecules, MM cells express and secrete a variety of chemokines and chemokine receptors, influencing migration and

homing [40]. One example is the macrophage inflammatory protein 1 α (MIP-1α), which seems to be involved in the induction of lytic bone lesions and is additionally able to stimulate proliferation, migration and survival of MM cells in the BM.

1.3 (Ga)lectins in MM - EC interactions

Glycans (complex carbohydrates) are major components of the outer cell surface and are attached to proteins via N- or O-linkage by an enzymatical process. EC glycosylation can be heavily altered in the tumor situation displaying or masking ligands for endogenous lectins. Both, selectins as well as integrins are glycosylation dependent and adhesion is influenced by alterations in their glycosylation patterns or the glycosylation of their ligands [42, 43]. During malignant transformation, tumor cells change their glycosylation patterns promoting tumor progression and metastasis. Common tumor cell epitopes are sialyl-Lewis^x, sialyl-Lewis^a (sLe^x, sLe^a), Thomsen-Friedenreich (T or TF) antigen (CD176), Thomsen-nouvelle antigen (Tn; CD175) or sialyl-Tn (sTn; CD175s). Enhanced sLe$^{x/a}$ expression correlates with an increased adherence to E-selectin [43]. Besides its influence on tumor adhesion processes, angiogenesis can also be influenced by altered glycosylation patterns. Gal-1, a member of the galectin family, has recently been shown to associate with glycosylated EC receptors influencing the resistance of tumors to anti-VEGF therapy [44]. It can be presumed that also other lectins can influence MM-EC interactions to promote angiogenesis in the tumor microenvironment. For MM it has been shown that the glycome is altered in many different ways during disease progression [45].

Lectins are defined by their selective binding to carbohydrates but they do not have any enzymatic activity. Originally they were classified as either C-type lectins (Ca^{2+} dependent) or S-type lectins, which are today known as galectins [46, 47]. By binding to surface carbohydrates, they "sense" the glycosylation patterns of cells and are able to induce signaling pathways.

Galectins represent a group of mammalian lectins which specifically bind β-galactosides [48]. Galectins are very conserved among species and can even be found in plants and fungi [49]. Today, 15 different mammalian galectins are known. Galectins consist of at least one carbohydrate recognition domain (CRD) and are further classified according to their structure [49, 50, 51]. Galectins that consist of only one CRD are termed prototype galectins (Gal-1, -2, -5, -7, -10, -11, -13, -14 and -15), whereas galectins consisting of two CRDs joined by a linker are named tandem repeat galectins (Gal-4, -6, -8, -9 and -12). One exception is Gal-3, which is

a so-called chimera galectin consisting of one CRD fused to a amino-acid tail (Figure 1.7). Each galectin has different sugar-binding specificities due to differences of amino acids in the binding pocket of the CRD.

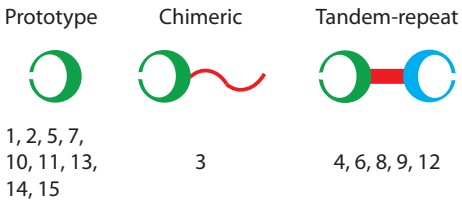

Figure 1.7: Galectins - classification
Galectins can be classified according to their structure in prototype galectins with one CRD, tandem repeat galectins with two CRDs joined by a linker and chimera galectins containing one CRD fused to an amino acid tail. (Figure according to Leffler *et al.* [50])

Prototype galectins such as Gal-1 and -7 have been shown to exist as dimers in solution, Gal-3 precipitates as a pentamer [52, 53]. This leads to bi -or multivalent molecules capable of binding more than one carbohydrate ligand. Tandem-repeat galectins occur per se as bivalent molecules which can possibly bind more than one ligand. For Gal-1 and Gal-3 it has been shown, that they are able to cluster receptors on T-cells to induce downstream signaling [54, 55, 56]. Additionally, multimerization on the cell surface of Gal-3 was visualized using fluorescence resonance energy transfer (FRET) [57]. Those observations lead to the suggestion of a model by Rabinovich and Toscano [58] that galectins form glycan-protein lattices on the cell surface in order to induce receptor clustering and downstream signaling (Figure 1.8) [58, 59].

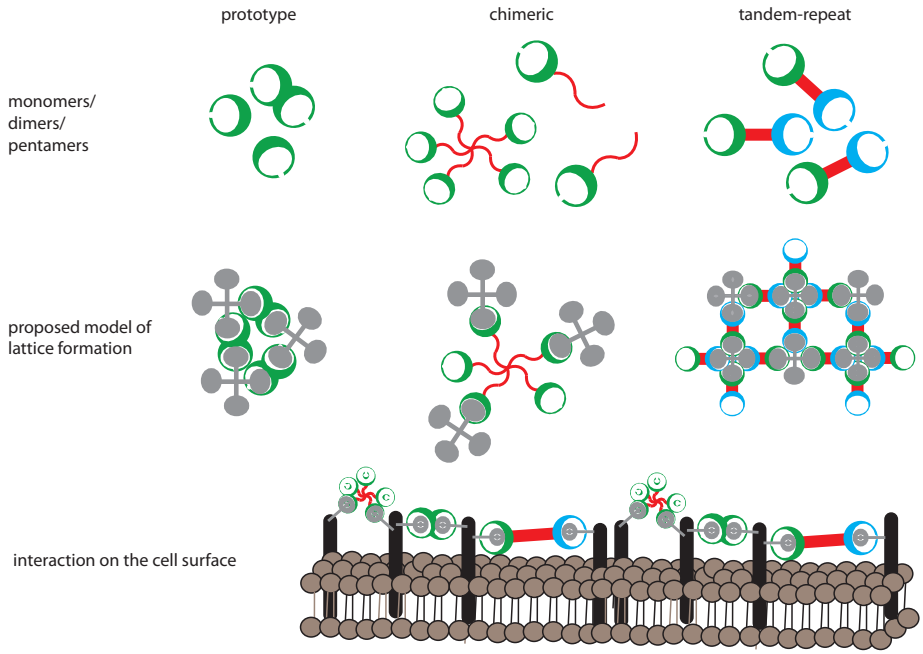

Figure 1.8: Formation of galectin-glycan lattices
Prototype galectins exist as monomers or dimers, chimeric Galectin-3 as mono-or pentamer. Those di- or multimers, as well as the tandem-repeat galectins (which already consist of two CRDs) are able to bind glycans on the cell surface and thereby crosslink cell surface receptors. (Figure modified according to Rabinovich *et al.* [58])

So far there is not much experimental evidence that these processes really occur for all known galectins besides Gal-1 and Gal-3 [54, 55, 56, 57]. In particular, not much is known about di- or multimerization of tandem-repeat galectins in the absence or presence of a ligand. Artificial linkage of two Gal-1 CRDs by several linking structures showed homodi - and multimerization by an artificial tandem repeat galectin, but there is no experimental evidence that "real tandem-repeat galectins" do so [60].

Galectins are ubiquitously expressed and can be found in the cytoplasm, on the cell surface and in the extracellular microenvironment after secretion via an unconventional pathway [61]. They are involved in many different cellular processes like cell-cell adhesion, apoptosis, angiogenesis and migration [59, 62]. Figure 1.9 gives an overview of galectin-involved cellular events.

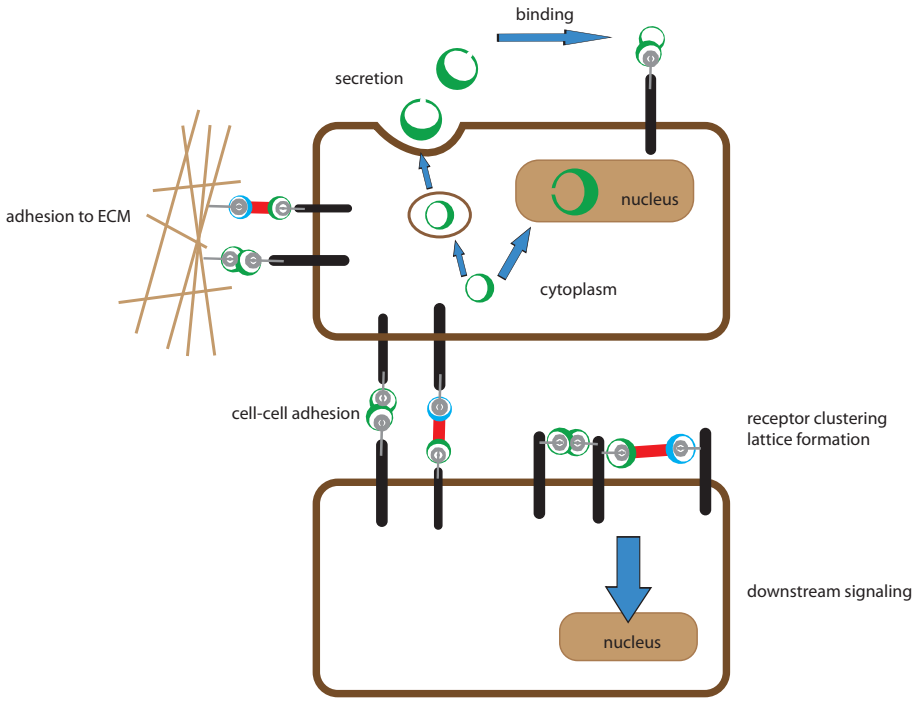

Figure 1.9: Galectins - biological roles
Galectins can be involved in many different cellular processes. They can be found in the nucleus, in the cytoplasm and on the cell surface. Secretion occurs by a non-classical secretion pathway. Binding to ligands on the cell surface leads to receptor clustering followed by downstream signaling, cell-cell or cell-ECM interactions.

Since galectins play a role in many basic cellular mechanisms, the dysregulation of galectin-expression can have an impact on tumorigenesis [62, 63, 64]. Several galectins are expressed in different tumor cells and tissues [64, 65]. The expression of the different galectins is highly variable in different tumors, thus linking of galectin-expression patterns to malignancy is difficult to achieve and has to be examined for each tumor-type and galectin separately. Changes in the expression and subcellular localization can occur during the transition of a normal cell to a cancer cell [63]. Gal-1 and -3 are the best studied galectins at the moment, but also Gal-8 seems to be involved in tumor biology. Table 1.4 summarizes the impact of Ga-1, -3 and -8 on tumor development and progression.

	Effect on	Reference
Gal-1	tumor transformation, binding H-Ras	[66]
	cell cycle regulation	[67]
Gal-3	tumor transformation, binding K-Ras	[68]
	cell cycle regulation	[69]
	anti-apoptosis	[70, 71]
	signal transduction	[72]
	cell-matrix interaction	[73]
Gal-8	modulation of cell adhesion	[74]
	binding of integrins	[75, 76, 77, 78]

Table 1.4: Impact of Gal-1, -3 and -8 on tumor progression

In MM, Gal-1, -3 and -9 have so far been described to play a role in the progression of the disease. Gal-1 supports the survival of MM cells by interaction with SDF-1 α [79], whereas Gal-3 is an anti-apoptotic factor in diffuse large B-cell lymphomas [80]. Furthermore, Gal-9 seems to have a rather inhibitory effect on the growth of cancer cells and leads to apoptosis in MM [81]. Additionally, in a first study it was shown, that the anti-Gal-3 compound GCS-100 could be used as a therapeutic molecule against MM. It modified intracellular signaling leading to an inhibition of proliferation and apoptosis [82]. This implies that galectins can be new targets for anti-myeloma therapy. The effect of other galectins on MM has not been investigated yet.

1.3.1 Galectin-8

Gal-8 was first described in 1995 as a rat lectin related to Gal-4 [83]. In 2000, it was found in humans as a surface marker associated with prostate cancer and named prostate carcinoma tumor antigen-1 (PCTA-1) [84]. Thereafter is was shown that PCTA-1 is a galectin that belongs to the family of tandem-repeat galectins consisting of two CRDs connected by a linker region and thus its name was changed to Gal-8. By alternative splicing, isoforms with differences in the length of the linker region are created [65, 84]. The linker of Gal-8 short (Gal-8S) consists of 34 amino acids whereas the Gal-8 long (Gal-8L) isoform linker consists of 76 amino acids. Gal-8 is expressed in many healthy and tumor tissues of different origins [65, 85, 86, 87, 88]. Depending on the tumor, Gal-8 is either increased or decreased in the progression of the disease [64, 65, 74, 87, 89, 90, 91, 92, 93].

As expected for a lectin with two CRDs, both domains are able to bind distinct glycan structures. The N-terminal CRD seems to have in general a higher binding affinity compared to the C-CRD [94]. The N-CRD prefers sialylated and sulfated oligosaccarides, whereas the C-CRD seems to prefer non-sialylated glycans like blood-group A and B antigen or polylactosamine [94, 95, 96, 97, 98, 99].

Although not much is known about the function of the lectin, it seems to play a role in the induction of apoptosis on different leucocytes [98, 100]. Furthermore, a pro-angiogenic role on bovine aortic endothelial cells (BAEC) has been shown [101]. Stimulation of EC with recombinant Gal-8 induces the secretion of pro-angiogenic cytokines and the expression of certain adhesion molecules [89]. Several studies display the lectins role in adhesion processes by binding of integrins [75, 76, 77, 78] and that it strengthens the adhesion of colon cancer cells to EC [74]. Recent publications report a critical role of Gal-8 in the defense of bacterial infections indicating the involvement of Gal-8 in the immune system [102, 103]. Still many questions are open regarding the function of Gal-8 and not much is known whether both isoforms have different effects on the biological functions. Only few studies deal with both isoforms, mostly the short-linker isoform has been used for published experiments so far.

1.4 Aim of the study

This study intends to investigate the role of Gal-8 in the progression of MM. Nothing is known yet about the influence of Gal-8 in MM, but there is some evidence that Gal-8 plays a role in angiogenesis as well as in adhesion processes. Since MM progression depends on both, tumor-angiogenesis and homing of the malignant cells into the bone marrow, I was wondering, whether Gal-8 plays a key role in the progression of the disease. In my study, I wanted to see whether the length of the linker influences the biological function of Gal-8. The linker region seems to have an impact on the function of the lectin [104], however the long-linker isoform has not been considered in most studies about Gal-8 function.

In a first step, the influence of Gal-8 expression in MM patients was analyzed using Gal-8 expression data from bone-marrow biopsies. It was important to investigate if Gal-8 is expressed in MM and if expression of the lectin differs during the progression of the disease or if it correlates with survival prognosis.

After preliminary tests, the study was divided into three different sub-projects, each focussing on different aspects of Gal-8 in MM biology. The working plan for my thesis was as follows:

1. Gal-8 in (tumor-) angiogenesis

Since MM progression is depending on tumor-angiogenesis, the impact of recombinant Gal-8 on angiogenesis was examined first. In order to find out if Gal-8 plays a critical role in this process the effect of Gal-8 on proliferation and migration in EC was examined. Additionally, an *in vitro* tube formation assay was performed, to detect if Gal-8 has any pro-angiogenic potential.

2. Gal-8 in MM homing

A second aspect in MM progression is the adhesion of MM cells to EC in the BM. In order to find out if Gal-8 is a factor promoting adhesion of MM to EC, an *in vitro* shear stress model was established. The influence of recombinant and MM cell derived Gal-8 on MM EC interaction was studied using this system.

3. Gal-8 multimerization

Dimerization and lattice formation has only been shown for prototype galectins and the chimeric Gal-3 so far. Using a new technique, microscale thermophoresis (MST), the capability of Gal-8 to built dimers or multimers was studied.

2

Materials & Methods

2.1 Materials

2.1.1 Primary Antibodies

Specificity (Clone)	Species	Isotype	Conjugate	Supplier	Application
Anti-human CD31	mouse	IgG_1	APC	RnD	FACS
Anti-human CD31	mouse	IgG_1	unconjugated	Dako	tube formation assay
Anti-human CD38	mouse	IgG_1	FITC	BD Biosciences	FACS
Anti-human CD54	mouse	IgG_1	APC	BD Biosciences	FACS
Anti-human CD56	mouse	IgG_1	APC	BD Biosciences	FACS
Anti-human CD59	mouse	IgG_{2A}	FITC	BD Biosciences	FACS
Anti-human CD62e	mouse	IgG_{2A}	PE	Biolegend	FACS
Anti-human CD138	mouse	IgG_1	PE	BD Biosciences	FACS
Anti-human CD144	mouse	IgG_{2B}	PE	RnD	FACS
Anti-human W6/32	mouse	IgG	unconjugated	Dr. Gerd Moldenhauer [105]	FACS

Specificity (Clone)	Species	Isotype	Conjugate	Supplier	Application
Anti-human Gal-8	mouse	IgG_{2A}	unconjugated	RnD	ELISA, IP
Anti-human Gal-8	goat	IgG polyclonal	biotin	RnD	Western Blot, ELISA

2.1.2 Secondary Antibodies

Specificity (Clone)	Species	Conjugat	Supplier	Application
Anti-mouse IgG+IgM	goat	APC	Dianova	FACS
Streptavidin		APC	Dianova	FACS
Streptavidin		FITC	BD Biosciences	FACS
Streptavidin		POX	Dianova	Western Blot, ELISA

2.1.3 Lectins

Galectins were kindly produced and provided by Prof. Hans-Joachim Gabius (LMU Munich) as described in the methods section.

Name	Specificity	Conjugate	Supplier	Application
Arachis hypogaea Peanut Agglutinin (PNA)	Galβ1-3GalNAcα1-Ser/Thr	biotin	Linaris/Vector Laboratories	FACS
Maackia amurensis lectin II (MAA)	Neu5Ac/Gcα2,3 Galβ1, Glc(NAc)	biotin	Linaris/Vector Laboratories	FACS
Sambucus nigra (Elderberry) bark lectin (SNA)	Neu5Acα2-6Gal(NAc)-R	biotin	Linaris/Vector Laboratories	FACS

2.1.4 Enzymes

Enzyme	Supplier
α-2-3,6,8 Neuraminidase from *Vibrio cholarae* (VCN)	Roche

2.1.5 Cell lines

Name	Origin	Supplier
HBMEC-60	bone marrow endothelium	Sanguin, Amsterdam
HUVEC	umbilical vein endothelium	Promocell
LP-1	peripheral blood of a MM patient	DSMZ
MOLP-8	peripheral blood of a MM patient	DSMZ
NHDF	adult breast skin (female)	Promocell

2.1.6 Sera

Sera from 42 MM patients were kindly provided by Drs. Anja Seckinger (Heidelberg) and Dirk Hose (Heidelberg).

2.1.7 Cell culture media and supplements

Medium / supplement	Supplier
AIM-V + AlbuMax (BSA) 1x	Gibco
Detach Kit	Promocell
Dulbeccos modified eagle medium (DMEM)	Sigma
Endothelial cell basal medium (ECBM)	Promocell
Endothelial cell growth medium supplement pack	Promocell
Fetal bovine serum (FBS)	Biochrome
Freezing medium	Ibidi
HEPES	Gibco
MEM non-essential amino acids (NEAA)	PAA
RPMI-1640 AQmedia	Sigma

2.1.8 Kits

Kit	Supplier
2x buffer SYBR green	Applied Biosystems
Dako LSAB2 System Hrp	Dako
High pure RNA isolation kit	Roche
Monolith NT.115 labeling kit red NHS	Nanotemper
Pierce BCA Protein Assay Kit	Thermo Scientific
Pierce Classic IP Kit	Thermo Scientific
Platinum Blue PCR Mix	Invitrogen
Super Script first strand cDNA synthesis system for RT-PCR	Invitrogen
Super Signal West Dura Extended duration substrate	Thermo Scientific
TMB substrate kit	Thermo Scientific
VenorGeMOneStep PCR kit	Minerva

2.1.9 Molecular weight markers

Marker	Supplier	Application
Gene ruler 100bp	Fermentas	DNA agarose gel electrophoresis
Rainbow marker full range	GE Healthcare	SDS gel electrophoresis

2.1.10 PCR primer for qRT-PCR

qRT-PCR primers were purchased from MWG operon and stocks were diluted to a concentration of 200µM in ddH_2O. Frozen stocks were thawed and further diluted to a concentration of 5µM prior to use.

Primer	Sequence
β-Actin fwd	5'- GCT CCT CCT GAG CGC AAG -3'
β-Actin rev	5'- CAT CTG CTG GAA GGT GGA CA -3'
Gal-8 fwd *	5'- CTT AGG CTG CCA TTC GCT -3'
Gal-8 rev *	5'- AAG CTT TTG GCA TTT GCA -3'
CD54 fwd	5'- GGG CAT AGA GAC CCC GTT GCC T -3'
CD54 rev	5'- GGG TGC CAG TTC CAC CCG TTC -3'

Primer	Sequence
CD31 fwd	5'- ATT GCA GTG GTT ATC ATC GGA GTG -3'
CD31 rev	5'- CTC GTT GTT GGA GTT CAG AAG TGG -3'
CD62e fwd	5'- ATC CAA AAG GCTCCA ATG TG -3'
CD62e rev	5'- CTC CAA TAG GGG AAT GAG CA -3'
CD144 fwd	5'- CGA TAC ATG AGC CCT CCC GCG -3'
CD144 rev	5'- GAT CTG CAG GAC CAG CTG GAA AA -3'

* primer sequence according to Thijssen *et al.* [88]. All other primers were designed according to their mRNA sequence and the specificity of the primers was checked using NCBI/ Primer-BLAST.

2.1.11 PCR primer

PCR primers were purchased from MWG operon and stocks were diluted to a concentration of 200µM in ddH_2O. Frozen stocks were thawed and further diluted to a concentration of 20µM prior to use.

Primer	Sequence
Gal-8 fwd *	5'- AGA ATG ATG TTG TCC TTA AAC -3'
Gal-8 rev *	5'- CTA CCA GCT CCT TAC TTC C -3'

* primer sequence according to Thijssen *et al.* [88]. The specificity of the primers was checked using NCBI/ Primer-BLAST.

2.1.12 Buffers & solutions

Application	Buffer	Contents	Molarity/ grams
ELISA	Coating buffer (pH9.6)	Na_2CO_3	0.52g
		Tween-20	0.05% (v/v)
		ddH_2O	100ml
		adjust pH with $NaHCO_3$	
	Wash buffer	PBS	
		Tween-20	0.05% (v/v)
Western Blot	Blotting buffer (pH7.5)	Trizma base	25mM
		NaCl	0.15M
		Tween-20	0.05% (v/v)
		adjust pH with HCl	
	Blocking buffer	non-fat dry milk	2% (w/v)
		in Blotting buffer	
	Antibody incubation buffer	non-fat dry milk	1% (w/v)
		in Blotting buffer	
	Transfer buffer 1 (pH9.4)	Aminocaproic acid	0.04M
		Trizma base	0.025M
		adjust pH with HCl	
	Transfer buffer 2 (pH10.4)	Trizma base	0.3M
		adjust pH with HCl	
	Transfer buffer 3 (pH10.4)	Trizma base	0.025M
		adjust pH with HCl	
Galectin dissolving buffer	10mM PB-buffer (pH7.2)	0,2M NaH_2PO_4	1.4ml
		0,2M Na_2HPO_4	3.6ml
		ad ddH_2O	100ml
FACS	FACS buffer	PBS	
		BSA	1% (w/v)
		NaN_3	0.1% (w/v)

Application	Buffer	Contents	Molarity/ grams
SDS Gel-electrophoresis	10x SDS running buffer	Trizma base	151.5g
		Glycine	720g
		ad ddH_2O	5l
Thermophoresis	MST-optimized buffer (pH 7.2)	Trizma base	50mM
		NaCl	150mM
		MgCl2	10mM
		Tween-20	0.05% (v/v)
		BSA	0.1% (w/v)
		adjust pH with HCl	
PCR	50x TAE buffer (pH 8.3)	Trizma base	2M
		Acetic acid (anhydrous)	1M
		EDTA	100mM
		adjust pH using acetic acid (anhydrous)	

2.1.13 Chemicals

Chemical	Supplier
16% Paraformaldehyde solution (PFA)	Thermo Scientific
[^{3}H]-Thymidine	PerkinElmer
6x DNA gel loading buffer	Novagen
7-Amino-Actinomycin-D (7-AAD) viability probe	BD Biosciences
Acetic acid (anhydrous)	Merck
ADEFO Citroline 2000	Adefo
Adefofix-Fixierer	Adefo
AEC+ high sensitivity substrate	Dako
Albumin standard	Thermo Scientific
Aminocaproic acid	Sigma
Ammonium persulfate (APS)	Sigma
Beta-lactose minimum 99% total lactose	Sigma
Betaplate Scint	Perkin Elmer
Blotto non-fat dry milk	Santa Cruz/Chem Cruz
Bovine serum albumin (BSA) fraction V	PAA
Calcein green AM	Invitrogen
Dako fluorescent mounting medium	Dako
Di-Sodium Hydrogenphosphate (Na_2HPO_4)	Merck
Dimethyl Sulfoxide (DMSO)	Eurolone
Dithiothreitol (DTT)	Sigma
Ethanol	Sigma
Ethidiumbromide solution 0,07%	AppliChem
Ethylenediaminetetraacetic acid (EDTA)	Acros
Gelatine from bovine skin type B	Sigma
Glycerine	AnalR Normapur
Glycine	Sigma
Hydrochloric acid (HCl) 37%	Normapur
Hydrocortisione acetate	Sigma
Hydrogen peroxide (H_2O_2)	Sigma
Isopropanol (2-Propanol)	J.T.Baker
LDS sample buffer	Expedeon
Magnesium chloride ($MgCl_2$)	Sigma
Methanol	Sigma
N,N,N',N'-Tetramethylendiamin (TEMED)	Roth

Chemical	Supplier
Phosphate buffered saline (PBS)	Sigma
PBS + Ca_2/Mg_2	Sigma
Protease-Phosphatase Inhibitor Cocktail	Thermo Scientific
Protein A/G Plus Agarose	Santa Cruz
recombinant human TNF-α	PromoKine
recombinant human VEGF-165	Thermo Scientific
Roti-Load 1 protein loading buffer reducing	Roth
Rotiphorese Gel 30 (Acrylamide/Bis)	Roth
RunBlue RAPID SDS Run Buffer	Expedeon
Silicon paste	Roth
Sodium azide (NaN_3)	Merck
Sodium carbonate (Na_2CO_3)	Merck
Sodium chloride (NaCl)	Sigma
Sodium di-hydrogenphosphate (NaH_2PO_4)	Merck
Sodium dodecyl sulfate (SDS) Powder	GERBU
Sodium hydrogencarbonate ($NaHCO_3$)	Roth
Sodium hydroxide (NaOH)	Isochim
Sulfuric acid (H_2SO_4)	Roth
Triton-X 100	Sigma
Trizma base	Sigma
Trypan blue	Biochrom
Tween-20	Sigma
Ultra Pure Agarose	Invitrogen
Water, DNase, RNase free	MP Biomedicals

2.1.14 Consumables

Sterile plastic-ware for cell culture was ordered from TPP or BD Biosciences if not indicated otherwise.

Consumable	Supplier
1x8 Stripwell plates high binding	Costar
24-well cell culture cluster	Costar
3mm Chr blotting paper	NeoLab
96-well qRT-PCR plate	StarLab
Amersham Hyperfilm ECL	GE Healthcare
Amicon Ultra-15	Millipore
C-Chip disposable hemocytometer	DigitalBio
Cell Scraper 320mm	CytoOne
Cellulose chromatography paper	Whatman
Cryo.S	Greiner bio One
Culture-inserts for self-insertion	Ibidi
HumanHT-12 v4 Expression BeadChip	Illumina
MicroAmp Optical Adhesive Film	Life Technologies
Millex GP filterunit 0.22µM	Millipore
NT.115 hydrophobic capillaries	Nanotemper
Nunc MicroWell 96-well plates	Thermo Scientific
Parafilm “M”	Sigma
Perfusion set red	Ibidi
Perfusion set white	Ibidi
Petri dishes 35x10mm	Falcon
Printed filtermat A	Perkin Elmer
RunBlue SDS precast gels 4-12%	Expedeon
Safe lock tubes 0.5ml; 1.5ml; 2ml	Eppendorf
Sample bag for MicroBeta	Perkin Elmer
Serial connector	Ibidi
Superdex 200 HR 10/30 column	GE Healthcare
Syringe 50ml without needle	Terumo
Transfer membrane Immobilion-P	Millipore
µ-Slide 8-well ibiTreat	Ibidi
µ-Slide angiogenesis ibiTreat	Ibidi
µ-Slide $I^{0.6}$ ibiTreat	Ibidi

2.1.15 Instruments

Instrument	Manufacturer
-20°C freezer comfort	Liebherr
-80°C freezer Hera freeze	Thermo Scientific
+4°C fridge Profiline	Liebherr
7300 Real Time PCR System	Applied Biosystems
Agarose-Gel-electrophoresis system	Hybaid
Allegra 218 centrifuge	Beckman
Cell Observer.Z1	Zeiss
Chicken egg incubator Termo-de-Luxe 150	J. Hemel Brutgeräte
Dyad DNA engine	BioRad
FACS CantoII	BD Biosciences
Heracell 204i CO_2 incubator	Thermo Scientific
Heraeus Fresco17 centrifuge	Thermo Scientific
Herasafe clean bench	Heraeus
Leica DM IL LED	Leica Microsystems
Leica TCS SP5 II	Leica Microsystems
Liquid nitrogen tank	Cryotherm
MicroBeta TriLux	Perkin Elmer
Microwave oven	Sharp
MilliQ water purification systems	Millipore
Monolith NT.115	Nanotemper
Mr. Frosty	Thermo Scientific
Multi image light cabinet	HeroLab
Multiscan EX	Thermo Scientific
Nanodrop 2000	Thermo Scientific
Optimax X ray film processor	PROTEC Medizintechnik
PEQ Power 300	PeqLab
pH meter pH525	WTW
Pipet boy	Integra
Pipettes 1000µl; 200µl; 100µl; 10µl; 2,5µl	Eppendorf
Promax 2020	Heidolph
Pump system	Ibidi
Rotana 460RC	Hettich Zentrifugen
SDS-chamber model V15.17	Biometra Analytik Jena
Stereomicroscope SMZ 800	Nikon

Instrument	Manufacturer
Thermomixer Comfort	Eppendorf
TomTec Harvester	SisLab
Viscotek TDAmax	Malvern
Water bath	Medingen E5
Western Blot transfer chamber	LTF Labortechnik

2.1.16 Software

Software	Supplier
Adobe Illustrator CS5	Adobe Systems GmbH
Adobe Photoshop CS5	Adobe Systems GmbH
Angiosys 1.0	TCS (Cellworks)
Chipster	The Finnish IT Center for Science CSC
Flow Jo 9.5.2	TreeStar
Igor Pro 6.3	Wave Metrics
Image J	Wayne Rasband (NIH)
Office 2008	Microsoft Corporation
Prism 5	GraphPad Software Incorporated

2.2 Methods

2.2.1 Cell culture

All cells were cultivated under sterile conditions at 37°C and in a 5% CO_2 atmosphere.
Human umbilical vein endothelial cells (HUVEC) and human bone marrow endothelial cells (HBMEC-60) were cultivated in endothelial cell basal medium (ECBM) supplemented with 10% FBS and growth factors. Cells were split twice per week and used in passage 4 or 5 (HUVEC) or up to passage 20 (HBMEC-60).
Normal human dermal fibroblasts (NHDF) were cultivated in Dulbeccos modified Eagle medium (DMEM) supplemented with 10% FBS, 1% non-essential amino acids (NEAA) and 1% HEPES. Medium was changed twice weekly, cells were split every 7-14 days (depending on confluency) and used until passage 15.
Adherent cell lines were detached using the detach kit containing HEPES for washing, Trypsin/EDTA for detaching and Trypsin-neutralizing solution (TNS).
The MM cell lines MOPL-8 and LP-1 were cultivated in RPMI containing 20% or 10% FBS respectively. Cells were split twice per week and used in passage up to passage 20.

Cells were counted diluting them 1:2 with trypan-blue for live-dead discrimination using a Neubauer counting chamber.

For cryoconservation, cells were adjusted in freezing medium to $1x10^6$/ml (adherent cells) or to $3x10^6$/ml (suspension cells) and frozen at -80°C using a Mr. Frosty according to the manufacturers protocol. Long-term storage was performed in a liquid nitrogen tank.
The cells were mycoplasma free as determined by the VenorGeMOneStep PCR kit. Multiplexion human cell line authentication test (MCA) was performed as described (www.multiplexion.de). Both MM cell lines are included in the MCA data base. Identity was confirmed to 100%, no cross-contamination with other cell lines was found. For HBMEC-60 a HeLa contamination was excluded, but the identity could not be confirmed, because the cell line is not included in the MCA database.

2.2.2 Preparation of cell culture supernatants

For Gal-8 detection in cell culture supernatants $7.5x10^5$EC or $2.5x10^6$MM cells were cultivated in the respective cell culture medium for 48h. Supernatants were centrifuged at 300g, cellular debris was discarded and the supernatants were mixed

with protease/phosphatase inhibitors.
Prior to shear stress experiments with conditioned supernatants, MOLP-8 cells were pre-cultured in RPMI-1640 supplemented with 10% FBS for at least 3 days. 5x10^6cells were transferred to 20ml AIM-V Medium and cells were cultivated at 37°C in a 5% CO_2 atmosphere for 72h. Supernatants were centrifuged at 300g, cellular debris was discarded and the supernatants were concentrated 20-fold using an Amicon Ultra-15 Centrifugal Filter Unit according to the manufacturer's protocol. Concentrated supernatants were supplemented with protease-phosphatase inhibitors and subsequently used for Gal-8 depletion.

2.2.3 Gal-8 depletion in cell culture supernatants

Concentrated supernatants were used for the Gal-8 depletion. 1ml of 20x supernatant was incubated with 5µg of anti-Gal-8 antibody (mouse monoclonal) over night at 4°C on a shaker. The following day the supernatants were incubated twice with 20µl Agarose A/G slurry for 30min. The mixture was centrifuged at 1000g and the supernatants were taken for further shear stress experiments. Gal-8 content of depleted cell culture supernatants was investigated using a Gal-8 specific ELISA.

2.2.4 Enzymatic treatment of cells

For VCN treatment, cells were diluted in RPMI-1640 and treated for 1h at 37°C with 5mU/5*10^6 cells. After the treatment, the cells were washed once with RPMI-1640 and used for further experiments.

2.2.5 Stimulation of cells with TNF-α

Cells were diluted in their regular cell culture medium and stimulated using 10ng/ml TNF-α for 24h prior to an experiment.

2.2.6 Calcein-green staining of cells

5*10^6 cells of the respective MM cell line were washed once with PBS and diluted in RPMI-1640 containing 1% HEPES. Cells were incubated with 5µM calcein-green for 30 minutes and washed twice with PBS afterwards. The stained cells were diluted in the respective medium needed for the following experiments.

2.2.7 Preparation of galectins

The preparation and lyophilization of galectins was kindly performed by Prof. Hans-Joachim Gabius (LMU Munich) [99, 106]. Wild type and variant proteins were obtained by recombinant production followed by chromatographic purification and quality controls. Protein concentrations were determined using the theoretical molar adsorption coefficient before lyophilization. Galectins were stored at -20°C and dissolved in 10mM PB buffer before use. Protein concentration after dissolving was determined using a BCA assay. Diluted proteins were stored in aliquots at -20°C. Proteins were not refrozen after thawing once.

2.2.8 BCA Assay

For quantification of protein-concentrations, the BCA assay was used. 10µl of the lysate or the standard protein were loaded into the wells of a 96-well plate. Standard-protein concentrations to calculate a calibration curve were ranging from 100µg/ml to 1500µg/ml. For detection, 200µl of a 50+1 mixture of reagent A and reagent B was added and the 96-well plate was incubated for 30min at 37°C. Absorption was measured in an ELISA reader at 540nm.

2.2.9 RNA-isolation and cDNA synthesis

Total cellular RNA was isolated from $1x10^6$ cells using the high pure RNA isolation kit according to the manufacturer's protocol. The concentration and purity of the isolated RNA was determined using a Nano-Drop 2000. cDNA synthesis was performed with 800ng RNA using the SuperScript First-Strand Synthesis System for RT-PCR according to the supplier's protocol.

Reagents	Volume/ concentration
RNA	800ng
dNTP mix (10mM)	1µl
Oligo(dt) 12-18 (0.5µg/µl)	1µl
water, DNase RNase free	ad 10µl
incubate at 65°C for 5min, put subsequently on ice for 1min	
10x RT buffer	2µl
$MgCl_2$(25mM)	4µl
DTT (0.1M)	2µl
RNase OUT	1µl
incubate at 42°C for 2min	
Superscript II RT (50U)	1µl
incubate at 42°C for 50min and subsequently for 15min at 72°C	
RNaseH	1µl
incubate at 37°C for 20min, use immediately or store at -20°C	

2.2.10 Real-time PCR

Real-Time PCR was performed on a 7300 Real Time PCR System using SYBR-green PCR Master mix. Each cDNA probe was measured in triplicates.

Reagents	Volume	PCR cycle	time (min)
2x buffer SYBR green	12.5µl	50°	2min (only at 1st cycle)
primer forward (fwd) (5µM)	3µl	95°C	10min (only at 1st cycle)
primer reverse (rev) (5µM)	3µl	95°C	15sec
water, DNase RNase free	4µl	60°C	1min
cDNA	2.5µl		repeat cycles 40 times
		add dissociation stage	
		95°C	15sec
		60°C	1min
		95°C	15sec

To calculate the gene expression relative to ß-actin, the cycle threshold (C_t) value was determined for each primer pair. The $C_t$value defines the cycle in which the sample fluorescence intensity overcomes the background fluorescence. This value can be used for relative quantification of the sample. Calculation of the relative expression level of the gene of interest (gene x), was performed using the ΔC_tmethod with following equation:

$$\Delta C_t = \bar{x}C_t{}^{\beta-actin} - \bar{x}C_t{}^{gene\ x}$$

The standard deviation was calculated with the following formula:

$$STDEV \triangle C_t = \sqrt{(STDEV\, C_t^{\beta-actin})^2 + (STDEV\, C_t{}^{gene\,x})^2}$$

To compare relative expression levels of different genes, the ΔC_tlevels of the respective genes were normalized to a control treated sample.

$$2^{-\triangle\triangle C_t} \text{ with } \triangle\triangle C_t = \triangle C_t^{control} - \triangle C_t^{gene\,x}$$

The normalized standard deviations were calculated as:

$$+STEDV = 2^{-\triangle\triangle C_t} + STEDV\, \triangle C_t$$

$$-STEDV = 2^{-\triangle\triangle C_t} - STEDV\, \triangle C_t$$

2.2.11 PCR

For Gal-8 full-length PCR 2µl of cDNA was mixed with the Gal-8 PCR primers and added to the Platinum Blue PCR Super Mix. Cycles were performed as suggested by the supplier on a DNA engine Dyad thermal cycler.

Reagents	**Volume**	**PCR cycle**	**time**
Platinum blue PCR Super Mix	45µl	94°C	1min (only at 1st cycle)
cDNA	2µl	94°C	30sec
primer fwd (20µM)	0,5µl	55°C	30sec
primer rev (20µM)	0,5µl	72°C	90sec
water, DNase RNase free	2µl		repeat cycles 30 times
		72°C	10min

Products were loaded on a 2% Agarose gel and run using 1x TAE buffer. Products were visualized using Ethidium Bromide.

2.2.12 Whole genome expression analyses

2.2.12.1 Affymetrix

For whole genome analysis of MM patients and MM cell lines, the Affymetrix protocol was used. The data was obtained from Dr. Dirk Hose (Heidelberg) and used for expression and survival analyses [107, 108, 109, 110].

2.2.12.2 Illumina

Whole genome expression analyses of HUVEC was performed using an Illumina HumanHT-12 v4. RNA was isolated from the cells as described above and processed according to the manufacturers protocol. Raw data were then obtained from the DKFZ Genomics and Proteomics Core Facility and results were analyzed using Chipster software.

2.2.13 Immunoprecipitation

Immunoprecipitation (IP) was performed using the Thermo Scientific Pierce Classic IP Kit. Either $5x10^6$ HUVEC or $2x10^7$ MM cells were lysed in 1x lysis buffer containing protease and phosphatase inhibitors. After 5 min incubation on ice, insoluble cellular debris was removed by centrifugation at 13.000g for 10 min. Protein concentration of the lysate was measured via BCA assay reagent and 1mg protein was used for the IP. The IP was performed according to the manufacturer's protocol using 3µg of anti-Gal-8 antibody (mouse monoclonal). The eluate was used for western blot analysis against Gal-8.

2.2.14 Sodium dodecyl sulfate polyacrylamide gel electrophoresis (SDS-PAGE)

Following the IP, proteins of the whole eluate from the IP (50µl) were separated using 15% SDS-PAGE gels.

Resolving gel reagents	**Volume**	**Stacking gel reagents**	**Volume**
ddH_2O	7.35ml	ddH_2O	6.1ml
1,5M Tris/HCl pH8,8	7.5ml	0,5M Tris/HCl pH6,8	2,5ml
Acrylamide/Bis	15ml	Acrylamid/Bis	1.33ml
TEMED	15µl	TEMED	10µl
APS 10%	150µl	APS 10%	50µl

SDS-Gels were loaded and electrophoresis was performed at 50mA constant in 1x SDS-running buffer.
For multimer gels of recombinant galectins, 2µg protein was loaded using 4x LDS sample buffer on 4-12% MOPS/SDS precast gels.
To determine protein-size, rainbow full range protein marker was loaded on the gels in parallel.

2.2.15 Western Blot analysis

Proteins separated on a SDS-PAGE were blotted on a Immobilion-P membrane using semi-dry blotting technique. The membrane was activated by rinsing with methanol followed by rinsing with transfer buffer 3. Six Whatman paper sheets were soaked with transfer buffer 2 and put on the anode (+) side of a transfer chamber. Three Whatman paper sheets soaked with transfer buffer 3, the Immobilion-P membrane and the SDS gel rinsed with transfer buffer 3 were put on top. These were covered with nine Whatman paper sheets soaked with transfer buffer 1. The cathode (-) was put on top of the filter system. For transfer of proteins to the Immobilion-P membrane, 0,8mA/cm^{2}were applied for 1h.
After the transfer, the membrane was blocked in blocking buffer followed by 5x 10min washing in blotting buffer, incubation with biotinylated anti-Gal-8 antibody at RT for 1 hour. The membrane was washed again 5x10min in blotting buffer and incubated with Streptavidin-POX (1:50.000) followed again by 5 washing steps for 10min each in blotting buffer. The proteins were visualized using a x-ray film processor after incubating the membrane with SuperSignal Chemiluminescent Substrate for 5min.

2.2.16 FACS

For FACS analyses 5x10^5 cells were incubated on ice for 30min with respective antibodies or lectins (table) followed by two washing steps in FACS-buffer. Detection antibodies were incubated for 30min on ice followed by two washing steps in FACS-buffer. Biotinylated antibodies or lectins were detected using Streptavidin-FITC. Primary unconjugated antibodies were detected using a secondary antibody with a fluorescently labeled conjugate appropriate for the species of the primary antibody. For live-dead discrimination of cells, viaprobe (7-AAD) was used. Fluorescence was measured using a BD FACS Canto II. Data was analyzed using FlowJo software.

Lectin / antibody	**concentration / dilution**
biotinylated recombinant Gal-8N	200nM
recombinant Gal-8 (S, L)	200nM
Streptavidin-FITC	1:800
anti-Gal-8 mouse monoclonal	1:100
secondary antibody with a fluorescently labeled conjugate	1:100
primary antibody with a fluorescently labeled conjugate	1:100
biotinylated SNA/MAA/PNA	10µg/ml

2.2.17 ELISA

High binding 96-well plates were coated with 2,5µg/ml anti-Gal-8 antibody (mouse monoclonal) in coating buffer over night at 4°C. The plates were washed three times with washing buffer and blocked for 1h with 1% gelatin in PBS. 50µl of samples were incubated for 2h at room temperature followed by three washing steps using washing buffer. Gal-8 was detected incubating with 0,6µg/ml biotinylated anti-Gal-8 antibody at RT for 1h followed by 0,5µg/ml Streptavidin-horseradish peroxidase (POX) for 20min. Peroxidase-activity was detected using TMB substrate following the manufacturer's instructions. The reaction was stopped using 50µl 2M H_2SO_4. For quantification, increasing concentrations of recombinant protein (Gal-8S) diluted in blocking buffer were used. Readout was performed on a ELISA plate reader (Multiscan EX) with 450nm filters (substrate) and 540nm filters (background).

2.2.18 Tritium-thymidine proliferation assay

Cells were seeded in 96-well plates (MM 2.5x10^4/well; EC and NHDF 1.5x10^3/well) and stimulated with the respective galectin at indicated concentrations for 24h. After the incubated, 1µCi [^{3}H]-thymidine/well were added for 8h. Adherent cells were washed with HEPES (detach kit) and detached with trypsin/EDTA (detach kit) for 10min at 37°C. The 96-well plates were frozen at -20°C and thawn for harvesting at 37°C. Transfer of the cells to filters was performed in a TomTec harvester. After transfer, filters were dried in a microwave oven at 150°C for 2-3min at 600watt. Radiation was visualized using Betaplate Scintillator and read out was performed in a MicroBeta TriLux.

2.2.19 Gap-closure assay

HUVEC were diluted to 3x10^5/ml in ECBM supplemented with 10% fetal bovine serum, 1% HEPES and growth factors. 70µl of the solution were applied in each well of a culture insert for self insertion in a chamber slide (ibi-treat). Cells were allowed to grow for 24h at 37°C, in a 5% CO_2 atmosphere. Then the culture insert was removed and Gal-8 at indicated concentrations was added to the medium. Gap-closure was monitored using a Zeiss Cell Observer.Z1 (objective: 5× / 0.16 EC Plan-NEO Ph1 DIC0) with incubation chamber at 37°C in a 5% CO_2 atmosphere. Pictures were taken every 30min for 24h. Image Analyses was performed using ImageJ software (http://www.le.ac.uk/biochem/microscopy/pdf/Wound%20healing%20assay.pdf).

2.2.20 Tube formation assay

NHDF were seeded in 24-well plates and cultured for 5 days in DMEM supplemented with 10% fetal bovine serum, 1% HEPES and 1% non-essential amino acids. HUVEC were seeded on the confluent NHDF layer and either VEGF-165 (concentrations ranging from 1.25ng/ml to 20 ng/ml) or the test compounds in concentrations as indicated were added to the respective wells. Growth medium including growth factors and test substances was changed at day 3 of co-culture. At day 3 or 7 medium was removed from the co-culture, cells were washed and fixed in ice-cold 70 % ethanol (v/v) for 30 min at RT, followed by a washing step and incubation in methanol/30% H_2O_2, 40:1 (v/v) for 10 min at RT. The cells were washed and incubated with a monoclonal antibody against CD31 (1:40) for 30 min followed by a washing step and incubated with a secondary goat anti-mouse IgG antibody coupled to biotin (LSAB2) for 20 min. After further washing, the cells were incubated for 20 min with streptavidin coupled to horseradish peroxidase (LSAB2). Antibody reactivity was visualized by adding AEC-substrate to the cells for 14 min in the dark. Enzymatic reaction was stopped by washing with water. Wells were sealed with mounting medium and microscopic quantitative analysis (Leica DM IL LED) of tube formation was performed with the software Angiosys 1.0.

2.2.21 Static adhesion assay

HUVEC were seeded in collagen-coated 48-well plates ($1.5x10^4$ cells/well) and grown until confluency for three days. At the day of experiment, medium of HUVEC was removed and 150µl ECBM supplemented with 1% HEPES and 200nM of the respective galectin was added to each well. Calcein stained MM cells were diluted in RPMI supplemented with 1% HEPES and $5x10^4$ cells were added to the HUVEC in a volume of 150µl medium. The final concentration was 100nM galectin/well. Cells were allowed to adhere for 60min at 37°C, in a 5% CO_2atmosphere and carefully washed twice with pre-warmed PBS Ca_2/Mg. 500µl of a mixture with equal volumes of RPMI and ECBM supplemented with 1% HEPES was added and quantitative observation of adherent cells was performed after microscopic observations (Zeiss Cell Observer.Z1 (objective: 5× / 0.16 EC Plan-NEO Ph1 DIC0)) of each well. 2 photos per well were taken and analyzed using the ImageJ software.

2.2.22 Shear stress assay

Pre-cultivation of HUVEC prior to the shear stress experiment was performed according to IBIDIs application note 13 (http://ibidi.com/fileadmin/support/application_notes/AN13_HUVECs_under_perfusion.pdf). Briefly, 2.5 x 10^5 HUVEC were seeded on a µ-Slide $I^{0.6}$ Luer in 150µl endothelial cell basal medium supplemented with 10% FCS and growth factors. After adhesion of cells to the µ-slide, the perfusion set red, filled with 12ml ECBM plus 10%FBS and growth factors, was connected to the µ-slide. Cells were cultured with increasing shear stress for 24h (30min 2dyn/cm^2; 30min 5dyn/cm^2; 23h 10dyn/cm^2). Prior to the shear stress experiment, 5 x 10^6 MM cells were stained with Calcein-green. Cells were resuspended in 25ml RPMI + 25ml ECBM containing 1%HEPES. For each slide, 12 ml cell suspension supplemented with the respective galectin was filled into a white perfusion set. MM cells were perfused at 1dyn/cm^2 for 30min and subsequently for 10min at 5dyn/cm^2. Images were taken on 4 different positions on each slide every 30sec using a Zeiss Cell Observer.Z1 (objective: 5× / 0.16 EC Plan-NEO Ph1 DIC0). Adherent cells were counted after microscopic observation using ImageJ.

2.2.23 Thermophoresis

Galectins were stained with a red fluorescent dye using nanotempers Protein Labeling Kit RED-NHS according to the manufacturer's protocol. 10µM of the respective galectin was mixed with 30µM of dye and incubated for 30min at RT in the dark. A gravity column removed free dye from the labeled protein. For MST-measurement, the labeled protein was kept constant at low concentrations (25nM) and mixed with increasing concentrations of the unlabeled protein in MST-optimized buffer. Measurements were performed in hydrophilic capillaries on a NanoTemper Monolith NT.115 (60% LED; 40% IR-laser power). The curves were fitted with Hill kinetics to obtain an EC_{50} and the dissociation constant for each Galectin. The software IGOR pro was used for the fitting of the graphs.

2.2.24 Static light scattering

Static light scattering was performed by Vladimir Rybin (EMBL, Heidelberg). Static light scattering (SLS) experiments were performed on a Viscotek TDAmax system, equipped with Superdex 200 HR 10/30 column. As a mobile phase 1xMST buffer without BSA and Tween-20 was used with a flow rate of 0.4 ml/min.

2.2.25 Gal-8 modeling

The calculation as well as the description of the method were performed by Sonu Kumar, Sanford-Burnham Medical Research Institute, San Diego.
The starting structures of short and long linker Gal-8 were retrieved from ModBase server [111] using their fasta sequence. Gal-8 long linker structure used PDB ID: 3VKL [112]where as short linker used PDB ID: 4HAN [113] as template for modeling. The template structure for linker is not available so it remained as extended loop between N- and C- domains. To explore the structure of linker molecular dynamics simulations were performed on both the Gal-8 structures along with linker in explicit solvent for 25 ns. For the simulations, the AMBER force field ff99SB was used for the protein [114]. The structures were solvated in a box of TIP3P water using periodic boundary conditions. Firstly, energy minimization was carried out for removal of initial unfavorable contacts made by the solvent using 10000 minimization cycles (500 steps of steepest descendent and 500 steps of conjugate gradient) keeping protein backbone atoms restrained. Then, protein side chain atoms and explicit water molecules were kept unrestrained followed by unrestrained minimization with 20000 cycles of the whole system. Secondly, the equilibration of the system was carried out by heating the system slowly from 0 to 300 K for 300 ps, followed by 500 ps of maintaining 300 K constant temperature at constant pressure of 1 atm. Then finally, production of dynamics were performed at 300 K for 25 ns using a 2-fs time step, with the SHAKE algorithm at constant pressure of 1 atm. During the simulations, SHAKE algorithm was turned on and applied to all hydrogen atoms and the particle-mesh Ewald method was used for treating the electrostatic interactions with a cutoff of 10 Å. Minimization, equilibration, and production phases were carried out by the SANDER module of AMBER 8.

2.2.26 Statistics

2.2.26.1 General

If not indicated otherwise, Prism 5 was used to calculate statistics. Figures depict mean +/- standard error of the mean (SEM). T-test was performed with the parameters: unpaired t-test, two-tailed, 95% confidence intervals. * $p<0,05$ / ** $p<0,01$ / *** $p<0,001$

2.2.26.2 Illumina Array

The expression data were normalized and log2 transformed by the Chipster software. Heatmap analyses were performed using the standard settings for annotated heatmap analyses in Chipster.

2.2.26.3 Affymetrix Array

Expression data were gcrma-preprocessed and log2 transformed. From 6 Gal-8 specific probesets, probeset 2 was chosen for further analyses, since it showed best correlation to overall survival. The probeset was validated by an independent cohort of patients treated within the total therapy 2 (TT2) or total therapy 3 (TT3) protocol [115, 116].
Survival analyses (Kaplan-Meyer) were performed according to standard settings of the software Prism 5.

3

Results

3.1 Gal-8 expression in MM and correlation to the progression of the disease

It has been shown before that Gal-8 expression is altered in various types of cancers in comparison to the corresponding healthy tissue. Depending on the tumor, Gal-8 is either increased or decreased in the progression of the disease [64, 65, 74, 87, 89, 90, 91, 92, 93]. No analyses are yet available which investigate the role of Gal-8 in MM. In order to explore the role of Gal-8 in MM disease, I examined the expression of the protein in patients serum and MM cells isolated from bone marrow biopsies. The expression was correlated to patients' survival by Kaplan-Meyer analysis and chromosomal aberrations common in MM in order to find out if Gal-8 is a prognostic marker for MM progression and disease.

3.1.1 Gal-8 in serum of MM patients

First, Gal-8 serum-levels of MM patients were measured by an ELISA (Figure 3.1). The Gal-8 level in sera of MM patients was higher compared to that of age-matched healthy donors (HD) (Figure 3.1 A). Only 22.2% (2/9) of HD in contrast to 45% (19/42) of MM patients had Gal-8 protein present in their serum. HD did not display elevated Gal-8 levels above 0.23ng/ml Gal-8, whereas Gal-8 levels in patients' serum had a maximum of 1.33ng/ml total protein content. It was not possible to perform extended statistical analysis on the data since too many patients as well as HD do not express Gal-8. This leads to a high variance within the expression data.

Subdivision of the patients' sera with regards to secreted protein showed that MM patients producing Bence-Jones (BJ) protein have the highest mean Gal-8 expression level compared to HD. The highest measured values were in patients with IgG seroprotein (Figure 3.1 B).

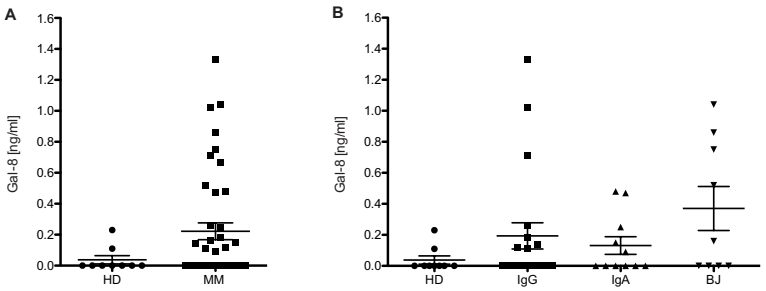

Figure 3.1: Gal-8 serum levels in MM patients compared to healthy donors
Gal-8 serum levels were measured in sera of 42 MM patients and compared to sera of 9 HD. The mean age of the MM patients was 55,95+/-8,35 years (39-70), the mean age of HD was 58.6+/-6.2 years (48-68years) A: The mean Gal-8 serum level was higher in patients compared to HD. B: Subdivision of MM sera according to types of secreted protein showed elevated levels of Gal-8 protein in all serotypes and the highest in IgG. The graph shows mean Gal-8 concentration +/-SEM.

3.1.2 Gal-8 expression in the progression of MM

MM development is accompanied by many genetic changes from the pre-stage MGUS which is defined by irregular serum protein in blood or urine. The mechanisms and how and why MGUS proceeds to a fully established MM are unclear. Gene expression data from BM biopsies of patients with MGUS, previously untreated MM and healthy normal donors were analyzed focussing on Gal-8 expression. Microarray analyses of gene expression profiles revealed that Gal-8 expression did not change significantly during the disease progression (Figure 3.2), but some patients showed elevated levels of Gal-8 transcription higher than the maximum gene expression in HD. Although the mean mRNA expression level is comparable, the range was higher in MM (min: 2.46; max: 8.74) than in HD (min: 5.37; max: 7.44).

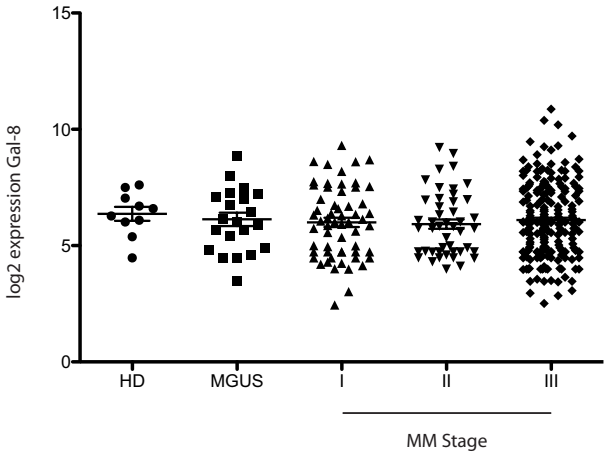

Figure 3.2: Gal-8 expression in MM patients compared to healthy donors
Microarray analyses of Gal-8 gene expression profiles in MGUS (n=22), MM stage I (n=59), stage II (n=46) and stage III (n=226) were compared to HD (n=10). There was no significant change in the Gal-8 expression during the disease progression, but the range of expression was higher in MM patients than in HD.

3.1.3 Gal-8 expression is correlated to over-all survival in MM patients

Next, I tested the prognostic value of Gal-8 expression with regard to MM progression by Kaplan-Meier survival analysis. Patients were classified in Gal-8^{high} and Gal-8^{low} using a median cut of the expression values (median=6.063+/-0.08). The over all survival (OAS) analysis showed that Gal-8 expression negatively correlates with survival of patients (Figure 3.3 A). The survival data was validated by two independent cohorts treated within the total therapy 2 (TT2) [115] or the total therapy 3 (TT3) [116] protocol (Figure 3.3 B, C).

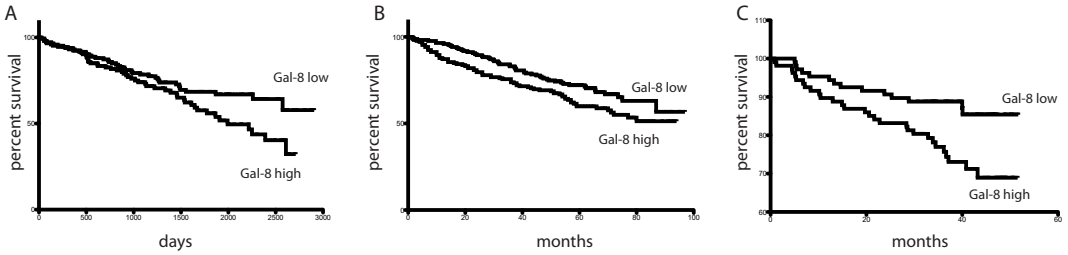

Figure 3.3: OAS of Gal-8 high vs. Gal-8 low patients
The prognostic value of Gal-8 expression for OAS was tested. Median cut was performed to distinguish Gal-8^{high} and Gal-8^{low} expressing patients. A: OAS of the test cohort showed a longer survival for patients with low Gal-8 expression (* p=0.0406). B: the data was validated on the TT2 dataset (* p=0.0435) and C: on the TT3 dataset (** p=0.0108).

The correlation of Gal-8 expression with OAS could also be confirmed with regard to the event-free survival (EFS) of the patients (Figure 3.4 A). Gal-8^{high} patients progress faster to the disease stage I than Gal-8^{low} patients. The EFS data was also validated by the TT2 and TT3 cohort (Figure 3.4 B, C).

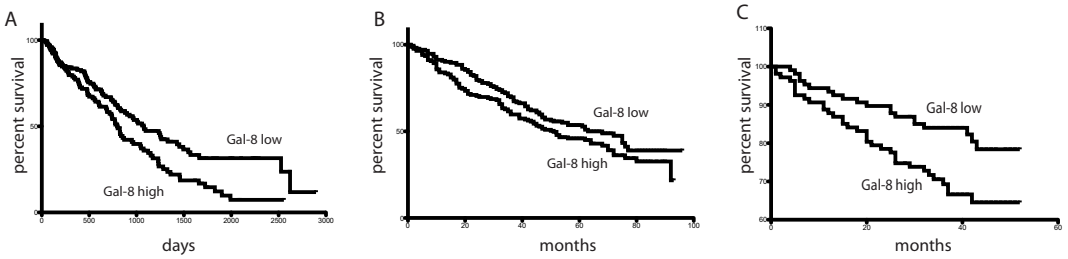

Figure 3.4: EFS of Gal-8 high vs. Gal-8 low patients
The prognostic value of Gal-8 expression for EFS was tested. Median cut was performed to distinguish Gal-8^{high} and Gal-8^{low} expressing patients. A: EFS of the test cohort showed a slower progression to stage I for patients with low Gal-8 expression (* p=0.047). B: the data was validated on the TT2 dataset (p=0.0873) and C: on the TT3 dataset (* p=0.0149).

MM is characterized by many chromosomal aberrations. Main mutations found in MM patients are gain of 1q21, the loss of 13q14 or the chromosomal translocation

t4;14. Correlation analyses showed, that Gal-8 expression is significantly higher in patients with a gain in 1q21 (Figure 3.5 A), a loss in 13q14 (Figure 3.5 B) or a translocation in t4;14 (Figure 3.5 C).

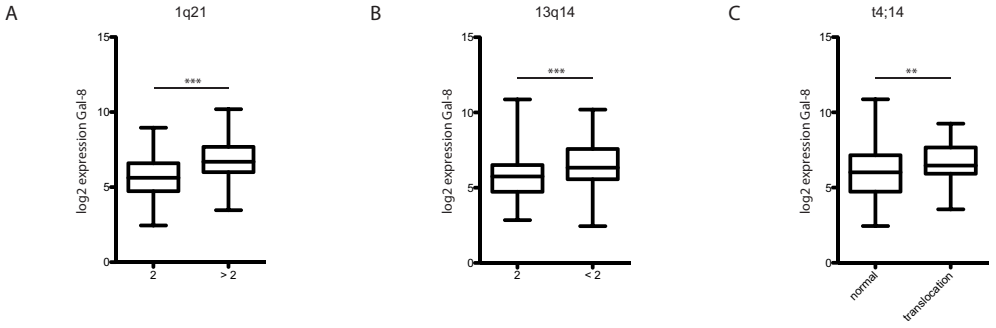

Figure 3.5: Gal-8 expression correlated to chromosomal aberrations
Gal-8 expression was plotted as log2 gene expression and correlated to A: 1q21 gene copy number B: 13q14 gene copy number and C: t4;14 translocation. All three chromosomal aberrations showed a significant up regulation of Gal-8 expression.

As further chromosomal abnormalities I analyzed translocation t11;14 and 17p deletion. These chromosomal aberrations did not show a significant change in Gal-8 gene expression.

The patients' data indicate that Gal-8 might play a role in MM progression. In order to investigate the influence of Gal-8 on MM disease progression on the molecular level, several *in vitro* angiogenesis and homing assays were performed analyzing the role of Gal-8 in MM.

3.2 Gal-8 expression in cell lines of MM and endothelial origin

For *in vitro* studies on synthesis and expression of Gal-8 in MM, Gal-8 transcription levels were measured in different cell lines of MM origin [117]. Microarray analysis of these cell lines revealed that Gal-8 expression is very heterogenous among them (Figure 3.6 A). This heterogeneity is also reflected in patients' data on the Gal-8 transcription level (Figure 3.6 B), from the 332 patients analyzed, the mRNA transcription levels varied among them. This very heterogenous gene expression is known for many proteins in MM [118, 119].

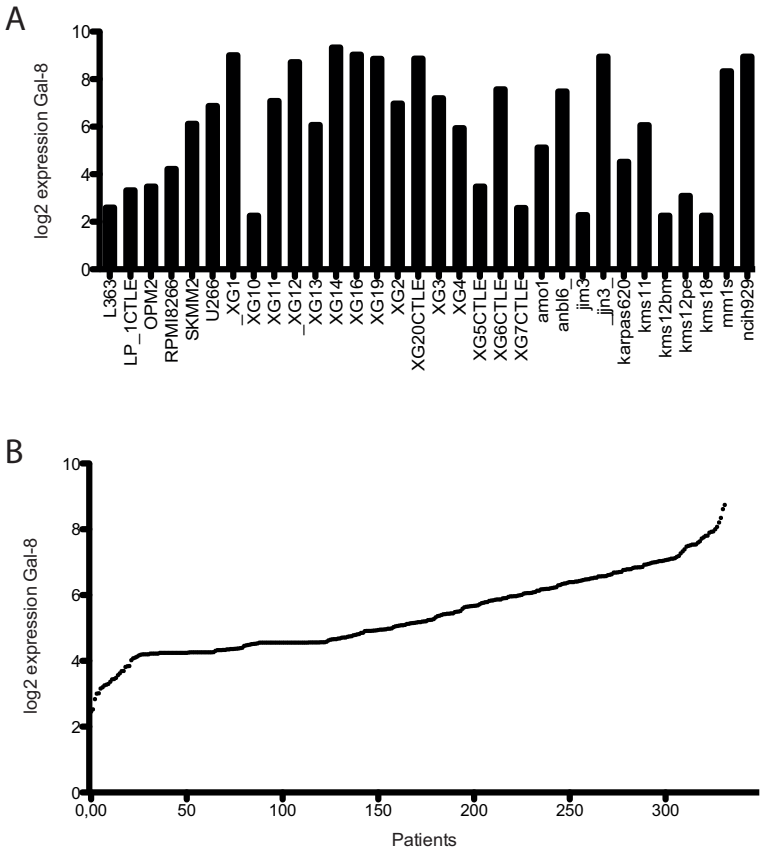

Figure 3.6: Gal-8 expression in several MM cell lines and 332 MM patients
Microarray analyses showed, that Gal-8 expression is very heterogenous in several MM cell lines (A) as well as in MM patients (B).

For further detailed analyses in this study, two different MM cell lines, the Gal-8 positive cell line MOLP-8 and the Gal-8 negative cell line LP-1, were chosen. Additionally, the endothelial cell line HBMEC-60 and primary endothelial cells (HUVEC) were included in this study. A qRT-PCR was performed to study the Gal-8

mRNA expression level of those cell lines (Figure 3.7 A). MOLP-8, as well as the endothelial cells express Gal-8 in contrast to the MM cell line LP-1. To determine if both isoforms (short and long linker) of Gal-8 are expressed, a PCR spanning the linker region was performed using the same mRNA isolates. The PCR showed, that both isoforms are expressed in MOLP-8 and the endothelial cells (Figure 3.7 B). In contrast to EC, MOLP-8 expressed more Gal-8S than Gal-8L on the mRNA level.

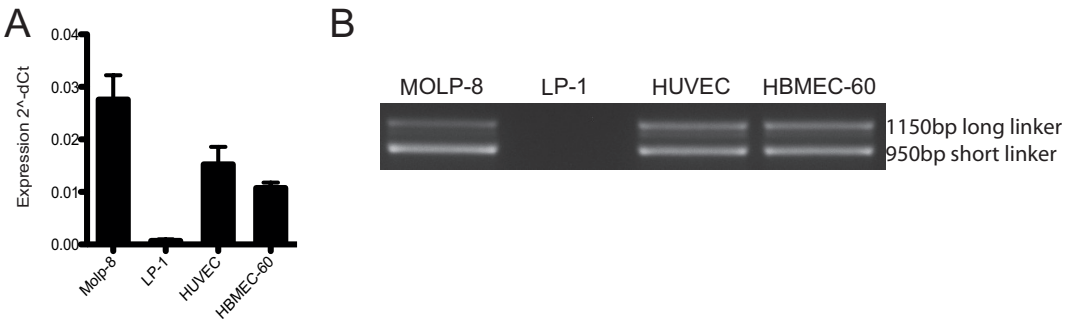

Figure 3.7: PCR analyses of Gal-8 expression in the different cell lines used in this study
A: Quantitative levels of Gal-8 expression were obtained using real-time PCR. MOLP-8 as well as both ECs express Gal-8 whereas the MM cell line LP-1 is Gal-8 negative B: To detect the expression of the different isoforms, PCR spanning the linker region was used. For the short-linker isoform a product with 950bp is expected, for the long-linker isoform a product with 1150bp. Both isoforms are expressed by MOLP-8 and the EC.

Protein levels of cells expressing Gal-8 were examined by Western blot analysis. Since protein levels are very low, an IP was performed prior to the Western blot. MOLP-8 as well as the ECs express Gal-8 protein (Figure 3.8 A). However, MOLP-8 expresses lower amounts of Gal-8L compared to Gal-8S, as it has also been seen on the mRNA level. A quantitative ELISA revealed that the cells were able to secrete Gal-8 into the supernatant (Figure 3.8 B), but it is not possible to define which isoform since the amount of protein was under the detection limit of the Western blot.

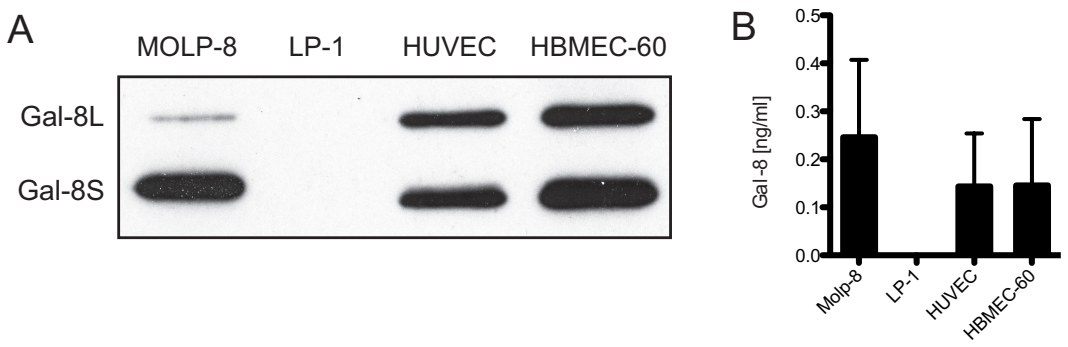

Figure 3.8: Gal-8 protein levels in cell lysates and cell culture supernatants of MM and EC
A: Western blot against Gal-8 protein after an IP of whole cellular lysates. The MM cell line MOLP-8 expressed Gal-8S stronger than Gal-8L. LP-1 was Gal-8 negative. HUVEC and HBMEC-60 express both isoforms in comparable amounts. B: Anti-Gal-8 ELISA of conditioned supernatants. MOLP-8 as well as both EC cells were able to release Gal-8 into cell culture supernatants. Representative data of three independent experiments is shown for the IP, cumulative data of three independent experiments is shown for the ELISA.

3.3 Binding of lectins to cell lines of MM and endothelial origin

Gal-8 is a lectin binding β-galactosides. The C-CRD prefers polyLacNac, blood group A and B structures, whereas the N-CRD recognizes lactosaminyl structures, but also sialylated and sulfated oligosaccarides [97]. It is noticeable that the N-CRD has in general a higher affinity to carbohydrate binding partners than the C-CRD [97].

3.3.1 Binding of SNA, MAA and PNA to MM and EC

The lectins PNA, MAA and SNA were used for MOLP-8 and LP-1 staining in order to compare the glycan structures important for Gal-8 binding expressed on the cell surface. Both, α2,3 as well as α2,6 sialylated structures are present on both cell lines as indicated by SNA and MAA binding. Stronger SNA staining indicates more α2,6 sialylated structures on both MM cell lines. PNA binds stronger to MOLP-8 than to LP-1, indicating more terminal galactose-containing carbohydrates, in particular those with a terminal Galβ1-3GalNac on MOLP-8 cells (Figure 3.9).

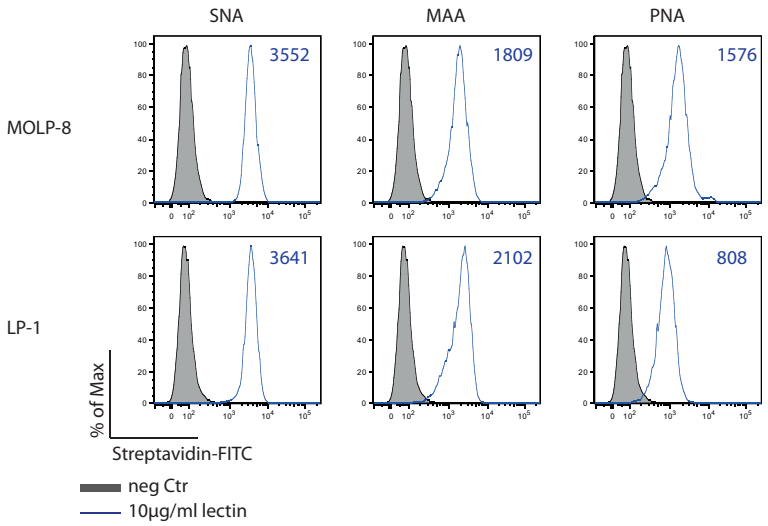

Figure 3.9: Binding of SNA, MAA and PNA to MM
MM were incubated with 10µg/ml of the indicated biotinylated lectins and binding was measured via FACS analyses. SNA, MAA and PNA were able to bind both MM cell lines. The median fluorescence intensity (MFI) is indicated in each histogram.

The same FACS experiment was performed on EC. HBMEC-60 have less α2,3 than α2,6 sialylated structures detectable on their surface. This is in contrast to HUVEC, which bind MAA better than SNA, indicating more α2,3 sialylation. But in general, HUVEC have less sialylated structures on their surface compared to HBMEC-60.

PNA, is also able to bind both EC, but HUVEC stronger than HBMEC-60 (Figure 3.10).

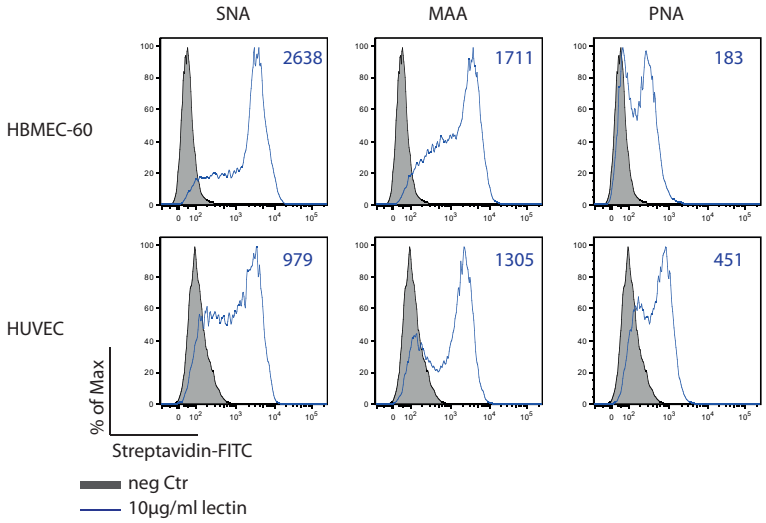

Figure 3.10: Binding of SNA, MAA and PNA to EC
EC were incubated with 10µg/ml of the indicated biotinylated lectins and binding was measured using FACS analyses. SNA, MAA and PNA were able to bind both EC cell lines. The MFI is indicated in each histogram.

3.3.2 Binding of different galectins to MM and EC

The ability of biotinylated Gal-1, -2, -3, -4, -8S and -9 to stain MM and EC cells was compared by flow cytometry. Gal-1 and -2 are prototype, Gal-3 is chimeric and Gal-4, -8S and -9 are tandem-repeat galectins. The median fluorescence intensity (MFI) was measured to compare the binding of the different galectins (Figure 3.11). Gal-1, -2, -3, -8S and -9 bound both EC. The strongest MFI was detected for Gal-8S in both, HUVEC and HBMEC-60. Differential staining was only observed for Gal-3 which bound strongly to HBMEC-60, but much weaker to HUVEC. In general, the affinity of the different galectins was weaker on MM. Gal-3 and Gal-8S were able to attach to both MM cell lines, binding of Gal-1 and -2 was only slightly above background fluorescence. Gal-4 was not able to recognize any cell line tested.

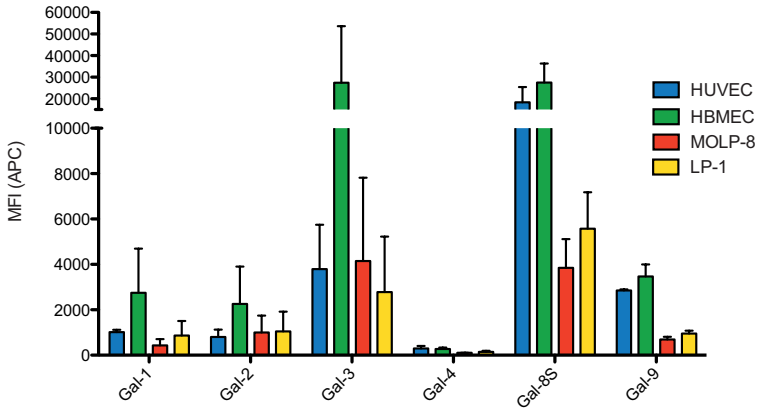

Figure 3.11: Binding of several galectins to cells of MM and endothelial origin
Binding of 1µg of the indicated biotinylated galectin to the endothelial cells HUVEC or HBMEC-60 or to the MM cell lines MOLP-8 and LP-1. EC as well as both MM cell lines bound strongest to Gal-3 and Gal-8S. Binding of Gal-8S was stronger of EC then of MM.

Gal-8 and Gal-3 have been the strongest binders to both, MM and EC, among all galectins tested in this study. As the influence of Gal-8 on MM and EC is the aim of this study, further analysis have been performed using also the long-linker isoform and the N-CRD of Gal-8.

3.3.3 Binding of Gal-8 to MM and EC

For the binding-analysis of both Gal-8 isoforms and the single N-terminal domain, I performed dose response tests to define the optimal concentration. For this initial experiment, HBMEC-60 and MOLP-8 were chosen. For further analysis, 200nM Gal-8 were used as an optimum concentration for both isoforms as well as for the N-terminal domain (Figure 3.12). The binding of the single C-terminal CRD could not be measured, because the biotinylated C-CRD was not available. The production of the single C-CRD is technically difficult and the low amount of protein I obtained was used for thermophoresis experiments (see below section Gal-8 multimerization).

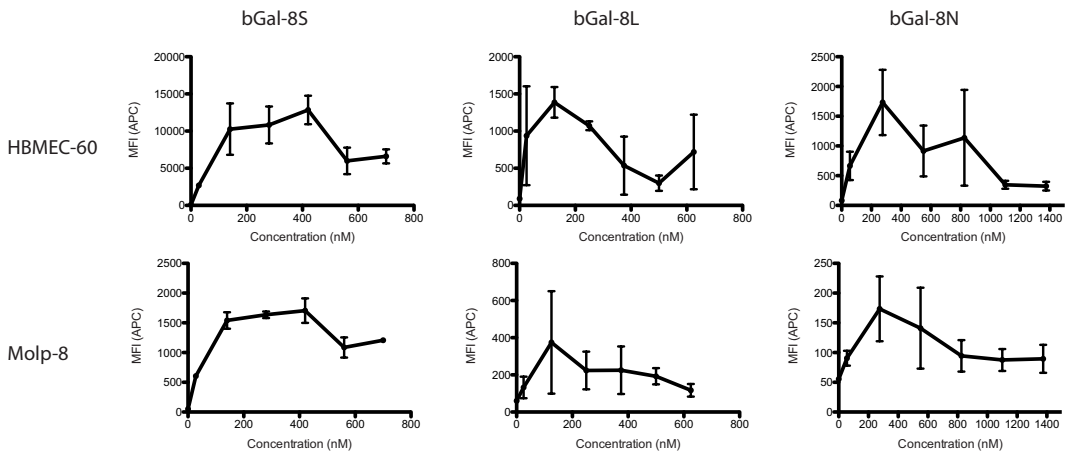

Figure 3.12: Concentration curves Gal-8 binding
HBMEC-60 and MOLP-8 cells were incubated with increasing concentrations of biotinylated Gal-8S, Gal-8L and Gal-8N in order to determine the optimal protein concentration for binding analyses. The binding was concentration dependent and an optimum for both cell lines and all Gal-8 isoforms was around 200nM.

The binding of both Gal-8 isoforms as well as the single N-terminal domain (Gal-8N) was tested by flow cytometry. For this purpose, 200nM of Gal-8S, Gal-8L or the biotinylated Gal-8 N-terminal CRD were incubated with either LP-1 or MOLP-8 cells. Both isoforms were able to recognize both MM cell lines (Figure 3.13). The N-terminal domain alone bound only LP-1, the staining of MOLP-8 was hardly above the fluorescence intensity of the negative control. The binding could be inhibited by addition of 100mM lactose, indicating that the binding of Gal-8 to MM cells is dependent on the cell surface expressed glycan structures. It is noticeable that Gal-8 bound LP-1 generally stronger than MOLP-8.

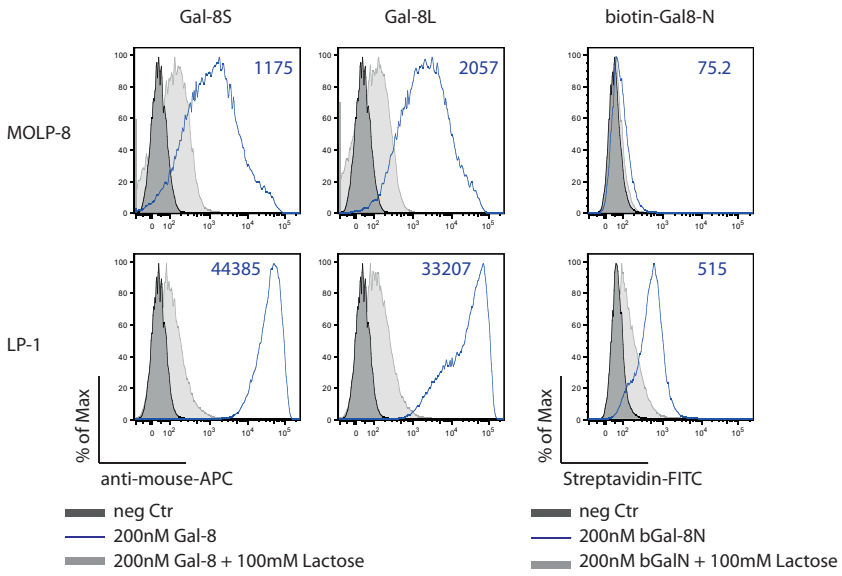

Figure 3.13: Binding of Gal-8 to MM cells
Binding of both Gal-8 isoforms and the N-terminal domain was investigated by incubation of the cells with 200nM of the respective recombinant Gal-8 protein followed by cytofluorographical analysis. Representative analyses of three independent experiments are shown. The MFI of bound Gal-8 is indicated in each histogram.

Also, Gal-8 binding efficiency to EC was measured showing that the two Gal-8 isoforms as well as the N-terminal domain were ably to bind both EC types (Figure 3.14). The binding was stronger to HUVEC than to HBMEC-60 and inhibited by addition of 100mM lactose indicating that the interaction is mediated by protein-glycan recognition and not by protein-protein interactions as already observed with MM cells.

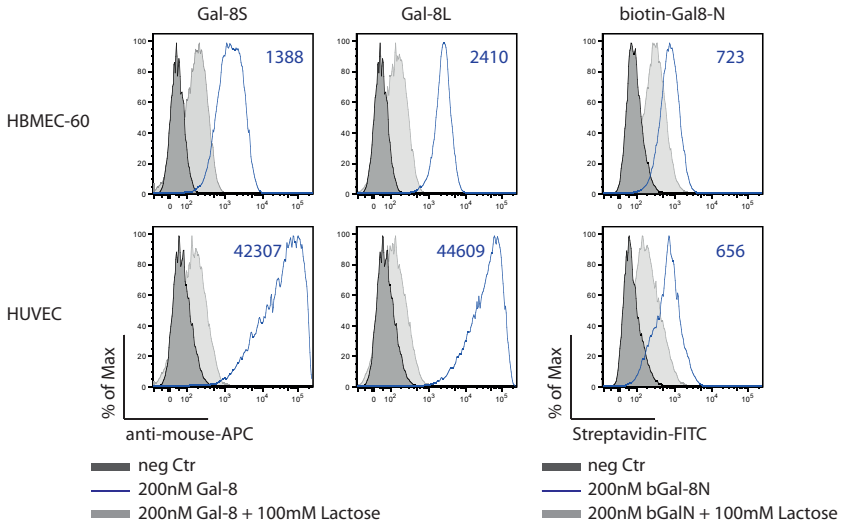

Figure 3.14: Binding of Gal-8 to EC
Binding of both Gal-8 isoforms and the N-terminal domain was investigated by incubation of the cells with 200nM of the respective protein followed by cytofluorographical analysis. Representative analyses of three independent experiments are shown. The MFI of bound Gal-8 is indicated in each histogram.

3.3.4 Gal-8 binding after VCN-treatment

VCN-treatment reduces terminal N-acetylneuraminic acids linked in α2,3-, α2,6-, or α2,8 fashion. As the Gal-8 N-terminal CRD prefers α2,3 sialylated structures for binding, VCN treatment on intact cells should reduce Gal-8N binding.

The effectiveness of VCN-treatment was exemplarily checked on MOLP-8 cells by SNA, MAA and PNA staining (Figure 3.15).

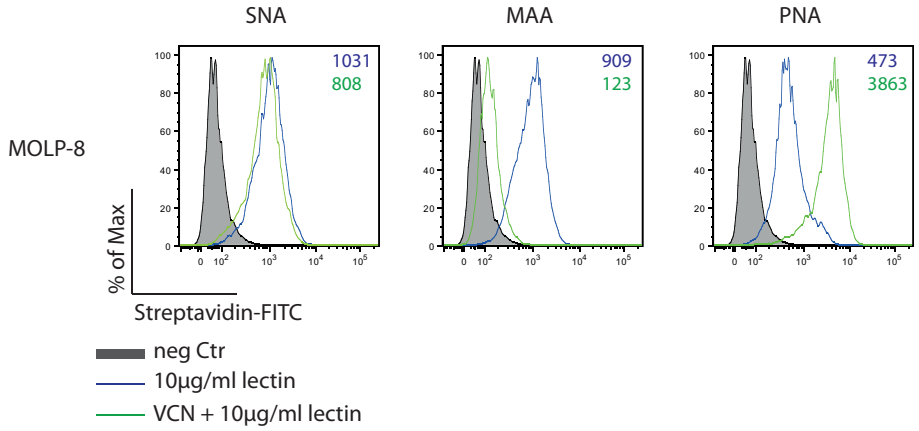

Figure 3.15: VCN treatment of MOLP-8
Cells were treated with VCN for 1h at 37°C and SNA, MAA and PNA binding was measured subsequently. The MFI of bound lectin is indicated in each histogram.

As expected, SNA and MAA binding is decreased after VCN-treatment, accordingly PNA staining increases. Terminal Galβ1-3GalNac are often masked by sialylation preventing PNA binding. It was remarkable that SNA-binding was only slightly altered indicating only a slight decrease of α2,6-sialylation, whereas MAA-binding was almost completely abolished showing an almost complete removal of α2,3-sialylation by VCN. Another explanation for this phenomenon is the possibility that α2,6 sialylated surface structures are not sterically available for the enzyme.

In order to determine whether Gal-8 binding is dependent on the sialylation of MM or EC, a Gal-8 staining was performed after VCN-treatment of the different cell lines (Table 3.1).

	MOLP-8		LP-1		HUVEC		HBMEC-60	
	UT	**VCN**	**UT**	**VCN**	**UT**	**VCN**	**UT**	**VCN**
Gal-8S	15,877*	34,141	28,158	18,934	56,130	32,217	32,957	24,050
Gal-8L	17,601	20,677	32,957	17,779	63,203	46,683	33,628	21,473
bGal-8N	260	225	149	126	467	228	511	153

Table 3.1: Impact of VCN treatment on Gal-8 binding
*Binding of Gal-8 is indicated by MFI values. UT=untreated, VCN=treated with VCN for 1h at 37°C

VCN-treatment reduces Gal-8S and Gal-8L binding on the cell surface of EC, pointing out the affinity of both isoforms to α2,3 sialylated structures, as α2,6 sialylation can not be recognized by Gal-8N [95]. On the MM side, LP-1 and MOLP-8 differed after VCN-treatment. Desialylation reduced binding of Gal-8 to LP-1, but increased binding on MOLP-8 indicating a difference in surface glycosylation of the two MM cell lines.

The MFI for Gal-8N binding was remarkably lower than the MFI for the full-length protein. This is possibly due to the biotinylation of the N-CRD leading to a lower affinity of the protein. Unbiotinylated Gal-8N can not be detected by the monoclonal antibody, as the full length protein, since the antibody binds an epitope in the C-CRD. Binding of the N-terminal domain is not altered after desialylation on the MM cell lines but decreases on both EC types. This points to the possibility, that EC are preferred targets for the N-CRD and MM cells might be preferably bound by the C-CRD.

3.4 Influence of Gal-8 on (tumor-) angiogenesis

The formation of new blood vessels is a tightly regulated process involving several signaling pathways and cell-cell interactions. In MM, tumor angiogenesis is a crucial step for the development and progression of the disease. MM cells are able to promote angiogenesis, a higher microvessel density in the BM of patients is a marker for faster progression [24]. Previously, Gal-8 has been described to be a pro-angiogenic factor [101]. I performed several *in vitro* angiogenesis assays in order to examine in more details whether Gal-8 induces angiogenesis.

3.4.1 Influence of Gal-8 on proliferation of EC and fibroblasts

The endothelium is usually quiescent after the formation of a vasculature. After pro-angiogenic stimuli, such as hypoxia, EC start to proliferate to form new blood vessels [14]. The influence of recombinant Gal-8 on EC proliferation was measured using a [^{3}H]-tymidine-incorporation assay. Neither Gal-8S nor Gal-8L had significant influence on the proliferation of HUVEC, solely the N-terminal domain at 0.5µM had negative effects on the proliferation (Figure 3.16 A). For HBMEC-60, both isoforms had a slightly positive effect on proliferation at 0.5µM. The N-terminal domain had, as seen before in HUVEC, a negative effect on proliferation (Figure 3.16 B).

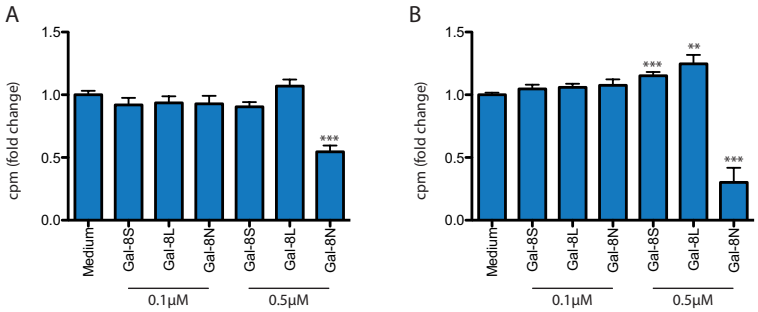

Figure 3.16: Influence of Gal-8 on proliferation of EC
EC were stimulated for 24h with the indicated concentration and isoform of Gal-8 prior to the addition of [^{3}H]-thymidine for 8h. Graphs show the proliferation of HUVEC (A) or HBMEC-60 (B) compared to medium control. 0.5µM Gal-8S and -8L have pro-proliferative effects on HBMEC-60, whereas 0.5µM of the N-terminal domain has negative effects on the proliferation of both EC. Cumulative data of three independent experiments are shown.

Besides EC, fibroblasts were used as feeder cells in the tube formation assay (see below) and ECM-derived components play a critical role in EC lumen formation [120]. Addition of Gal-8 did not significantly influence the proliferation of fibroblasts. (Figure 3.17).

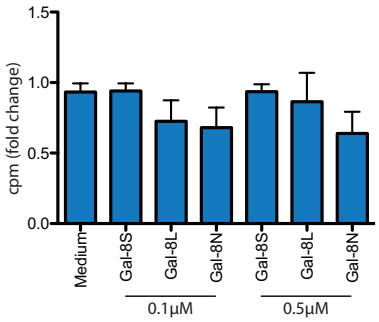

Figure 3.17: Influence of Gal-8 on proliferation of fibroblasts
Fibroblasts were treated as described above (Figure 3.16). The graph shows the proliferation of fibroblasts compared to medium control. No effects of Gal-8 on fibroblasts was observed. Cumulative data of three independent experiments is shown.

For further angiogenesis-experiments, HUVEC were used. Although HBMEC-60 cells were originally isolated from the bone marrow and are derived from a typical microenvironment of MM, they can not be used for the tube formation assay. For reasons not clearly understood the retrovirally immortalized HBMEC-60 have lost the capability to form tubes *in vitro.* HUVEC are a primary cell line and are therefore more suitable for angiogenesis assays.

3.4.2 Influence of Gal-8 on EC migration

Another mechanism influencing the formation of new blood vessels is the ability of EC to migrate. In the course of sprouting angiogenesis, EC line up and follow a tip cell to built a new blood vessel [14]. The influence of recombinant Gal-8 on EC migration was analyzed using a gap closure assay. For this purpose, HUVEC were seeded in IBIDI cell culture inserts and grown until confluency. The inserts were removed leaving a gap in the confluent HUVEC layer and Gal-8S or Gal-8L were added in different concentrations (0.1µM or 0.5µM) to the medium. Photos were taken every 20min for 10 hours and the percentage of uncovered area was calculated. Neither Gal-8S nor Gal-8L had a significant influence on the migratory potential of HUVEC (Figure 3.18).

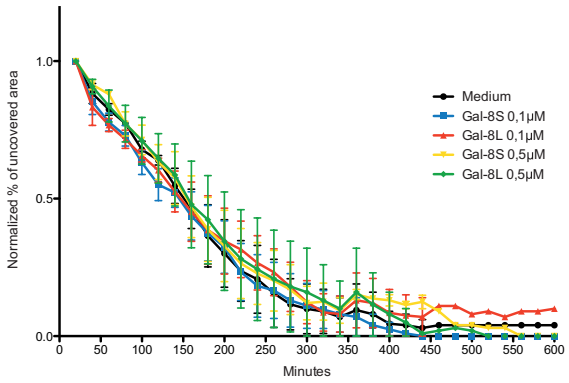

Figure 3.18: Influence of Gal-8 on wound healing
HUVEC were seeded in IBIDI cell culture inserts and grown for 24h and cell migration after addition of indicated amounts of Gal-8 was monitored using a Zeiss Cell Observer. The percentage of uncovered area, dependent on the time after removal of the insert, was measured using the ImageJ program. Addition of Gal-8 to the culture medium did not affect HUVEC migration. Cumulative data of three independent experiments is shown, mean+/-SEM is depicted.

3.4.3 Influence of Gal-8 on *in vitro* tube formation

Former studies on the influence of Gal-8 on angiogenesis used the matrigel-assay which is rather a network-formation assay than a 3D angiogenesis assay in which tube formation can be observed [101]. Therefore, a tube formation assay was performed which consists of a co-culture based on a fibroblast-feeder layer and ECs seeded on top. Addition of VEGF-165 to the co-culture was used as a positive control for tube formation. Tubes were visualized by CD31 staining (Figure 3.19).

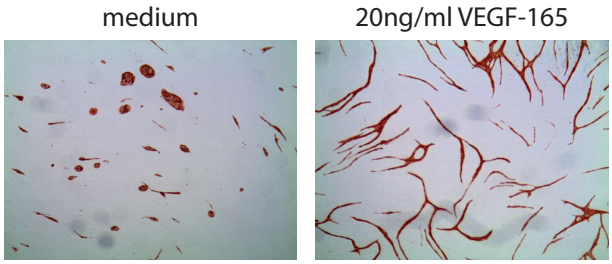

Figure 3.19: Tube formation assay
EC were cultured on top of a fibroblast feeder layer and tube formation was induced with 20ng/ml VEGF-165. Tubes were visualized by staining of CD31. VEGF-165 was able to induce tube formation on the HUVEC. The figure shows representative pictures of three independent experiments.

The angiogenic potential of Gal-8 was tested by the addition of the lectin to the co-culture. Tube formation was quantified by counting the number of tubes. Incubation of the fibroblast-EC co-culture with 0.1µM Gal-8 in addition to VEGF-165 for three

or seven days did not lead to any significant increase in tube formation (Figure 3.20 A, B).

Using 0.5µM Gal-8 without parallel application of VEGF-165, a slight increase in tube formation was observed after 3 days of the co-culture for Gal-8S. But this effect was lost again after seven days (Figure 3.20 C, D). Gal-8 in combination with VEGF-165 did not lead to any positive effect on tube formation.

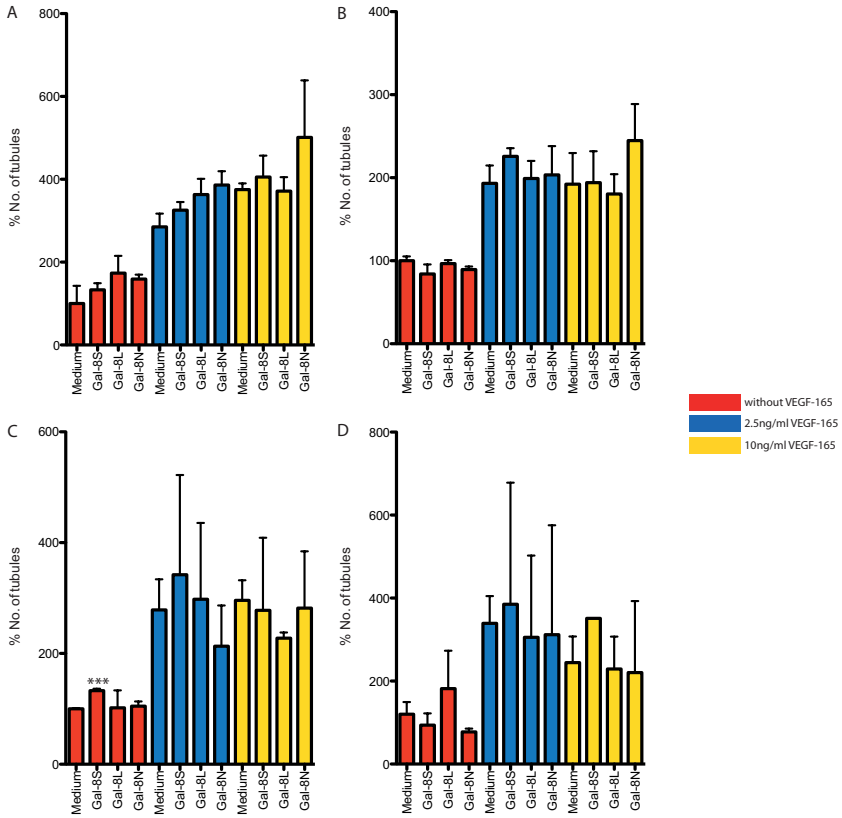

Figure 3.20: Tube formation assay
Fibroblast were seeded and grown till confluency prior to the addition of endothelial cells. No VEGF-165 (red bars), 2.5ng/ml VEGF-165 (blue bars) or 10ng/ml VEGF-165 (yellow bars) were applied in parallel with 0.1µM (A, B) or 0.5µM (C, D) of the indicated Gal-8 isoform. The cells were cultured for either 3 days (A, C) or 7 days (B, D). Tubes were visualized by CD31 staining, the tube formation was quantified by counting the number of tubes per picture using the software Angiosys. A slight increase in tube formation was seen after three days using 0.5µM Gal-8S without parallel application of VEGF-165. Addition of lower concentrations of Gal-8S or the other isoforms did not increase tube formation. Cumulative data of three independent experiments is shown.

Summarizing all results of the angiogenesis experiments, no pro-or anti-angiogenic effect was observed for Gal-8. There was only a slight effect of Gal-8S in high concentration on the tube formation potential of HUVEC, but there was no clear pro-angiogenic effect detectable.

3.5 Gal-8 in MM biology

Besides tumor-angiogenesis, MM proliferation and homing of the tumor cells into the bone marrow play crucial roles in the development of the disease. Since Gal-8 has been shown to influence adhesion processes by binding to integrins in other cell lines [75, 76, 77, 78], the effect of Gal-8 on MM proliferation and homing was examined.

3.5.1 Influence of Gal-8 on proliferation of MM

Massive proliferation of MM cells in the BM leads to a rapid progression of the disease. A [^{3}H]-thymidine proliferation assay was performed investigating the influence of Gal-8 on MM proliferation. MM cells were seeded and treated with 0.1µM or 0.5µM of the indicated Gal-8 for 24h. For both cell lines tested, Gal-8N at high concentrations had a negative effect on proliferation (Figure 3.21). For LP-1, Gal-8S had a slightly positive effect on proliferation (Figure 3.21 B).

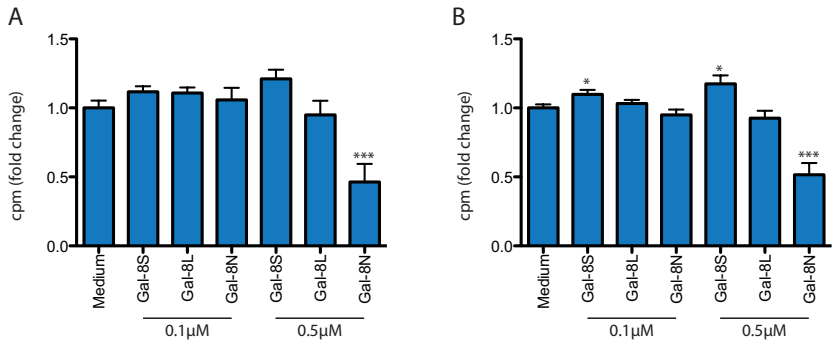

Figure 3.21: Influence of Gal-8 on proliferation of MM
MM were stimulated for 24h with the indicated concentration and isoform of Gal-8 prior to the addition of [^{3}H]-thymidine for 8h. Graphs show the proliferation of MOLP-8 (A) or LP-1 (B) compared to medium control. Gal-8S had a slightly positive effect on the proliferation of LP-1. 0.5µM Gal-8N had a negative effect on the proliferation of both MM cell lines. Cumulative data of three representative experiments are shown.

Overall, it seems that Gal-8 has only minor influence on the proliferation rates of MM cells *in vitro*.

3.5.2 Gal-8 in MM homing

Homing of the MM cells to EC in the BM is an initial step for invasion of MM into the bone. The impact of Gal-8 on homing of MM to EC was investigated next. In literature, Gal-8 has been described to be able to influence cell-cell as well as cell-ECM adhesion processes in several biological systems [75, 76, 77, 78].

3.5.2.1 Static adhesion

In order to investigate if Gal-8 is a pro-adhesive effector on MM adhesion to EC, HUVEC were seeded and grown until confluency prior to the addition of calcein-green stained MM cells. MM cells were allowed to adhere for 30min at 37°C, then non-adherent cells were gently washed away and adherent cells were counted. Addition of 0.1µM Gal-8 led to a stronger adhesion of both MM cell lines to the EC. Gal-8L had a stronger effect compared to Gal-8S, whereas the N-terminal domain alone did not influence adhesion. The addition of 100mM lactose led to an inhibition of the pro-adhesive effect of Gal-8 (Figure 3.22). This indicates that the positive effect on adhesion is mediated by galectin-glycan interactions. Additionally it shows that the N-terminal domain alone did not have such positive effect indicating that either both domains are necessary for the pro-adhesive effect or the single C-CRD.

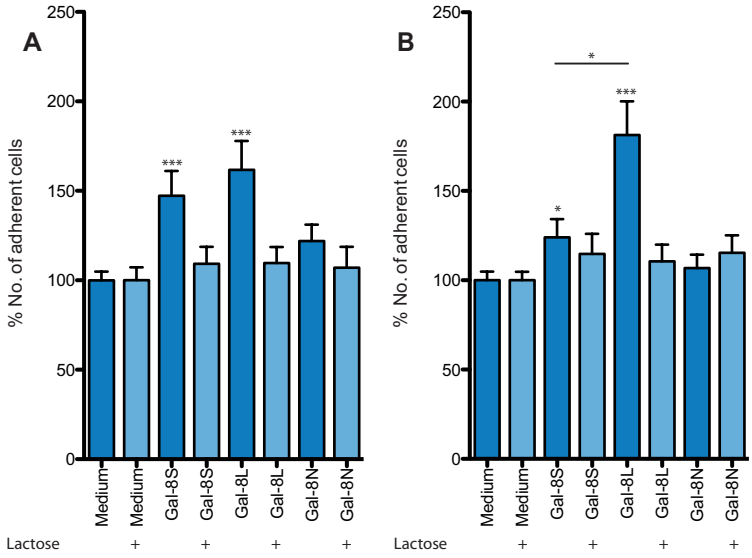

Figure 3.22: Static adhesion of MM to EC
MM cells were stained with calcein-green and adhesion of the cells to HUVEC was measured. MOLP-8 (A) as well as LP-1 (B) were able to adhere stronger in the presence of recombinant Gal-8. Gal-8L had a significantly stronger effect than Gal-8S in LP-1. The N-terminal domain had no pro-adhesive effect. The adhesion was inhibited in the presence of 100mM lactose (light blue bars). The graph shows cumulative data of three independent experiments and depicts mean +/- SEM

Since the adhesion assay showed that Gal-8S and Gal-8L had distinct effects on the adhesion, different mutants, lacking parts of the linker region, were used for further experiments. Figure 3.23 displays the deleted regions. The deletion of amino acids led to linker sizes ranging in between the long and the short linker isoform. In the following experiment the questions which parts of the linker lead to the stronger effect on adhesion, were addressed.

Gal-8L	GFSFSSDLQSTQASSLELTEISRENVPKSGTPQLPSNRGGDISKIAPRTVYTKSKDSTVNHTLTCTKIPPMNYVSK	76 AA
Gal-8S	GFSFSSDLQSTQASSLELTEISRENVPKSGTPQL———————————————————	34 AA
Gal-8 mut1	GFSFSSDLQSTQASSLELTEISRENVPKSGTPQLPSNRGGDISKIAPR———————————	48 AA
Gal-8 mut2	GFSFSSDLQSTQASSLELTEISRENVPKSGTPQLPSNRGGDISKIAPRTVYTKSKDSTVNHT———————	62 AA
Gal-8 mutA	GFSFSSDLQSTQASSLELTEISRENVPKSGTPQL————————————LTCTKIPPMNYVSK	48 AA
Gal-8 mutB	GFSFSSDLQSTQASSLELTEISRENVPKSGTPQL——————TVYTKSKDSTVNHTLTCTKIPPMNYVSK	62 AA

Figure 3.23: Mutation of the Gal-8 linker region
Comparison of the linker region amino-acid sequence of Gal-8S, Gal-8L and mutants with a partly deleted linker region. The deletions are indicated as a black lines, number of amino-acids in the linker region are displayed.

All Gal-8 linker mutants,with or without the addition of 100mM lactose, did not have any significant effect on the adhesion of MM to EC (Figure 3.24). Although not significant, Mut2 and MutA slightly increased the adhesion of MOLP-8 to HUVEC.

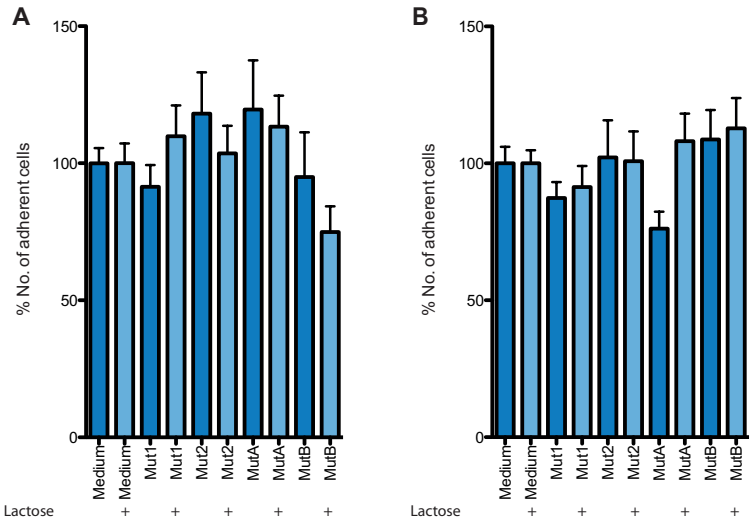

Figure 3.24: Static adhesion - Gal-8 linker mutants
MM cells were stained with calcein-green and adhesion of the cells to HUVEC was measured. Gal-8 mutants with partly deletions of the linker region did not change the adhesion of MOLP-8 (A) or LP-1 (B) to the EC. Only Mut2 and MutA were able to slightly increase the adhesion of MOLP-8 to HUVEC. Additionally, addition of 100mM lactose did not affect binding. The graph shows cumulative data of three independent experiments.

It seems that all mutant isoforms of Gal-8 are non-functional in terms of adhesion of MM to EC. This is possibly due to the deletions of essential amino acids in the linker region. This might have caused a general unstable and therefore non-functional protein.

Since it was shown that Gal-8 has an effect on adhesion of MM to EC, more experiments were performed to go further into details. The following paragraph will focus on the question if the pro-adhesive effect of Gal-8 is also present under shear stress conditions. Additionally, the impact of an inflammatory environment on the adhesion was examined.

3.5.2.2 Changes in the expression of surface molecules after TNF-α stimulation in MM

Stimulation with TNF-α mimics an inflammatory environment. The expression of the glycoproteins neuronal cell adhesion molecule (NCAM; CD56) and MAC-inhibitory protein (MAC-IP; CD59), cyclic ADP ribose hydrolase (CD38), the MM cell marker syndecan I (CD138) as well as HLA class 1(W6/32) were measured after stimulation of the MM cells with 10ng/ml TNF-α for 24h (Figure 3.25). Unexpectedly, HLA-surface expression was decreased on LP-1 after TNF-α stimulation. This effect was seen in two independent measurements and could be due to tumor-escape mechanisms. Major difference between LP-1 and MOLP-8 is the expression of NCAM which is present on the surface of MOLP-8, but not or only to a small amount on LP-1. All other molecules tested were expressed on both cell lines and not strongly altered by TNF-α treatment.

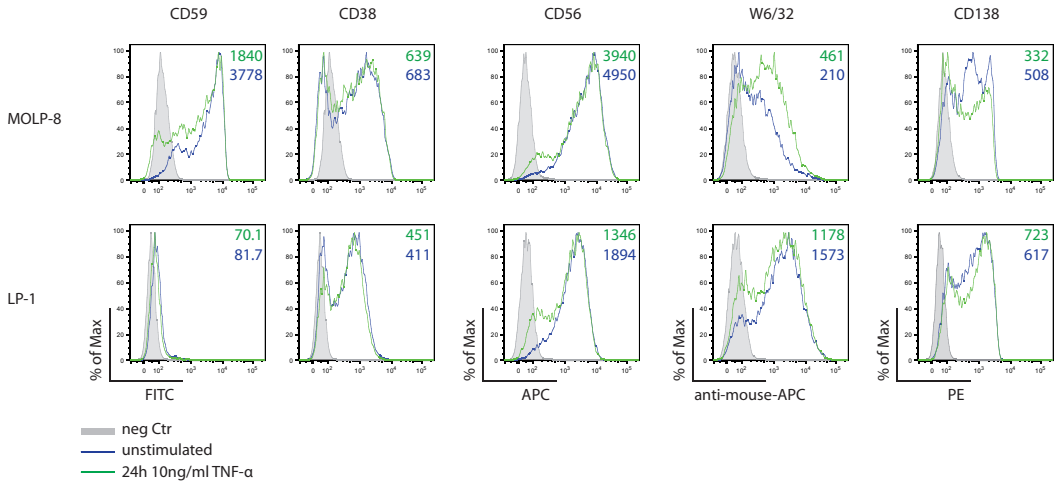

Figure 3.25: Expression of MM surface markers after TNF-α stimulation
MM cells were stimulated for 24h with 10ng/ml TNF-α. Expression of indicated surface markers was detected by FACS analyses.

It seems that surface expression of the adhesion molecules tested are not strongly activated in the presence of TNF-α in both MM cell lines.

3.5.2.3 Changes in the expression of adhesion molecules in EC

Vascular shear stress is an important factor for the homeostasis in the circulation. Since vascular EC are constantly exposed to shear stress and respond to it, this must be also considered by the investigation of homing processes. One example that shows the importance of shear stress is that selectin-mediated rolling depends on

shear stress, since the adhesion stops under static conditions [42]. It has also been shown that shear stress regulates the expression of certain adhesion molecules e.g. the expression of VCAM-1 decreases remarkably in cells exposed to shear stress *in vitro* [42, 121]. Microarray analyses revealed that around 3% of 5600 genes tested respond to shear stress stimulation [122]. It is also noticeable, that cells cultured under shear stress conditions change their morphology, they become more streched, line up and their actin skeleton is remodeled [121, 123]. Those responses to shear stress indicate that ECs are able to sense shear stress specifically, but the mechanisms of mechanotransduction and are not fully understood yet [121].

In order to obtain a comprehensive view on the influence of shear stress or inflammatory stimulation on the expression profile of EC whole genome analyses of HUVECs treated with either 10 ng/ml TNF-α for 24h, 10 dyn/cm^2 shear stress for 24h or both were performed. 188 genes that are important for adhesion processes were extracted from the dataset using a gene list according to the KEGG-pathway 4514 (http://www.genome.jp/dbget-bin/www_bget?pathway:map04514). The resulting heatmap shows, that HUVEC change their expression profile of adhesion molecules upon stimulation with shear stress, as well as after stimulation with TNF-α or both (Figure 3.26). All four datasets show different clusters of genes expressed resulting in a selective expression pattern for each group.

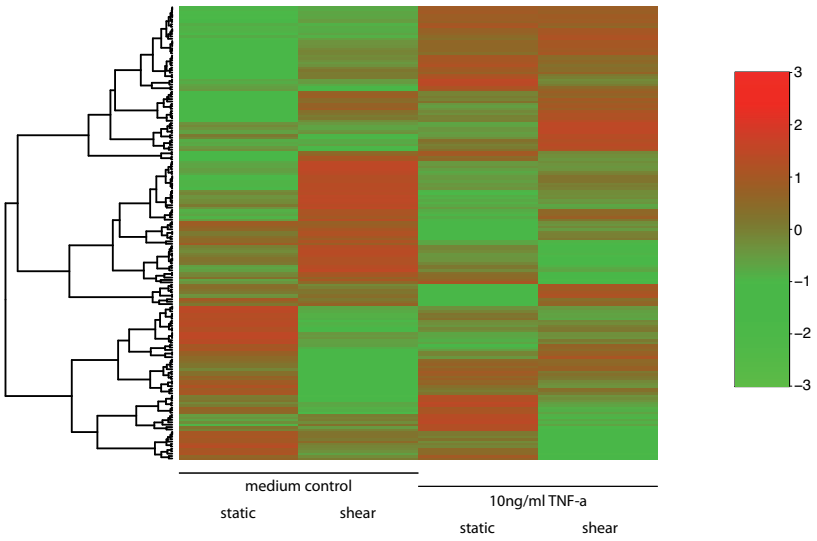

Figure 3.26: Heatmap of adhesion molecules under inflammatory stimulation or shear stress HUVEC were treated with 10ng/ml TNF-α for 24h, 10dyn/cm^{2}shear stress or both prior to the mRNA-analyses. Whole genome analysis was performed on a Illumina HT12 Chip and 188 genes from the KEGG pathway 4514 were selected for the heatmap analysis. Red color indicates upregulated genes, green color indicates downregulated genes. The x-axis indicates the treatment of the cells, the y-axis shows the hierarchical clustering of the selected genes. Different gene-expression patterns were seen comparing the four different treatments. Shear stress as well as stimulation with TNF-α altered the expression profile of HUVEC remarkably.

The data obtained from the heatmap analysis was verified by qRT-PCR on selected genes (Figure 3.27). The expression of ICAM-1 (CD54) was slightly upregulated by shear stress, but the expression of E-selectin (CD62E) was suppressed. The stimulation with TNF-α for 24h in addition to shear stress led to a massive increase of ICAM-1 and E-selectin expression on the mRNA level. The expression of PECAM-1 (CD31) and VE-cadherin (CD144) was not altered.

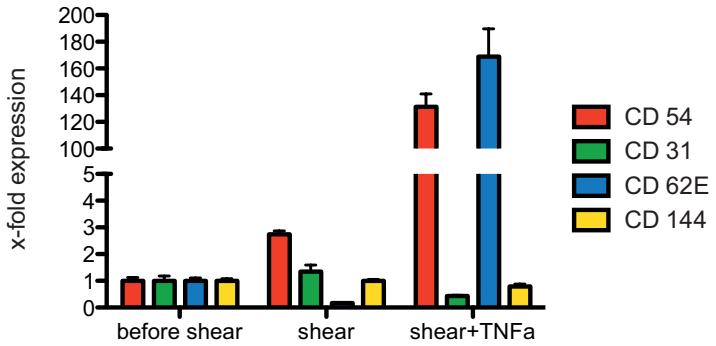

Figure 3.27: mRNA expression of surface markers after 24h shear stress +/- TNF-α
HUVEC were seeded and grown in a µSlide for 24h at 10dyn/cm^2. Cells were additionally stimulated with 10ng/ml TNF-α, as indicated. Shear stress suppresses the expression of the adhesion molecule CD62E, stimulation with TNF-α strongly increases the expression of CD62E and CD54. The expression of CD31 and CD144 are not altered by shear stress or TNF-α stimulation. Graph shows representative data of three independent experiments.

FACS analyses were performed in order to check the regulation of the selected genes on the cell surface. It is not possible to perform this experiment on cells stimulated with shear stress, due to limited numbers of cells to recover from the shear stress system. However, the change of expression of surface markers was measured after TNF-α stimulation under static conditions by FACS analysis (Figure 3.28). According to the qRT-PCR data, the expression of the adhesion molecules CD54 and CD62E is increased on HUVEC after stimulation with TNF-α. The positive control HLA class 1 is also upregulated after TNF-α stimulation. The expression of CD144 and CD31 was not changed. HUVEC and HBMEC-60 are comparable in the expression of the tested surface molecules, except for CD62E, which seemed not to be expressed on HBMEC-60, even after stimulation with TNF-α. This has also been described before in our group by Willhauck-Fleckenstein *et al.* [124].

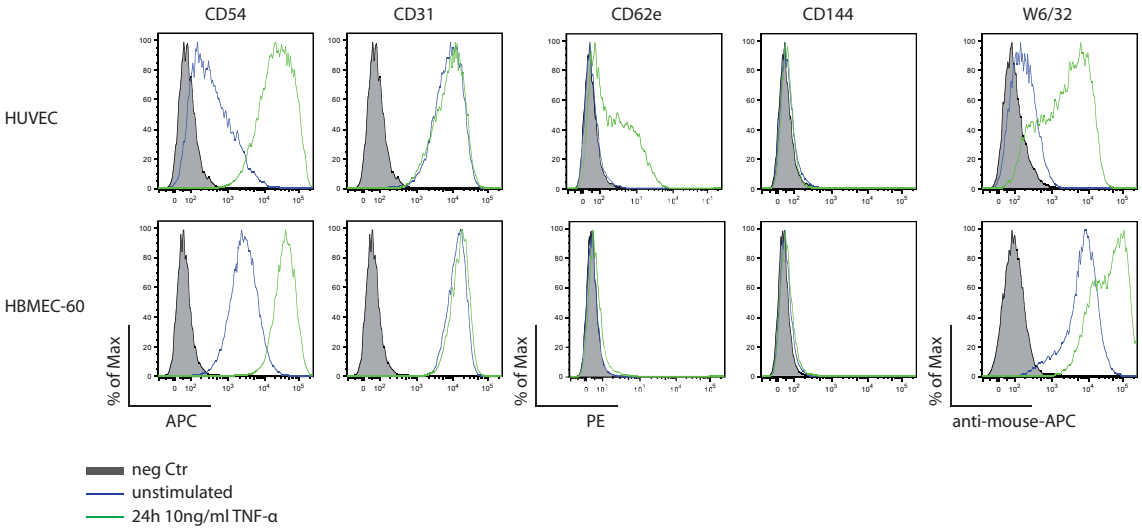

Figure 3.28: Expression of EC surface markers after TNF-α stimulation
EC were stimulated for 24h with 10ng/ml TNF-α. Expression of indicated surface markers was detected by FACS analyses. The expression of CD31 and CD144 remains stable, as has been shown before by qRT-PCR analysis. CD54 and CD62E expression is increased after inflammatory stimulation, as expected, as well as the positive control W6/32.

In summary, it was shown that due to inflammatory or shear stress conditions, HUVEC change their expression of characteristic cell surface molecules. These changes in the expression of adhesion molecules need to be considered for adhesion experiments, since both, shear stress and TNF-α can alter the expression of them. Therefore, the results of the static adhesion experiments were confirmed in an adhesion assay under shear stress conditions and by the combination of shear stress and TNF-α stimulation during the experiments.

3.5.2.4 Homing of MM to EC in shear stress conditions

Adhesion experiments were performed mimicking a blood vessel. The experiment was performed as shown in Figure 3.29. HUVEC were seeded and grown for 24h at 10 dyn/cm^2 with or without the addition of 10ng/ml TNF-α. After the pre-stimulation, calcein-green stained MM cells were first perfused at lower shear stress (1 dyn/cm^2) for 30 minutes to mimic shear stress in small vessels. Afterwards, shear stress was raised to 5 dyn/cm^2 to check if the cells adhere firmly or were just loosely attached.

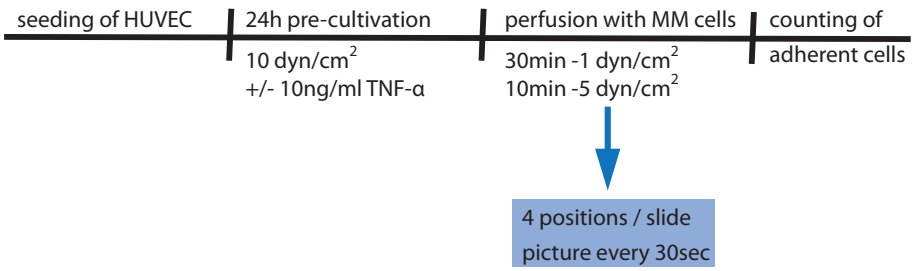

Figure 3.29: Schematic overview of shear stress experiments
The figure shows how shear stress experiments were performed in general. HUVEC were seeded and pre-cultivated under shear stress for 24h prior to an experiment. During the experiment, microscopic pictures using a Zeiss Cell Observer.Z1 (objective: 5× / 0.16 EC Plan-NEO Ph1 DIC0) were taken and calcein-green stained cells were counted for quantification.

Initial shear-stress experiments were performed with non-inflammatory HUVEC. Although only a few cells were able to adhere, the Gal-8 expressing MM cell line MOLP-8 adhered stronger to HUVEC under shear stress than the Gal-8 negative cell line LP-1 (Figure 3.30).

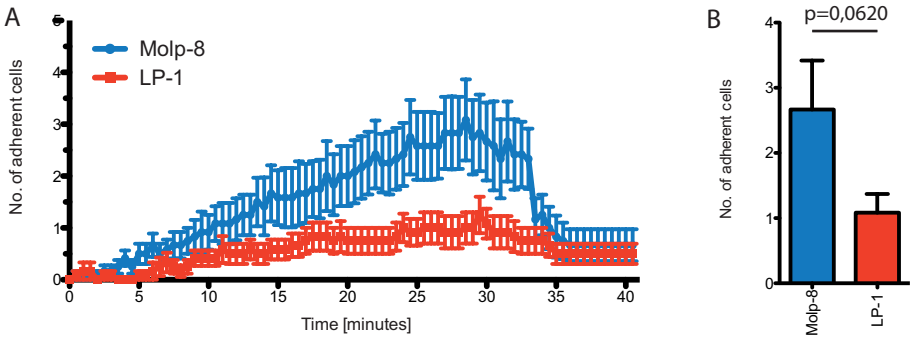

Figure 3.30: Adhesion of MM to EC under shear stress
Adhesion of MOLP-8 or LP-1 MM cells to HUVEC during 30 min of 1dyn/cm^{2}followed by shear stress of 5dyn/cm^{2}for 10 min. Adherent cells were counted every 30 sec during shear stress (A). The number of adherent cells/position after 30 min was used for statistical analyses (B). The Gal-8 positive cell line MOLP-8 was able to adhere stronger than the Gal-8 negative cell line LP-1. But only a few cells were able to adhere in general. The graph shows cumulative data of three independent experiments.

The expression of adhesion molecules on the surface of HUVEC was induced by pre-stimulation with TNF-α before the adhesion experiments. After pre-stimulation with TNF-α, approximately 100-fold more cells were able to adhere. In this case, the Gal-8 negative cell line LP-1 showed stronger binding compared to MOLP-8 (Figure 3.31).

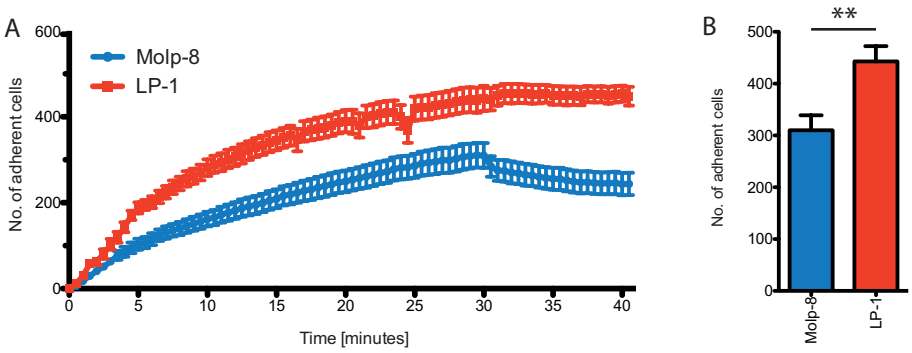

Figure 3.31: Adhesion of MM to EC under shear stress
HUVEC were pre-stimulated with 10 ng/ml TNF-α before the perfusion with MM cells as described above. Adherent cells were counted every 30 sec during shear stress (A). The number of adherent cells/position after 30 minutes was used for statistical analyses (B). Under inflammatory stimulation, about 100-fold more MM cells were able to adhere. LP-1 adhered stronger than MOLP-8. Graph shows cumulative data of three independent experiments.

The influence of recombinant Gal-8 on the adhesion under shear stress conditions was measured by the addition of 0.1µM Gal-8S or Gal-8L to the perfusion medium. After 30 minutes of perfusion at 1 dyn/cm^2, cells were able to adhere stronger if Gal-8 was present in the medium (Figure 3.32). For both, LP-1 and MOLP-8, the adhesion was significantly stronger if Gal-8L was present compared to Gal-8S. For Gal-8S the adhesion was enhanced approximately 15-fold, for Gal-8L 40 to 60-fold.

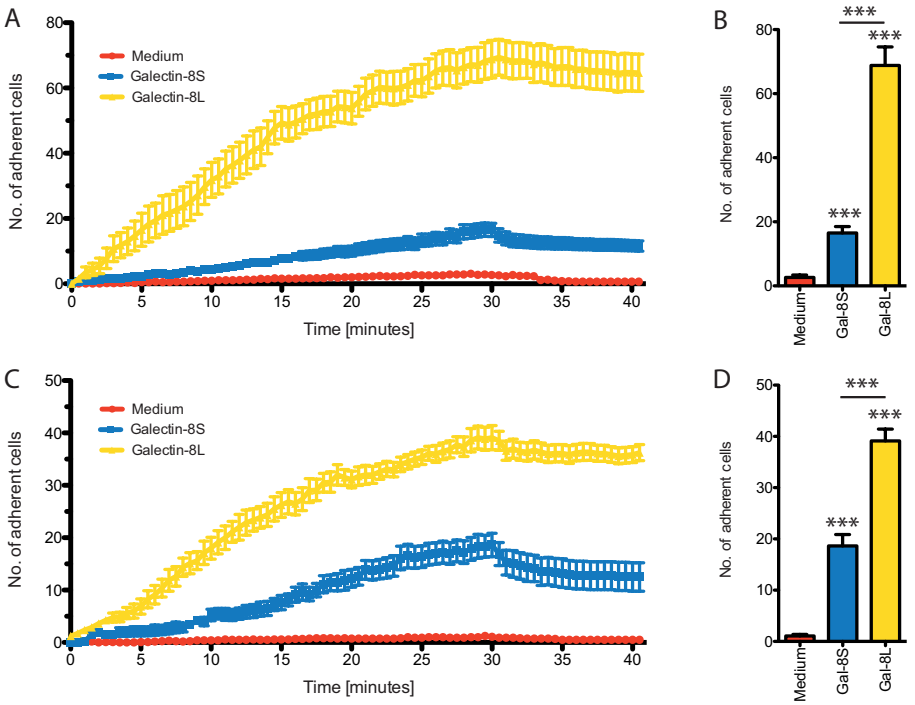

Figure 3.32: Influence of recombinant Gal-8 on adhesion
Adhesion of MOLP-8 (A, B) or LP-1 (C, D) MM cells to HUVEC during 30 min of 1 dyn/cm^2 followed by shear stress of 5 dyn/cm^2 for 10 min. If indicated, 0.1µM Gal-8S or Gal-8L was added to the perfusion medium. Adherent cells were counted every 30 sec during shear stress (A, C). The number of adherent cells/position after 30 minutes was used for statistical analyses (B, D). The addition of Gal-8S as well as Gal-8L increased the number of adherent MM cells significantly in both cell lines. Gal-8L increased the adhesion significantly stronger then Gal-8S. Graph shows cumulative data of three independent experiments.

Since it was shown before that pre-stimulation with TNF-α influences the expression of cell surface molecules and could thereby influence the adhesion of MM to EC too, HUVEC were pre-treated with 10ng/ml TNF-α prior to the adhesion experiment. As seen before, more MM cells were able to adhere to the HUVEC layer after inflammatory stimulation. Addition of recombinant Gal-8 even increased the already strong binding of MM to EC, but under these conditions there was no significant difference between Gal-8S and Gal-8L (Figure 3.33).

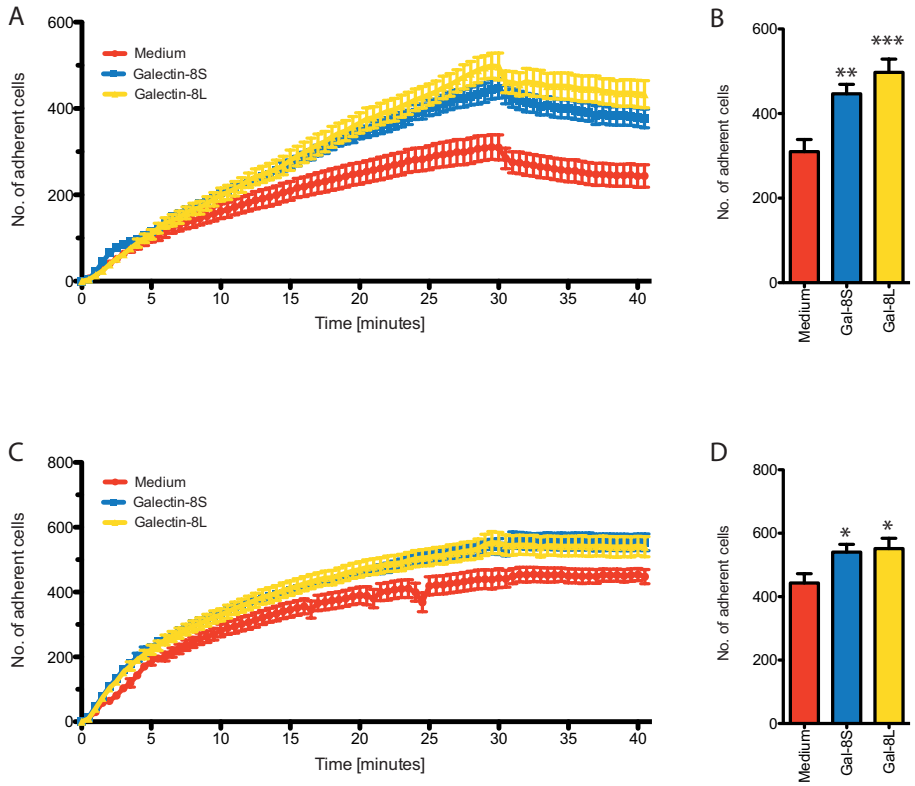

Figure 3.33: Influence of recombinant Gal-8 on adhesion to TNF-α stimulated HUVEC
HUVEC were pre-stimulated with 10 ng/ml TNF-α before the perfusion with MM cells (MOLP-8 A, B; LP-1 C, D) as described above. If indicated, 0.1µM Gal-8S or Gal-8L was added to the perfusion medium. Adherent cells were counted every 30 sec during shear stress (A, C). The number of adherent cells/position after 30 min was used for statistical analyses (B, D). Gal-8S as well as Gal-8L were able to increase the adhesion of MM to EC also after pre-stimulation with TNF-α. But there was no significant difference between Gal-8S and Gal-8L. Graph shows cumulative data of three independent experiments.

The role of Gal-8 secreted by MM on the MM adhesion to EC was assessed using conditioned supernatants of MOLP-8 cells. For this purpose, the cells were cultured for 72h in serum-free AIM medium, which was then concentrated 20-fold. The concentrated medium was split into two parts and half of the supernatant was Gal-8 depleted prior to the shear stress experiment. The depletion was checked using a Gal-8 specific ELISA (Figure 3.34 A). The conditioned supernatant and the Gal-8 depleted supernatant were added to the perfusion medium and the adhesion of MOLP-8 cells to HUVEC under shear stress was measured (Figure 3.34 B, C). After 30 minutes, a significant difference in adherent cells comparing Gal-8 conditioned against Gal-8 depleted supernatant was detected (Figure 3.34 C).

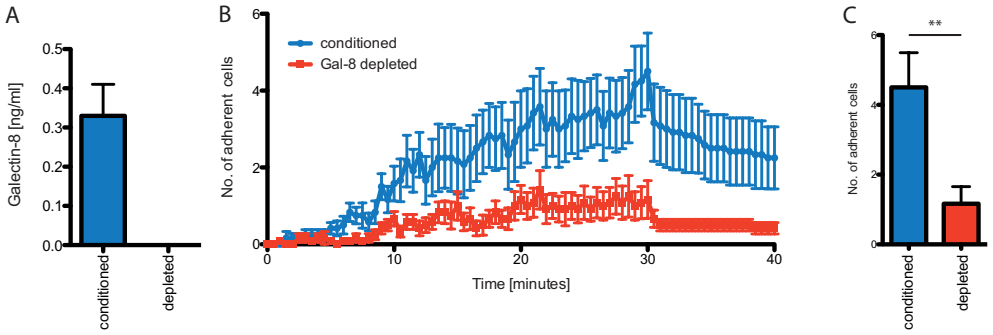

Figure 3.34: Shear stress using MOLP-8 conditioned supernatants
HUVEC were grown and perfused with MM cells as described above. Half of MOLP-8 conditioned supernatant was Gal-8 depleted. Depletion was measured using a Gal-8 specific ELISA (A). The supernatant was added to the perfusion medium. Adherent cells were counted every 30 sec during shear stress (B). The number of adherent cells/position after 30 min was used for statistical analyses (C). The depletion of Gal-8 in the conditioned supernatant lead to a significantly decrease in adherent MM cells. Graph shows cumulative data of three independent experiments.

In conclusion, it was shown that Gal-8 has an effect on the adhesion of MM to EC in static as well as in shear stress conditions. Gal-8L has a stronger pro-adhesive effect in both systems than Gal-8S indicating that the two isoforms of Gal-8 differ in their biological activity.

3.6 Gal-8 multimerization

Seeing differences between the long- and short-linker isoform of Gal-8 in biological assays, the question arises concerning the molecular background of this differential behavior. Multimerization or galectin-glycan lattice formation is a process often described for different galectins [58, 125, 126]. But there is only little experimental evidence proving that these processes occur [60]. For Gal-8 it has been shown that it can form dimers using chemical crosslinking [98]. For two Gal-1 CRDs connected by artificial linkers homodi - and multimerization was shown, but this has never been shown for tandem-repeat galectins [60]. Using SDS-PAGE analysis, static light scattering and thermophoresis measurements it was investigated if differences in the ability to form dimers or multimers occur in the two isoforms.

3.6.1 Non-reducing SDS-Gels

Gal-8 has been show to run as a dimer in SDS-PAGE after chemical crosslinking [98], but it was not shown if this dimerization is also present without chemical modification. Recombinant Gal-8 was loaded on MOPS/SDS gels using non-reducing loading buffer without the prior addition of a crosslinker. For the short-linker isoform, a band was observed at 36kDa. After longer exposure, a second signal appeared at approximately 75kDa (Figure 3.35). For the long linker isoform 3 bands appeared, a monomer at around 40kDa, a dimer at approximately 80kDa and a third band at about 120kDa, representing most likely a trimer. The ratios of multimer to dimer to monomer Gal-8L were 1:4.4:8.6. The ratios were investigated by calculating the pixel density using the ImageJ software.

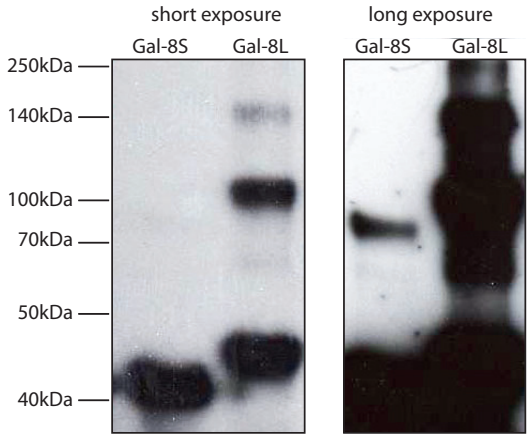

Figure 3.35: Non-reducing SDS-Gels of Gal-8S and Gal-8L
2µg of the indicated recombinant protein were loaded per lane of a 4%-12% MOPS/SDS precast gel. For Gal-8S a monomer (36kDa) and a dimer (72kDa) band were observed, for Gal-8L a monomer (40kDa), dimer (80kDa) and trimer (120kDa) were seen.

In order to investigate if the dimer-or multimerization is forced by either the single N-or C-terminal CRD, both domains were loaded on a gel as described above. Both showed the formation of a dimer (Figure 3.36), using longer exposure times did not show any tri- or multimers (data not shown). The ratio of dimers to monomer was 1:3.7 for Gal-8C and 1:7.4 for Gal-8N.

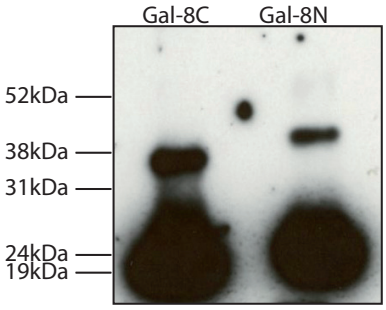

Figure 3.36: Non-reducing SDS-Gels of Gal-8N and Gal-8C
2µg of the indicated recombinant protein were loaded per lane on a 4%-12% MOPS/SDS precast gel. For Gal-8C a monomer (17kDa) and a dimer (34kDa) band was observed. The same was shown for for Gal-8N, a monomer (18kDa), dimer (36kDa) was visible.

It seems that more Gal-8C dimer is present than Gal-8N dimer, but this is due to a general higher protein content for Gal-8C in the gel. Although the protein-concentration of the suspension was determined before loading on the gel, it seems that more Gal-8C was loaded than Gal-8N. The pixel intensity for both bands is higher for Gal-8C (221.470) than for Gal-8N (207.603) indicating more total Gal-8C protein. A possibility is that Gal-8N is more degraded than Gal-8C and that the degradation products ran out the gel and are not visible anymore.

3.6.2 Static light scattering

SDS-PAGE separation indicated that Gal-8S and Gal-8L differ in their ability to di - or multimerize in solution. Using a second method, static light scattering (SLS) analysis (performed by Dr. Vladimir Rybin, EBML, Heidelberg), the presence of dimers in both, Gal-8S and Gal-8L could be confirmed by the appearance of two peaks (Figure 3.37). The ratio of dimer to monomer was 1:50 for Gal-8S and 2:3 for Gal-8L. The calculated size for the monomers was 33kDa for Gal-8L and 35kDa for Gal-8S, the size of the dimers was calculated with 67kDa for Gal-8L and 68kDa for Gal-8S.

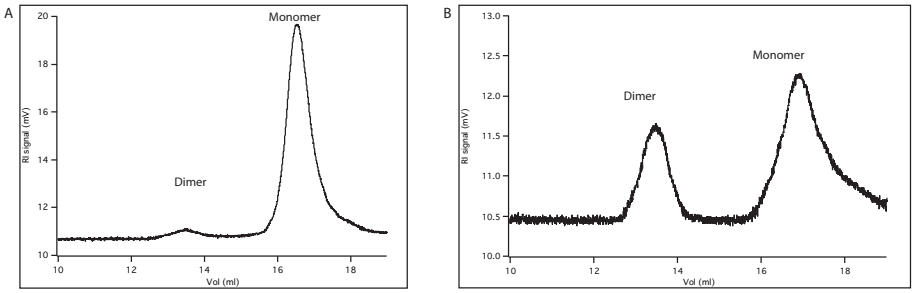

Figure 3.37: Static light scattering of Gal-8S and Gal-8L
For static light scattering, proteins were loaded on a Superdex 200 column and elution of the protein was detected by the refractive index (RI) at defined elution volumes. The RI signal is depicted on the y-axis, the elution volume on the x-axis. Both, Gal-8S as well as Gal-8L have peaks for monomers and dimers (indicated). But the ratio of dimers to monomers differs in both isoforms. For Gal-8S the ratio is 1:50 (A), for Gal-8L 2:3 (B). The measurement was performed by Dr. Vladimir Rybin(EBML, Heidelberg).

The fact that Gal-8S has a higher calculated molecular weight than Gal-8L might be due to differences in the protein folding influencing the migration of the protein through the column. But the clear difference in the ration of monomer to dimer in Gal-8S an Gal-8L indicates, that Gal-8L is more capable to build dimers in solution.

3.6.3 Thermophoresis

Since differences between Gal-8S and Gal-8L in the formation of dimers or trimers were seen in the SDS gels and SLS analysis, thermophoresis was used to calculate binding coefficients of the self-interaction. Thermophoresis is a process that describes the movement of a molecule along a temperature gradient. By fluorescence labeling of one interaction partner, the movement can be tracked. If two molecules interact with each other, a concentration dependent change in the movement is observed (e.g. gets slower or faster) and this can be measured using the label of one of the interaction partners (Figure 3.38) [127].

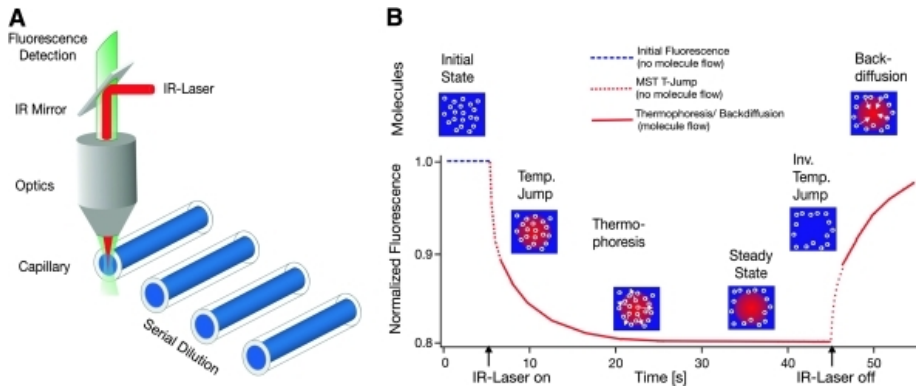

Figure 3.38: Schematic overview of thermophoresis
A: For MST measurements, serially diluted samples are filled into capillaries. A punctual temperature gradient is created by a IR-laser, the movement of molecules is detected using a fluorescence detector. B: By turing the laser on, the molecules move out the temperature gradient which is detected by a drop of the fluorescence (temperature jump) leading to a steady state situation after about 20 sec. After turning the laser off, the molecules move back. This is detected by an increasing fluorescence signal. If molecules interact with each other, the movement changes. The figure was taken from Jerabek-Willemsen *et al.* [127].

For the analysis of Gal-8 self-interactions, the protein was fluorescently labeled and incubated with unlabeled protein in increasing concentrations of the same isoform. A first change in the movement was seen for Gal-8S, Gal-8L and the N-terminal domain very early during thermophoresis, at the initial temperature jump (Figure 3.39). This change shows probably the formation of a dimer and was present at very low nano-molar concentrations (table 3.2). Gal-8L was about 5-fold stronger in dimerization comparing the obtained EC_{50} values. A second, very weak event occurred later during the thermophoresis for Gal-8L and Gal-8C (Figure 3.39). This is seen by a change in the direction of the amplitude. The second event might be the formation of a trimer for Gal-8L and the formation of a dimer for the C-terminal domain. The obtained EC_{50} values were much higher as at the early event (table 3.2).

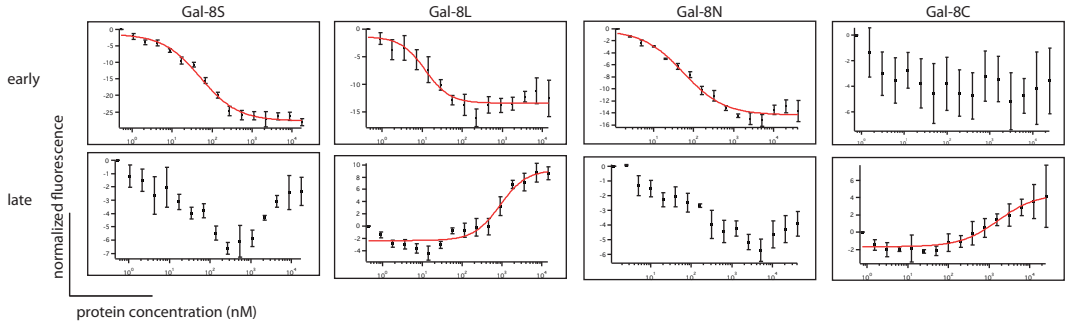

Figure 3.39: Thermophoresis of Gal-8 isoforms and the single CRDs
The early phase describes the decrease in fluorescence at the temperature jump. A high affinity binding event is seen for Gal-8S, Gal-8L and the N-terminal CRD. The late phase describes an increase in fluorescence at the late phase of thermophoresis. This indicates a low-affinity binding event for Gal-8L and the C-terminal CRD. The graphs show cumulative data of three independent experiments.

Lactose is a natural ligand for Gal-8 and used for inhibition of the lectin function. 100mM lactose was added to the MST-buffer prior to the measurement in order to find out if a glycan ligand could interfere with di-or multimerization. Lactose was able to inhibit all interactions and binding events were not visible anymore (Figure 3.40).

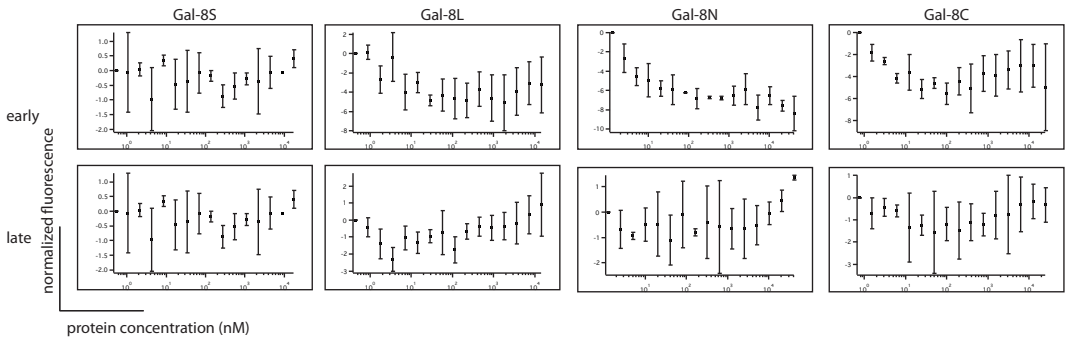

Figure 3.40: Inhibition of di- or multimerization with lactose
The experiment was performed as described above. 100mM lactose was added to the MST-buffer, inhibiting all binding events. The graph shows cumulative data of three independent experiments.

Mutants with partly deleted linker regions, as described above (Figure 3.23), were additionally used for the measurements since the linker region seemed to be important for multimerization. Mut1, Mut2 and MutA showed both binding events, whereas MutB only was able to show the low affinity binding event (Figure 3.41).

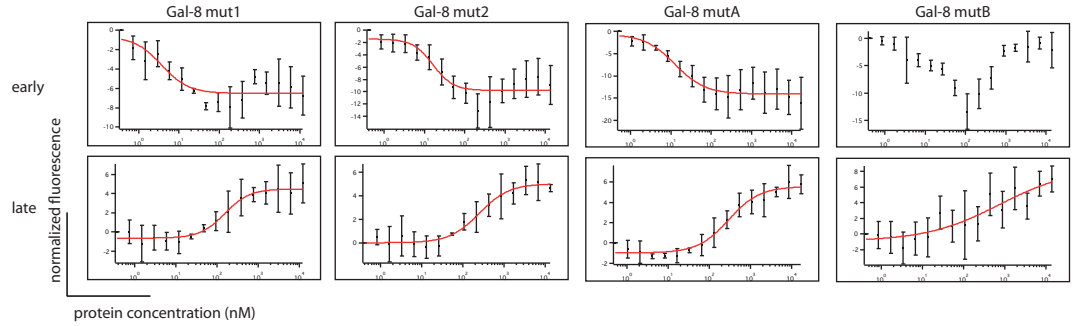

Figure 3.41: Thermophoresis of Gal-8 mutants
The early phase describes the decrease in fluorescence at the temperature jump. A high affinity binding event is seen for Gal-8mut1, Gal-8mut2 andGal-8mutA. The late phase describes an increase in fluorescence at the late phase of thermophoresis. This indicates a low-affinity binding event for all mutants used. The graphs show cumulative data of three independent experiments.

The calculated binding affinities for for all Gal-8 proteins used for thermophoresis measurements are summarized in table 3.2.

Protein	early EC_{50}(nM)	late EC_{50}(nM)
Gal-8S	50,619 +/-7,17	none
Gal-8L	11,816 +/-3,25	893,6 +/-281
Gal-8N	55,401 +/-13,9	none
Gal-8C	none	1670,5 +/-801
Mut1	3,7258 +/-2,41	153,1 +/-28,9
Mut2	116,24 +/-5,92	521,96 +/-53
MutA	12,476 +/-3,39	297,24 +/-63,1
MutB		736,13 +/-1650

Table 3.2: Summary of calculated EC_{50} values
To calculate the EC_{50} values for the different Gal-8 proteins used in thermophoresis, curves were fit using Hill-Equation.

The measurements indicate that the high affinity binding event is most likely due to a dimerization of the N-terminal domain in all isoforms. The second, weaker event only occurring in the long linker isoform might be due to the C-CRD, since this only shows the second, weaker binding event. This differences in dimer- or multimerization might contribute to the differences in the activity of the two isoforms.

3.6.4 Galectin-8 computational modeling

The following computer simulation was performed by Dr. Sonu Kumar (Sanford-Burnham Medical Research Institute, San Diego).

Both isoforms of Gal-8 were computationally modeled for the linker structure. The crystal structure for both, the N-and the C-CRD is available [112, 113], but the 3D-structure of the linker remains unknown. Additionally, the orientation of the CRDs to each other is not known yet. Since crystallization of the full length protein is not possible due to the flexibility of the linker region, a computational models was used to get information about a possible protein structure. The model shows that the CRDs in Gal-8L seem to be more distant from each other compared to Gal-8S (Figure 3.42). Additionally, the orientation is different in both isoforms.

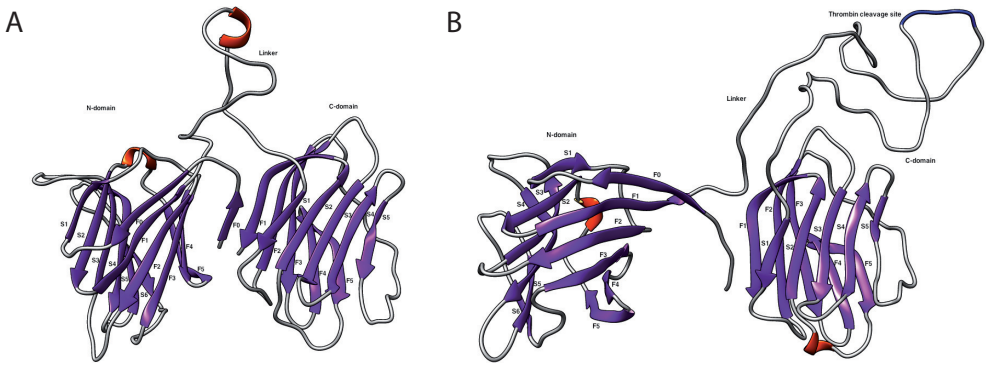

Figure 3.42: Computational model of Gal-8S and Gal-8L
The linker structures were modeled for Gal-8S (A) and Gal-8L (B) in explicit solvent for 25 ns. The model shows that the CRDs seem to be closer to each other for Gal-8S then for Gal-8L. The experiment was performed by Dr. Sonu Kumar (Sanford-Burnham Medical Research Institute, San Diego).

By dimerization of the N-terminal CRD of both isoforms, a further multimerization could possibly be blocked due to sterical hindrances in Gal-8S. The linker of Gal-8S is shorter, the space between the two CRDs seems to be fewer in Gal-8S. Additionally, the CRDs are facing more outwards in Gal-8L, possibly displaying the binding sites necessary for further multimerization. These calculations could possibly explain, why the isoforms differ in their ability to built multimers in solution and why they differ in their biological activity.

4

Discussion

This thesis intended to investigate the role of Gal-8 in MM with regard to interactions between MM cells and EC. I focussed on angiogenesis and homing of the tumor cells to the BM since these are crucial steps in the progression of the disease. It has been shown before that Gal-8 can influence angiogenesis as well as adhesion processes, but it has never been investigated in MM and with regard to the two different isoforms of the lectin. For Gal-9, another tandem-repeat galectin, it has already been shown that the isoforms have different effects on angiogenesis and adhesion [128, 129] indicating an impact of the linker region on the biological function of the lectin.

In my study, I was able to show that Gal-8 has no effect on angiogenesis, since recombinant Gal-8 was not able to enhance proliferation or the migratory potential of EC and did not influence tube formation in an *in vitro* tube formation assay. But I could reveal a pro-adhesive effect of Gal-8 in static as well as under shear stress conditions which is higher for the Gal-8L isoform. This pro-adhesive effect could promote the progression of the disease *in vivo* as Gal-8^{high} patients have a lower survival and a faster progression of the disease. The stronger pro-adhesive effect of Gal-8L might be explained by multimerization of the protein which was investigated by native SDS-PAGE, SLS analysis and thermophoresis.

4.1 Influence of Gal-8 on angiogenesis

As angiogenesis is crucial for the progression of MM and mainly induced by pro-angiogenic factors produced by MM cells, I was wondering whether Gal-8, secreted by MM cells, is able to promote angiogenesis in the BM. In my study, recombinant Gal-8 neither had a positive effect on migration in a gap closure assay nor on tube formation in a fibroblast-EC co-culture using the human primary cells HUVEC

for the experiments. Additionally, proliferation of the cells is not enhanced by the addition of Gal-8 to the medium.

These results are in contrast to Delgado *et al.* [101]. They proposed that Gal-8 induces angiogenesis which was shown by an improved network-formation using a matrigel assay and faster migration in a wound-scratch assay in the presence of Gal-8. These experiments were performed using bovine aortic endothelial cells (BAEC). Additionally, they showed promotion of angiogenesis in an *in vivo* matrigel plug assay in mice. Based on this publication, I wanted to validate their data using cells of human origin since they combined bovine or mouse models with human Gal-8. Although galectins are generally highly conserved among species, mouse, human and bovine Gal-8 share only 70-80% sequence homology. Furthermore, the matrigel-assay is rather a network-formation assay than a tube formation assay, since it shows only the interconnection of plated cells. Using cell lines of human origin, I could not confirm a pro-angiogenic effect of Gal-8. A recent publication by Chen *et al.* [89] showed that Gal-8 is enhanced in the circulation of cancer patients and stimulation of human micro-vascular lung endothelial cells (HMVEC-L) with Gal-8 induces the secretion of pro-angiogenic cytokines. HUVECs are, in contrast to HMVEC-L, derived from the macrovasculature. Maybe the pro-angiogenic effect depends on the EC subtype or in general on the model system used for the experiments. Further research has to be performed in order to investigate the function of Gal-8 in angiogenesis.

4.2 Influence of Gal-8 on MM homing

Previous studies described that Gal-8 influences cell-cell interactions in general [75, 76, 77, 78]. But it has not been assessed whether it also influences the adhesion of MM cells to EC, which is a crucial step in the progression of MM. I was able to show that Gal-8 enhances the adhesion of MM cells to HUVEC in a static environment. Gal-8L had a stronger pro-adhesive effect than Gal-8S. This is the first study showing that the Gal-8 isoforms differ in their biological activity. The N-terminal domain alone had no such effect, indicating that either both domains or the C-CRD is important for the adhesion.

Since whole genome microarray analyses revealed that the expression of adhesion molecules changes remarkably after shear stress or during inflammatory stimulation using TNF-α, interaction studies between MM and ECs were also performed under shear stress conditions. Even under flow, recombinant as well as MM cell derived Gal-8 was able to significantly promote adhesion indicating that Gal-8 could be an

important factor in MM homing in the absence of an inflammatory environment. As Gal-8 is a galectin consisting of two CRD connected by a linker region, one idea explaining this pro-adhesive effect was that one CRD could possibly bind MM cells while the other prefers EC and connects thereby the two cells. As the N-terminal domain prefers sialylated structures for binding and the C-terminal domain binds non-sialylated glycans such as blood-group A and B antigens, the sialylation status of MM and EC was investigated by MAA and SNA binding in order to find out whether one cell type possibly prefers binding of one of the CRDs. MM as well as EC have both, α2,3 and α2,6 sialylated structures on their cell surface. But Gal-8N binding after VCN treatment was only affected on EC as seen by a reduction of the MFI after desialylation. The binding on MM cells was not reduced after neuraminidase-treatment and on MOLP-8, both isoforms of the full-length protein even displayed increased binding after VCN-treatment. For LP-1, binding of both full-length isoforms was decreased after desialylation, as in EC. These experiments indicate that the C-CRD might favor MM cells, whereas the N-CRD prefers EC. Of course, the VCN treatment only gives a rough estimate. Binding specificities of both CRDs on the respective cellular partner certainly also depend on other conditions, as for example the arrangement of glycoconjugates on the cell surface (microdomains) or the length of a receptor candidate. This fact might explain, why the MM cells lines MOLP-8 and LP-1 differ in binding of Gal-8 after VCN treatment.

Still, ligands for the binding of Gal-8 to the surface of MM and EC have to be identified. One possible group of candidates for this type of interaction are integrins, which are expressed on both cell types and have been reported before to bind Gal-8 [77, 130]. Integrins are known to play key roles in the firm adhesion of leucocytes to EC during the rolling/adhesion cascade. Gal-8 could possibly strengthen the leucocyte-EC interactions as a co-factor for firm adhesion. Also, other glycosylated targets are possible and Gal-8 might play a role very early in homing comparable to selectins promoting the first rolling events during the adhesion cascade. But in general not much is known about Gal-8 binding partners and identification of those is difficult since there are many possible targets. Galectins can either bind carbohydrate-specific via their CRDs or use protein-protein interactions for binding. For MM and EC, binding seems to be carbohydrate-dependent, since the binding was inhibited by the addition of lactose.

4.3 Differences in biological activity of the isoforms

In this work, different than in other studies, both Gal-8 isoforms were used for the *in vitro* experiments. Most research done on Gal-8 claims that the isoforms do not

differ in their biological activity using only the short-linker isoform for experiments. In our group we were able to show on the one hand that Gal-8L has stronger pro-adhesive effects on MM adhesion to EC (my study) and on the other hand that only Gal-8L, but not Gal-8S is able to induce apoptosis in the pre-B cell line NALM-6 (Master thesis of Michal Stanczak). These results lead to the question, why these differences in biological activity of Gal-8 isoforms occur and what the mechanism behind this phenomenons are. For the pro-apoptotic effect of Gal-8L and the N-terminal CRD, a protease cleavage site present in the long-linker but not in the short-linker isoform could possibly explain the difference in biological activity. Proteolytic cleavage of Gal-8L results in single CRDs but with a shorter linker part. Both, the single recombinant N-CRD without a linker and the proteolytically cleaved N-CRD with a shortened linker part could induce apoptosis in NALM-6. Therefore, the N-CRD may be the driving force for induction of apoptosis and the C-CRD may be, at least for this biological function, not essential. In contrast, the difference in homing can not be explained by proteolytic cleavage of Gal-8L, since both domains seemed to be necessary for the pro-adhesive effect.

As galectins have been described to be able to form complex glycan-galectin lattices, the question arises whether multimerization processes or lattice formation influence cell-cell adhesion. Using non-reducing SDS-PAGE, I was able to show that Gal-8 can exists as di- or multimers, depending on the isoform, without the need of chemical crosslinking. Gal-8L was present as a trimer, whereas for Gal-8S only dimers were visible in the gel. These findings were confirmed by SLS analysis and indicate that Gal-8L more readily builds dimers in solution and has a stronger capability of self-interaction. The calculated size for monomers as well as dimers in SLS analysis differed from a theoretical size of the proteins. This could point to the possibility that Gal-8S and Gal-8L differ in their conformation.

MST analysis revealed that Gal-8L, in contrast to Gal-8S, shows two different binding events. The first high affinity binding might be due to a interaction of two N-terminal CRDs and is also present in Gal-8S. The second, weaker binding event is possibly a non-covalent interaction of two C-CRDs which is not seen for Gal-8S. Due to sterical hindrances caused by the shorter linker and less flexibility, a second binding event might not be possible for Gal-8S, but for Gal-8L. After the addition of lactose to the MST-buffer in order to mimic binding of a natural ligand during di- or multimerization in solution, no self-interaction was measured anymore, indicating that self-interaction of Gal-8 is independent of a ligand in solution and even interrupted when a ligand is present. Carbohydrate binding could lead to a conformational change in the CRD masking the regions important for dimerization of the single CRDs. As Gal-8 is present in serum, the question arises whether it

exists as di- or multimers or if carbohydrates present in the serum prevent the self-interaction of Gal-8 *in vivo*. It has to be noticed, that the dimerization of Gal-8 occurs with very high affinity with a EC_{50} of 12nM for Gal-8L and 50nM for Gal-8S. The highest serum Gal-8 concentration measured in MM patients was 37pM which is approximately 1000-fold less than necessary for self-aggregation. So it is unlikely that Gal-8 is present as di- or multimers in the serum. Still, local concentrations of the protein could be in nano-molar ranges allowing for dimerization. In this case the aggregated Gal-8 may prevent "unwanted" interactions with glycoproteins in the blood stream, as dimerization could block the binding of certain ligands. At the cell surface, aggregated Gal-8L may help to bring distinct binding partners into proximity and thereby facilitate adhesion processes.

Since crystallization of the full-length protein has not been performed yet, no data about the structure of the complete protein is available. There are only crystal-structures of the single N- or C-CRDs available and a mutant without a linker between the CRDs. Computational modeling using the crystal structure of the single CRDs connected by the insertion of the linker amino acid sequence for both isoforms was performed by Sonu Kumar in order to obtain more insights into the possible structure of the entire protein and whether the conformation of the linker influences the positions of the CRDs to each other. The model suggests that the linker is rather twisted and not stretched forming a loop bringing the CRDs in close proximity to each other. The carbohydrate binding grooves face outwards away from each other. For Gal-8S, the CRDs seem to be closer to each other than for Gal-8L possibly causing a steric hindrance for further multimerization after the formation of a Gal-8S dimer. For Gal-8L, the CRDs are further away from each other, enabling a second binding event. Additionally, as the linker in Gal-8S is shorter, the long linker isoform might be more flexible in stretching of the linker region after dimerization of one of the CRDs allowing further multimerization.

In 2007, Rabinovich *et al.* [58] predicted a model for galectin-multimerization and proposed a theory for the formation of galectin-glycan lattices on the cell surface. The model is shown in the introduction Figure 1.8 and Figure 4.1. Although it is frequently used, several papers question this model. Lepur *et al.* [131] were able to show in 2012 that Gal-3 seems not to be a pentamer in solution if a ligand is present and rather multimerizes via the CRDs and not by binding the amino-acid tail. The Gal-8 N-CRD has been shown to run as a dimer in a SDS-PAGE after chemical crosslinking without a ligand present [98], two Gal-1 CRDs connected by artificial linkers have been shown to homodi - and multimerize [60]. These findings indicate, that galectin-glycan lattice formation and multimerization is a much more complex process than it has been assumed up to now. Additionally, it has to be mentioned

that di- or multimerization is a mechanism that must not be connected to lattice formation. Both processes can occur in absence or presence of a ligand and have to be investigated separately. Even though some galectins are able to di- or multimerize it does not necessarily implicit lattice formation on the cell surface.

Taken together all results of my and published interaction-studies, I conclude that Gal-8S and Gal-8L differ in their ability of self-interaction. This self-interaction is independent of a ligand and occurs in solution. The lattice-formation model of Rabinovich *et al.* [58] has to be extended. From my finding, I propose that the tandem-repeat Gal-8 is able to form dimers or even multimers, depending on the isoform. Binding of a ligand leads to the abrogation of the self-interaction (Figure 4.1).

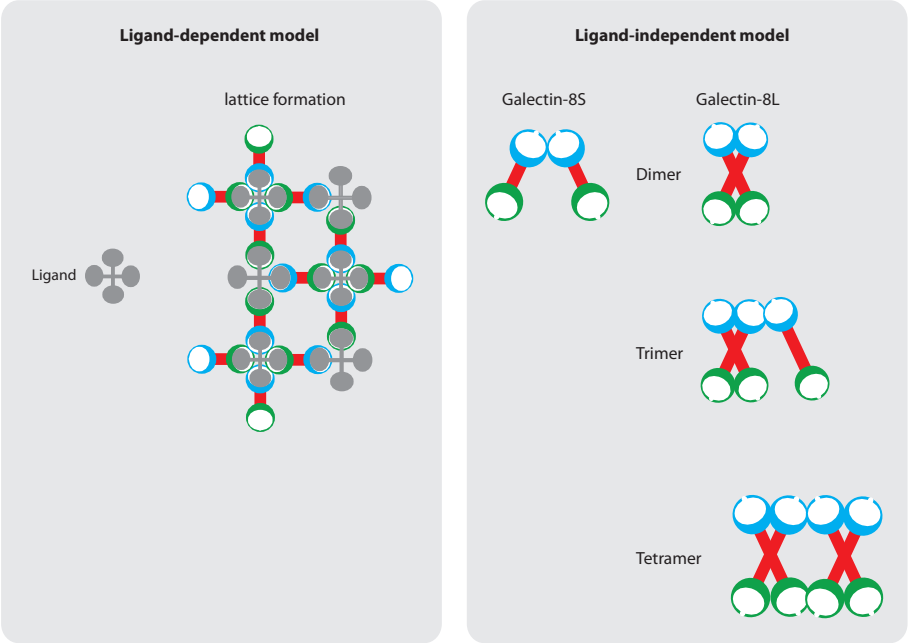

Figure 4.1: Model for ligand-independent di- or multimerization of Gal-8
The ligand-dependent lattice formation model was proposed by Rabinovich *et al.* [58] in 2007. It describes the interaction of tandem-repeat galectins with ligands on the cell surface crosslinking cell surface receptors. There is no experimental evidence that this process occurs *in vivo* and *in vitro*. I propose a ligand independent di- or multimerization for the tandem-repeat Gal-8, depending on the isoform. This self interaction is abrogated if a ligand is present in the solution.

The difference in their ability of self-interaction could also explain differences in the biological activity of both isoforms in terms of homing. The activity of the lectin could be influenced by the di- or multimerization of the protein. As Gal-8L is able to form higher-ordered aggregates, more proteins can bind to the cell surface in closer proximity to each other without sterical hindrances as compared to Gal-8S. This could result in better pro-adhesive capacities of Gal-8L by binding more carbohydrate ligands on MM and EC surfaces as shown in Figure 4.2.

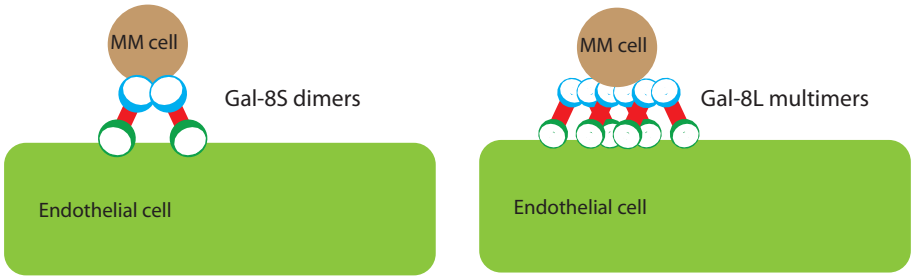

Figure 4.2: Homing of MM to EC
Possible influence of Gal-8 di- or multimerization on adhesion of MM to EC.

4.4 Gal-8 in MM disease progression

MM is a very heterogenous disease in terms of gene expression, hence it is difficult to identify and define prognostic markers or new treatment targets. Today, still many patients have a relapse due to treatment-resistant MM clones and a cure of the disease is not possible at the moment. Identifying novel drug-targets may improve clinical outcomes, new prognostic markers could help for the selection of treatment options according to a patients' risk type and give the opportunity of individualized therapy.

My studies showed that Gal-8 serum levels were higher in many, but not all, MM patients compared to HD and further survival analysis revealed that patients expressing high Gal-8 mRNA levels have a shorter survival and a faster progression compared to patients with low Gal-8 expression. This negative effect of Gal-8 transcription is also reflected by the correlation of high Gal-8 expression with chromosomal aberrations that are known to occur frequently in MM. The gal-8 gene is located on chromosome 1 (1q43), one frequent aberration correlating with Gal-8 expression is the gain of 1q21. As the positions 1q21 and 1q43 are close to each other, duplication of 1q21 could possibly also regulate the expression of Gal-8 leading to higher transcription of the gene. The analysis of MM patients' samples indicated that Gal-8 influences MM progression. According to my observations, Gal-8 could be used as an additional prognostic marker for MM since the disease seems to progress more aggressively in individuals with high Gal-8 expression.

It is noticeable that the mean Gal-8 concentration in the serum of HD as well as in MM patients was much lower as compared to other studies that measured Gal-8 serum levels in colon and breast cancer patients [74]. In those studies the Gal-8 concentration was determined to be an average of 10ng/ml ranging from approximately 0.1 to 100ng/ml. These differences to my study may be due to the specificity of the Gal-8 ELISA. Barrow *et al.* [74] used a polyclonal catcher antibody and the

same antibody coupled to biotin for detection. Performing an ELISA with two polyclonal antibodies may cause unspecific binding as well as detection of other serum galectins, since they are very homologous. In my study, I applied a monoclonal antibody as catcher antibody and the biotinylated polyclonal antibody for detection. Using a monoclonal catcher antibody leads to a higher specificity of the ELISA and therefore more reliable data with regard to Gal-8 serum concentrations.

Observing the pro-adhesive effect of Gal-8 a question that arises is: where does Gal-8 actually come from *in vivo*? Both, MM cells as well as EC are able to produce and secrete Gal-8. Therefore, the protein in the serum could come from both or from other sources. But due to experimental constraints, the isoforms present in the serum could not be defined. Intracellularly, MOLP-8 produces less Gal-8L than Gal-8S, EC produce both isoforms in comparable amounts. The question is whether MOLP-8 is able to selectively secrete Gal-8L into the supernatant because of its stronger pro-adhesive properties. Nevertheless, even if only Gal-8S is secreted and present in the serum, this also has an pro-adhesive effect though with lower affinities. For further experiments an isoform-specific ELISA should be developed in order to define the ratios of Gal-8S to Gal-8L in the sera and supernatants used for adhesion assays.

To solve the question where Gal-8 originates from, further *in vivo* studies have to be performed. Histopathology of BM sections could show if Gal-8 is present in the BM microenvironment and which cells could be the main producers.

In which stage of the disease is a pro-adhesive effect of Gal-8 in a non-inflammatory environment beneficial? Usually, an inflammatory environment is crucial for the adhesion of leucocytes, since most adhesion molecules are only expressed in inflamed tissues. Gal-8 promotes adhesion even without prior stimulation of the EC. Since the whole genome array covers both isoforms for expression analysis, the effect of the isoforms could not be taken into account. Nevertheless in view of Gal-8^{high} patients' lower survival rate and faster progression of the disease, Gal-8 could either promote the first homing steps of MM cells to the BM or allow the circulating MM cells to home into different sites of the disease without the dependance on other adhesion molecules. Still, it must be noticed that Gal-8 also has a beneficial, though small effect on adhesion in an inflammatory environment. During the progression of the disease, many pro-inflammatory cytokines are produced by MM cells leading to an inflammatory situation in the BM microenvironment [1]. Gal-8 has also been shown to further increase the adhesion of MM cells to EC, which is already strong after TNF-α stimulation due to the expression of many other adhesion molecules like E-selectin or ICAM-I. So even in later stages of the disease, Gal-8 expression

and secretion can be beneficial for MM cells in terms of homing and spreading of the disease.

Comparing the experimental set-up with the *in vivo* situation, one recognizes that the serum level in MM patients had a maximum at 1.33ng/ml (37pM), the mean concentration was 0.22ng/ml (6pM). This is around 5000-fold lower than the concentration used for *in vitro* adhesion assays which was 100nM. It has to be considered that serum was used for the analysis and not fresh plasma or whole-blood samples. Some Gal-8 might be lost during the coagulation of blood proteins since galectins are rather sticky proteins with a tendency for aggregation. Additionally, the local concentrations e.g. in the bone marrow might be higher in sites of MM adhesion. Furthermore, Gal-8 conditioned medium with mean concentration of 0.33ng/ml (9pM) Gal-8 was able to enhance adhesion compared to Gal-8 depleted medium indicating that lower Gal-8 concentrations might still be effective. SDS gels stained with Comassie brilliant blue showed some degradation products in the recombinant protein. So may be lower concentrations of active protein were actually used in this study.

4.5 Gal-8 as target for anti-myeloma therapy

Targeting homing mechanisms in MM treatment seems to be beneficial and prevention of MM-EC interactions could disrupt the disease spreading in the BM. Furthermore, more cells could be forced to circulate in the blood stream by the inhibition of MM-EC interactions leading to an improved susceptibility for other drugs.

Since it has been described that galectins might play a role in cancer and other diseases, anti-galectin compounds may be used for treatment. For this purpose, several modes of galectin-intervention could be tried, for example natural ligands, carbohydrate analogues of natural ligands or anti-galectin antibodies [132]. For Gal-1 and Gal-3, several trials have been made using different galectin antagonists. DB21, an allosteric antagonist of Gal-1 was used to inhibit tumor angiogenesis and tumor growth in mouse models [133], in a breast cancer model Gal-1 blocking disaccharides were successfully administered as an adjuvant therapy promoting immune responses [134]. Two studies using the Gal-3 inhibitors GR-MD-01 and GR-MD-02 reveal their function in treatment of liver fibrosis and steatohepatitis in mice [135, 136]. In MM GCS-100, a Gal-3 antagonist, was shown to inhibit tumor cell growth *in vitro* [82]. But no clinical studies in humans proofing the effectiveness of these drugs in patients have been published yet.

These studies show in principle, that galectin-antagonists are a therapeutic option that should be considered in diseases where galectins are involved. Up to now, no Gal-8 specific inhibitor has been developed which may be an option for treatment of Gal-8^{high} MM patients. But still more experiments have to be performed, in order to find out which role Gal-8 plays in MM and how it influences the progression of the disease. Pro-adhesive effects of Gal-8 have not only been shown concerning MM-EC interactions, PBMC from healthy donors are also able to adhere stronger to HUVEC in the presence of Gal-8 [137]. Blocking these interactions could interfere with basic functions of the immune system, more experiments need to be performed in order to investigate the role of Gal-8 in healthy individuals.

In conclusion, I was able to show that Gal-8 influences MM biology by enhancing the binding of MM cells to EC and thereby possibly influencing the progression of the disease and the survival time of the patients. Additionally, this study shows for the first time that the two isoforms of Gal-8 have different activities *in vitro*. These differences must be considered in further studies by taking both isoforms into account.

A

Publications

Götschel F, Berg D, Gruber W, Bender C, Eberl M, **Friedel M**, Sonntag J, Rüngeler E, Hache H, Wierling C, Nietfeld W, Lehrach H, Frischauf A, Schwartz-Albiez R, Aberger F, Korf U: Synergism between Hedgehog-GLI and EGFR Signaling in Hedgehog-Responsive Human Medulloblastoma Cells Induces Downregulation of Canonical Hedgehog-Target Genes and Stabilized Expression of GLI1. PLoS ONE 2013, 8(6):e65403

B

Danksagung

An dieser Stelle möchte ich mich bei allen bedanken, die zum Erstellen und Gelingen meiner Doktorarbeit beigetragen haben.
Besonders bedanken möchte ich mich bei:

PD Dr. Reinhard Schwartz-Albiez, für die Möglichkeit meine Doktorarbeit in seiner Arbeitsgruppe anzufertigen, die Gedult, Kritik und die Bereitschaft zur Diskussion.

Prof. Dr. Rainer Zawatzky, für die Bereitschaft sowohl die Tätigkeit als Erstgutachter zu übernehmen als auch in meinem TAC mitzuwirken.

Prof. Dr. Christian Körner, für die Übernahme des Prüfungsvorsitzes und der Bereitschaft sich an meiner Verteidigung als Prüfer beteiligen.

Dr. Markus Feuerer, für die Beteiligung am Prüfungsauschuss.

Prof. Dr. Inaam Nakchbandi, für die Bereitschaft an meinem TAC mitzuwirken.

Prof. Dr. Dr. h.c. Hans-Joachim Gabius, für die Produktion und Bereitstellung der Galektine.

Der kompletten Arbeitsgruppe Glykoimmunologie, für den Spaß im Labor, ein stets offenes Ohr für alle Probleme, gelungene Laborausflüge und die schöne Zeit mit Euch während der letzten Jahre.

Sandra Bondong und Martin Heinemann, für die Hilfe mit dem Layout, dem Erstellen der Doktorarbeit und die gemeinsamen Kaffeepausen.

Meiner Familie, im besonderen bei meinen Eltern Ina Schlesinger-Friedel und Peter Friedel: Ohne Eure Unterstützung hätte ich weder Biologie studiert noch meine Doktorarbeit gemacht. Ihr seit mein Rückhalt und ich bin dankbar, dass ich mich immer auf Euch verlassen kann und auf darauf vertrauen kann, dass Ihr hinter mir steht.

Die vorliegende Arbeit wurde von der “Deutsche José Carreras Leukämie-Stiftung e.V.” (Stipendium DJCLS R10/32f) finanziert.

Bibliography

[1] Antonio Palumbo and Kenneth Anderson. Multiple myeloma. *N Engl J Med*, 364(11):1046–1060, Mar 2011.

[2] N. Howlader, AM. Noone, M. Krapcho, J. Garshell, N. Neyman, SF. Altekruse, CL. Kosary, M. Yu, J. Ruhl, Z. Tatalovich, H. Cho, A. Mariotto, DR. Lewis, HS. Chen, EJ. Feuer, and KA (eds) Cronin. Seer cancer statistics review, 1975-2010. 2012.

[3] Kenneth C. Anderson and Ruben D. Carrasco. Pathogenesis of myeloma. *Annu Rev Pathol*, 6:249–274, 2011.

[4] Robert A. Kyle, Terry M. Therneau, S Vincent Rajkumar, Dirk R. Larson, Matthew F. Plevak, Janice R. Offord, Angela Dispenzieri, Jerry A. Katzmann, and L Joseph Melton, 3rd. Prevalence of monoclonal gammopathy of undetermined significance. *N Engl J Med*, 354(13):1362–1369, Mar 2006.

[5] Dean Smith and Kwee Yong. Multiple myeloma. *BMJ*, 346:f3863, 2013.

[6] Gareth J. Morgan, Brian A. Walker, and Faith E. Davies. The genetic architecture of multiple myeloma. *Nat Rev Cancer*, 12(5):335–348, May 2012.

[7] W Michael Kuehl and P Leif Bergsagel. Multiple myeloma: evolving genetic events and host interactions. *Nat Rev Cancer*, 2(3):175–187, Mar 2002.

[8] Joseph R. Mikhael, David Dingli, Vivek Roy, Craig B. Reeder, Francis K. Buadi, Suzanne R. Hayman, Angela Dispenzieri, Rafael Fonseca, Taimur Sher, Robert A. Kyle, Yi Lin, Stephen J. Russell, Shaji Kumar, P Leif Bergsagel, Steven R. Zeldenrust, Nelson Leung, Matthew T. Drake, Prashant Kapoor, Stephen M. Ansell, Thomas E. Witzig, John A. Lust, Robert J. Dalton, Morie A. Gertz, A Keith Stewart, Keith Stewart, S Vincent Rajkumar, Asher Chanan-Khan, Martha Q. Lacy, and Mayo Clinic . Management of newly diagnosed symptomatic multiple myeloma: updated mayo stratification of myeloma and risk-adapted therapy (msmart) consensus guidelines 2013. *Mayo Clin Proc*, 88(4):360–376, Apr 2013.

[9] Jean-Paul Fermand, Sandrine Katsahian, Marine Divine, Veronique Leblond, Francois Dreyfus, Margaret Macro, Bertrand Arnulf, Bruno Royer, Xavier Mariette, Edouard Pertuiset, Coralie Belanger, Maud Janvier, Sylvie Chevret, Jean Claude Brouet, Philippe Ravaud, and Group Myelome-Autogreffe . High-dose therapy and autologous blood stem-cell transplantation compared with conventional treatment in myeloma patients aged 55 to 65 years: long-term results of a randomized control trial from the group myelome-autogreffe. *J Clin Oncol*, 23(36):9227–9233, Dec 2005.

[10] S. Manier, A. Sacco, X. Leleu, I. M. Ghobrial, and A. M. Roccaro. Bone marrow microenvironment in multiple myeloma progression. *J Biomed Biotechnol*, 2012:157496, 2012.

[11] Teru Hideshima, Constantine Mitsiades, Giovanni Tonon, Paul G. Richardson, and Kenneth C. Anderson. Understanding multiple myeloma pathogenesis in the bone marrow to identify new therapeutic targets. *Nat Rev Cancer*, 7(8):585–598, Aug 2007.

[12] Guido Pagnucco, Giovanni Cardinale, and Francesco Gervasi. Targeting multiple myeloma cells and their bone marrow microenvironment. *Ann N Y Acad Sci*, 1028:390–399, Dec 2004.

[13] Peter Carmeliet and Rakesh K. Jain. Molecular mechanisms and clinical applications of angiogenesis. *Nature*, 473(7347):298–307, May 2011.

[14] P. Carmeliet and R. K. Jain. Angiogenesis in cancer and other diseases. *Nature*, 407(6801):249–257, Sep 2000.

[15] Gabriele Bergers and Laura E. Benjamin. Tumorigenesis and the angiogenic switch. *Nat Rev Cancer*, 3(6):401–410, Jun 2003.

[16] P. Carmeliet. Mechanisms of angiogenesis and arteriogenesis. *Nat Med*, 6(4):389–395, Apr 2000.

[17] Peter Carmeliet. Angiogenesis in life, disease and medicine. *Nature*, 438(7070):932–936, Dec 2005.

[18] Areck A. Ucuzian, Andrew A. Gassman, Andrea T. East, and Howard P. Greisler. Molecular mediators of angiogenesis. *J Burn Care Res*, 31(1):158–175, 2010.

[19] Michael Simons. Angiogenesis: where do we stand now? *Circulation*, 111(12):1556–1566, Mar 2005.

[20] Hira Lal Goel and Arthur M. Mercurio. Vegf targets the tumour cell. *Nat Rev Cancer*, 13(12):871–882, Dec 2013.

[21] D. Hanahan and R. A. Weinberg. The hallmarks of cancer. *Cell*, 100(1):57–70, Jan 2000.

[22] Douglas Hanahan and Robert A. Weinberg. Hallmarks of cancer: the next generation. *Cell*, 144(5):646–674, Mar 2011.

[23] Adriana Albini, Francesca Tosetti, Vincent W. Li, Douglas M. Noonan, and William W. Li. Cancer prevention by targeting angiogenesis. *Nat Rev Clin Oncol*, 9(9):498–509, Sep 2012.

[24] A. Vacca, D. Ribatti, L. Roncali, G. Ranieri, G. Serio, F. Silvestris, and F. Dammacco. Bone marrow angiogenesis and progression in multiple myeloma. *Br J Haematol*, 87(3):503–508, Jul 1994.

[25] T. M. Moehler, A. D. Ho, H. Goldschmidt, and B. Barlogie. Angiogenesis in hematologic malignancies. *Crit Rev Oncol Hematol*, 45(3):227–244, Mar 2003.

[26] A. Vacca and D. Ribatti. Bone marrow angiogenesis in multiple myeloma. *Leukemia*, 20(2):193–199, Feb 2006.

[27] H. De Raeve, E. Van Marck, B. Van Camp, and K. Vanderkerken. Angiogenesis and the role of bone marrow endothelial cells in haematological malignancies. *Histol Histopathol*, 19(3):935–950, Jul 2004.

[28] Grzegorz S. Nowakowski, Thomas E. Witzig, David Dingli, Michal J. Tracz, Morie A. Gertz, Martha Q. Lacy, John A. Lust, Angela Dispenzieri, Philip R. Greipp, Robert A. Kyle, and S Vincent Rajkumar. Circulating plasma cells detected by flow cytometry as a predictor of survival in 302 patients with newly diagnosed multiple myeloma. *Blood*, 106(7):2276–2279, Oct 2005.

[29] Isabelle Vande Broek, Karin Vanderkerken, Benjamin Van Camp, and Ivan Van Riet. Extravasation and homing mechanisms in multiple myeloma. *Clin Exp Metastasis*, 25(4):325–334, 2008.

[30] T. E. Witzig, T. K. Kimlinger, G. J. Ahmann, J. A. Katzmann, and P. R. Greipp. Detection of myeloma cells in the peripheral blood by flow cytometry. *Cytometry*, 26(2):113–120, Jun 1996.

[31] E. C. Butcher and L. J. Picker. Lymphocyte homing and homeostasis. *Science*, 272(5258):60–66, Apr 1996.

[32] Klaus Ley, Carlo Laudanna, Myron I. Cybulsky, and Sussan Nourshargh. Getting to the site of inflammation: the leukocyte adhesion cascade updated. *Nat Rev Immunol*, 7(9):678–689, Sep 2007.

[33] Rodger P. McEver. Selectins: lectins that initiate cell adhesion under flow. *Curr Opin Cell Biol*, 14(5):581–586, Oct 2002.

[34] E. B. Finger, K. D. Puri, R. Alon, M. B. Lawrence, U. H. von Andrian, and T. A. Springer. Adhesion through l-selectin requires a threshold hydrodynamic shear. *Nature*, 379(6562):266–269, Jan 1996.

[35] M. B. Lawrence, G. S. Kansas, E. J. Kunkel, and K. Ley. Threshold levels of fluid shear promote leukocyte adhesion through selectins (cd62l,p,e). *J Cell*

Biol, 136(3):717–727, Feb 1997.

[36] Bryan T. Marshall, Mian Long, James W. Piper, Tadayuki Yago, Rodger P. McEver, and Cheng Zhu. Direct observation of catch bonds involving cell-adhesion molecules. *Nature*, 423(6936):190–193, May 2003.

[37] Richard O. Hynes. Integrins: bidirectional, allosteric signaling machines. *Cell*, 110(6):673–687, Sep 2002.

[38] Dermot Cox, Marian Brennan, and Niamh Moran. Integrins as therapeutic targets: lessons and opportunities. *Nat Rev Drug Discov*, 9(10):804–820, Oct 2010.

[39] Marcelina E. Janik, Anna Litynska, and Pierre Vereecken. Cell migration-the role of integrin glycosylation. *Biochim Biophys Acta*, 1800(6):545–555, Jun 2010.

[40] Rohit Aggarwal, Irene M. Ghobrial, and G David Roodman. Chemokines in multiple myeloma. *Exp Hematol*, 34(10):1289–1295, Oct 2006.

[41] Marisa Parmo-Cabañas, Rubén A. Bartolomé, Natalia Wright, Andrés Hidalgo, Angelika M. Drager, and Joaquin Teixidó. Integrin alpha4beta1 involvement in stromal cell-derived factor-1alpha-promoted myeloma cell transendothelial migration and adhesion: role of camp and the actin cytoskeleton in adhesion. *Exp Cell Res*, 294(2):571–580, Apr 2004.

[42] Yue Geng, Jocelyn R. Marshall, and Michael R. King. Glycomechanics of the metastatic cascade: tumor cell-endothelial cell interactions in the circulation. *Ann Biomed Eng*, 40(4):790–805, Apr 2012.

[43] Irina Häuselmann and Lubor Borsig. Altered tumor-cell glycosylation promotes metastasis. *Front Oncol*, 4:28, 2014.

[44] Diego O. Croci, Juan P. Cerliani, Tomas Dalotto-Moreno, Santiago P. Méndez-Huergo, Ivan D. Mascanfroni, Sebastián Dergan-Dylon, Marta A. Toscano, Julio J. Caramelo, Juan J. García-Vallejo, Jing Ouyang, Enrique A. Mesri, Melissa R. Junttila, Carlos Bais, Margaret A. Shipp, Mariana Salatino, and Gabriel A. Rabinovich. Glycosylation-dependent lectin-receptor interactions preserve angiogenesis in anti-vegf refractory tumors. *Cell*, 156(4):744–758, Feb 2014.

[45] Thomas M. Moehler, Anja Seckinger, Dirk Hose, Mindaugas Andrulis, Jèrôme Moreaux, Thomas Hielscher, Martina Willhauck-Fleckenstein, Anette Merling, Uta Bertsch, Anna Jauch, Hartmut Goldschmidt, Bernard Klein, and Reinhard Schwartz-Albiez. The glycome of normal and malignant plasma cells. *PLoS One*, 8(12):e83719, 2013.

[46] Susumu Nakahara and Avraham Raz. Biological modulation by lectins and their ligands in tumor progression and metastasis. *Anticancer Agents Med*

Chem, 8(1):22–36, Jan 2008.

[47] Nathan Sharon and Halina Lis. History of lectins: from hemagglutinins to biological recognition molecules. *Glycobiology*, 14(11):53R–62R, Nov 2004.

[48] S. H. Barondes, V. Castronovo, D. N. Cooper, R. D. Cummings, K. Drickamer, T. Feizi, M. A. Gitt, J. Hirabayashi, C. Hughes, and K. Kasai. Galectins: a family of animal beta-galactoside-binding lectins. *Cell*, 76(4):597–598, Feb 1994.

[49] D. N. Cooper and S. H. Barondes. God must love galectins; he made so many of them. *Glycobiology*, 9(10):979–984, Oct 1999.

[50] Hakon Leffler, Susanne Carlsson, Maria Hedlund, Yuning Qian, and Francoise Poirier. Introduction to galectins. *Glycoconj J*, 19(7-9):433–440, 2004.

[51] J. Hirabayashi and K. Kasai. The family of metazoan metal-independent beta-galactoside-binding lectins: structure, function and molecular evolution. *Glycobiology*, 3(4):297–304, Aug 1993.

[52] Nisar Ahmad, Hans-J. Gabius, Sabine André, Herbert Kaltner, Subramanian Sabesan, René Roy, Bingcan Liu, Frank Macaluso, and C Fred Brewer. Galectin-3 precipitates as a pentamer with synthetic multivalent carbohydrates and forms heterogeneous cross-linked complexes. *J Biol Chem*, 279(12):10841–10847, Mar 2004.

[53] Stephanie Morris, Nisar Ahmad, Sabine André, Herbert Kaltner, Hans-J. Gabius, Michael Brenowitz, and Fred Brewer. Quaternary solution structures of galectins-1, -3, and -7. *Glycobiology*, 14(3):293–300, Mar 2004.

[54] C Fred Brewer, M Carrie Miceli, and Linda G. Baum. Clusters, bundles, arrays and lattices: novel mechanisms for lectin-saccharide-mediated cellular interactions. *Curr Opin Struct Biol*, 12(5):616–623, Oct 2002.

[55] K. E. Pace, C. Lee, P. L. Stewart, and L. G. Baum. Restricted receptor segregation into membrane microdomains occurs on human t cells during apoptosis induced by galectin-1. *J Immunol*, 163(7):3801–3811, Oct 1999.

[56] Brianna N. Stillman, Daniel K. Hsu, Mabel Pang, C Fred Brewer, Pauline Johnson, Fu-Tong Liu, and Linda G. Baum. Galectin-3 and galectin-1 bind distinct cell surface glycoprotein receptors to induce t cell death. *J Immunol*, 176(2):778–789, Jan 2006.

[57] Julie Nieminen, Atsushi Kuno, Jun Hirabayashi, and Sachiko Sato. Visualization of galectin-3 oligomerization on the surface of neutrophils and endothelial cells using fluorescence resonance energy transfer. *J Biol Chem*, 282(2):1374–1383, Jan 2007.

[58] Gabriel A. Rabinovich, Marta A. Toscano, Shawn S. Jackson, and Gerardo R. Vasta. Functions of cell surface galectin-glycoprotein lattices. *Curr Opin Struct*

Biol, 17(5):513–520, Oct 2007.

[59] Gabriel A. Rabinovich and Marta A. Toscano. Turning 'sweet' on immunity: galectin-glycan interactions in immune tolerance and inflammation. *Nat Rev Immunol*, 9(5):338–352, May 2009.

[60] Lesley A. Earl, Shuguang Bi, and Linda G. Baum. Galectin multimerization and lattice formation are regulated by linker region structure. *Glycobiology*, 21(1):6–12, Jan 2011.

[61] R. C. Hughes. Secretion of the galectin family of mammalian carbohydrate-binding proteins. *Biochim Biophys Acta*, 1473(1):172–185, Dec 1999.

[62] Gerardo R. Vasta. Roles of galectins in infection. *Nat Rev Microbiol*, 7(6):424–438, Jun 2009.

[63] Fu-Tong Liu and Gabriel A. Rabinovich. Galectins as modulators of tumour progression. *Nat Rev Cancer*, 5(1):29–41, Jan 2005.

[64] Arun Satelli, Prema S. Rao, Prem K. Gupta, Paul R. Lockman, Kalkunte S. Srivenugopal, and U Subrahmanyeswara Rao. Varied expression and localization of multiple galectins in different cancer cell lines. *Oncol Rep*, 19(3):587–594, Mar 2008.

[65] H. Lahm, S. André, A. Hoeflich, J. R. Fischer, B. Sordat, H. Kaltner, E. Wolf, and H. J. Gabius. Comprehensive galectin fingerprinting in a panel of 61 human tumor cell lines by rt-pcr and its implications for diagnostic and therapeutic procedures. *J Cancer Res Clin Oncol*, 127(6):375–386, 2001.

[66] A. Paz, R. Haklai, G. Elad-Sfadia, E. Ballan, and Y. Kloog. Galectin-1 binds oncogenic h-ras to mediate ras membrane anchorage and cell transformation. *Oncogene*, 20(51):7486–7493, Nov 2001.

[67] Christian Fischer, Hugo Sanchez-Ruderisch, Martina Welzel, Bertram Wiedenmann, Toshiyuki Sakai, Sabine André, Hans-Joachim Gabius, Levon Khachigian, Katharina M. Detjen, and Stefan Rosewicz. Galectin-1 interacts with the alpha5beta1 fibronectin receptor to restrict carcinoma cell growth via induction of p21 and p27. *J Biol Chem*, 280(44):37266–37277, Nov 2005.

[68] Galit Elad-Sfadia, Roni Haklai, Eyal Balan, and Yoel Kloog. Galectin-3 augments k-ras activation and triggers a ras signal that attenuates erk but not phosphoinositide 3-kinase activity. *J Biol Chem*, 279(33):34922–34930, Aug 2004.

[69] Emily A. Partridge, Christine Le Roy, Gianni M. Di Guglielmo, Judy Pawling, Pam Cheung, Maria Granovsky, Ivan R. Nabi, Jeffrey L. Wrana, and James W. Dennis. Regulation of cytokine receptors by golgi n-glycan processing and endocytosis. *Science*, 306(5693):120–124, Oct 2004.

[70] S. Akahani, P. Nangia-Makker, H. Inohara, H. R. Kim, and A. Raz. Galectin-3: a novel antiapoptotic molecule with a functional bh1 (nwgr) domain of bcl-2 family. *Cancer Res*, 57(23):5272–5276, Dec 1997.

[71] R. Y. Yang, D. K. Hsu, and F. T. Liu. Expression of galectin-3 modulates t-cell growth and apoptosis. *Proc Natl Acad Sci U S A*, 93(13):6737–6742, Jun 1996.

[72] Huei-Min Lin, Richard G. Pestell, Avraham Raz, and Hyeong-Reh Choi Kim. Galectin-3 enhances cyclin d(1) promoter activity through sp1 and a camp-responsive element in human breast epithelial cells. *Oncogene*, 21(52):8001–8010, Nov 2002.

[73] J. Ochieng, M. L. Leite-Browning, and P. Warfield. Regulation of cellular adhesion to extracellular matrix proteins by galectin-3. *Biochem Biophys Res Commun*, 246(3):788–791, May 1998.

[74] Hannah Barrow, Xiuli Guo, Hans H. Wandall, Johannes W. Pedersen, Bo Fu, Qicheng Zhao, Chen Chen, Jonathan M. Rhodes, and Lu-Gang Yu. Serum galectin-2, -4, and -8 are greatly increased in colon and breast cancer patients and promote cancer cell adhesion to blood vascular endothelium. *Clin Cancer Res*, 17(22):7035–7046, Nov 2011.

[75] Claudia Cárcamo, Evelyn Pardo, Claudia Oyanadel, Marcela Bravo-Zehnder, Paulina Bull, Mónica Cáceres, Jorge Martínez, Loreto Massardo, Sergio Jacobelli, Alfonso González, and Andrea Soza. Galectin-8 binds specific beta1 integrins and induces polarized spreading highlighted by asymmetric lamellipodia in jurkat t cells. *Exp Cell Res*, 312(4):374–386, Feb 2006.

[76] Y. R. Hadari, R. Arbel-Goren, Y. Levy, A. Amsterdam, R. Alon, R. Zakut, and Y. Zick. Galectin-8 binding to integrins inhibits cell adhesion and induces apoptosis. *J Cell Sci*, 113 (Pt 13):2385–2397, Jul 2000.

[77] Y. Levy, R. Arbel-Goren, Y. R. Hadari, S. Eshhar, D. Ronen, E. Elhanany, B. Geiger, and Y. Zick. Galectin-8 functions as a matricellular modulator of cell adhesion. *J Biol Chem*, 276(33):31285–31295, Aug 2001.

[78] Nozomu Nishi, Hiroki Shoji, Masako Seki, Aiko Itoh, Hiroshi Miyanaka, Kouichi Yuube, Mitsuomi Hirashima, and Takanori Nakamura. Galectin-8 modulates neutrophil function via interaction with integrin alpham. *Glycobiology*, 13(11):755–763, Nov 2003.

[79] Saeid Abroun, Ken-Ichiro Otsuyama, Karim Shamsasenjan, Abul Islam, Jakia Amin, Mohd S. Iqbal, Toshikazu Gondo, Hideki Asaoku, and Michio M. Kawano. Galectin-1 supports the survival of cd45ra(-) primary myeloma cells in vitro. *Br J Haematol*, 142(5):754–765, Sep 2008.

[80] Katrina K. Hoyer, Mabel Pang, Dorina Gui, I Peter Shintaku, Ichiro Kuwabara, Fu-Tong Liu, Jonathan W. Said, Linda G. Baum, and Michael A. Teitell. An anti-apoptotic role for galectin-3 in diffuse large b-cell lymphomas. *Am J Pathol*, 164(3):893–902, Mar 2004.

[81] T. Kobayashi, J. Kuroda, E. Ashihara, S. Oomizu, Y. Terui, A. Taniyama, S. Adachi, T. Takagi, M. Yamamoto, N. Sasaki, S. Horiike, K. Hatake, A. Yamauchi, M. Hirashima, and M. Taniwaki. Galectin-9 exhibits anti-myeloma activity through jnk and p38 map kinase pathways. *Leukemia*, 24(4):843–850, Apr 2010.

[82] Matthew J. Streetly, Lenushka Maharaj, Simon Joel, Steve A. Schey, John G. Gribben, and Finbarr E. Cotter. Gcs-100, a novel galectin-3 antagonist, modulates mcl-1, noxa, and cell cycle to induce myeloma cell death. *Blood*, 115(19):3939–3948, May 2010.

[83] Y. R. Hadari, K. Paz, R. Dekel, T. Mestrovic, D. Accili, and Y. Zick. Galectin-8. a new rat lectin, related to galectin-4. *J Biol Chem*, 270(7):3447–3453, Feb 1995.

[84] R. V. Gopalkrishnan, T. Roberts, S. Tuli, D. Kang, K. A. Christiansen, and P. B. Fisher. Molecular characterization of prostate carcinoma tumor antigen-1, pcta-1, a human galectin-8 related gene. *Oncogene*, 19(38):4405–4416, Sep 2000.

[85] Nathalie Bidon-Wagner and Jean-Paul Le Pennec. Human galectin-8 isoforms and cancer. *Glycoconj J*, 19(7-9):557–563, 2004.

[86] I. Camby, N. Belot, S. Rorive, F. Lefranc, C. A. Maurage, H. Lahm, H. Kaltner, Y. Hadari, M. M. Ruchoux, J. Brotchi, Y. Zick, I. Salmon, H. J. Gabius, and R. Kiss. Galectins are differentially expressed in supratentorial pilocytic astrocytomas, astrocytomas, anaplastic astrocytomas and glioblastomas, and significantly modulate tumor astrocyte migration. *Brain Pathol*, 11(1):12–26, Jan 2001.

[87] N. Nagy, Y. Bronckart, I. Camby, H. Legendre, H. Lahm, H. Kaltner, Y. Hadari, P. Van Ham, P. Yeaton, J-C. Pector, Y. Zick, I. Salmon, A. Danguy, R. Kiss, and H-J. Gabius. Galectin-8 expression decreases in cancer compared with normal and dysplastic human colon tissue and acts significantly on human colon cancer cell migration as a suppressor. *Gut*, 50(3):392–401, Mar 2002.

[88] Victor L. Thijssen, Sarah Hulsmans, and Arjan W. Griffioen. The galectin profile of the endothelium: altered expression and localization in activated and tumor endothelial cells. *Am J Pathol*, 172(2):545–553, Feb 2008.

[89] C. Chen, C. A. Duckworth, B. Fu, D. M. Pritchard, J. M. Rhodes, and L-G. Yu. Circulating galectins -2, -4 and -8 in cancer patients make important

contributions to the increased circulation of several cytokines and chemokines that promote angiogenesis and metastasis. *Br J Cancer*, 110(3):741–752, Feb 2014.

[90] Stéphanie Cludts, Christine Decaestecker, Virginie Mahillon, Dominique Chevalier, Herbert Kaltner, Sabine André, Myriam Remmelink, Xavier Leroy, Hans-Joachim Gabius, and Sven Saussez. Galectin-8 up-regulation during hypopharyngeal and laryngeal tumor progression and comparison with galectin-1, -3 and -7. *Anticancer Res*, 29(12):4933–4940, Dec 2009.

[91] Geun Woo Dong, Jun Kim, Jun Hee Park, Ji Yun Choi, Sung Il Cho, and Sung Chul Lim. Galectin-8 expression in laryngeal squamous cell carcinoma. *Clin Exp Otorhinolaryngol*, 2(1):13–19, Mar 2009.

[92] Mario Wolfgang Kramer, Sandra Waalkes, Jürgen Serth, Jörg Hennenlotter, Hossein Tezval, Arnulf Stenzl, Markus Antonius Kuczyk, and Axel Stuart Merseburger. Decreased galectin-8 is a strong marker for recurrence in urothelial carcinoma of the bladder. *Urol Int*, 87(2):143–150, 2011.

[93] S. Savin, D. Cveji?, M. Jankovi?, T. Isi?, I. Paunovi?, and S. Tati? Evaluation of galectin-8 expression in thyroid tumors. *Med Oncol*, 26(3):314–318, 2009.

[94] Susanne Carlsson, Christopher T. Oberg, Michael C. Carlsson, Anders Sundin, Ulf J. Nilsson, David Smith, Richard D. Cummings, Jenny Almkvist, Anna Karlsson, and Hakon Leffler. Affinity of galectin-8 and its carbohydrate recognition domains for ligands in solution and at the cell surface. *Glycobiology*, 17(6):663–676, Jun 2007.

[95] Hiroko Ideo, Tsutomu Matsuzaka, Takamasa Nonaka, Akira Seko, and Katsuko Yamashita. Galectin-8-n-domain recognition mechanism for sialylated and sulfated glycans. *J Biol Chem*, 286(13):11346–11355, Apr 2011.

[96] Hiroko Ideo, Akira Seko, Ineo Ishizuka, and Katsuko Yamashita. The n-terminal carbohydrate recognition domain of galectin-8 recognizes specific glycosphingolipids with high affinity. *Glycobiology*, 13(10):713–723, Oct 2003.

[97] Sonu Kumar, Martin Frank, and Reinhard Schwartz-Albiez. Understanding the specificity of human galectin-8c domain interactions with its glycan ligands based on molecular dynamics simulations. *PLoS One*, 8(3):e59761, 2013.

[98] Sean R. Stowell, Connie M. Arthur, Kristin A. Slanina, John R. Horton, David F. Smith, and Richard D. Cummings. Dimeric galectin-8 induces phosphatidylserine exposure in leukocytes through polylactosamine recognition by the c-terminal domain. *J Biol Chem*, 283(29):20547–20559, Jul 2008.

[99] O. A. Vokhmyanina, E. M. Rapoport, I. M. Ryzhov, E Yu Korchagina, G. V. Pazynina, V. V. Severov, H. Kaltner, S. André, H-J. Gabius, and N. V. Bovin.

Carbohydrate specificity of chicken and human tandem-repeat-type galectins-8 in composition of cells. *Biochemistry (Mosc)*, 76(10):1185–1192, Oct 2011.

[100] Andrés Norambuena, Claudia Metz, Lucas Vicuña, Antonia Silva, Evelyn Pardo, Claudia Oyanadel, Loreto Massardo, Alfonso González, and Andrea Soza. Galectin-8 induces apoptosis in jurkat t cells by phosphatidic acid-mediated erk1/2 activation supported by protein kinase a down-regulation. *J Biol Chem*, 284(19):12670–12679, May 2009.

[101] Víctor M Cárdenas Delgado, Lorena G. Nugnes, Lucas L. Colombo, María F. Troncoso, Marisa M. Fernández, Emilio L. Malchiodi, Isabel Frahm, Diego O. Croci, Daniel Compagno, Gabriel A. Rabinovich, Carlota Wolfenstein-Todel, and María T. Elola. Modulation of endothelial cell migration and angiogenesis: a novel function for the "tandem-repeat" lectin galectin-8. *FASEB J*, 25(1):242–254, Jan 2011.

[102] Kim Hodges and Gail Hecht. Bacterial infections of the small intestine. *Curr Opin Gastroenterol*, 29(2):159–163, Mar 2013.

[103] Teresa L M. Thurston, Michal P. Wandel, Natalia von Muhlinen, Agnes Foeglein, and Felix Randow. Galectin 8 targets damaged vesicles for autophagy to defend cells against bacterial invasion. *Nature*, 482(7385):414–418, Feb 2012.

[104] Yifat Levy, Sofia Auslender, Miriam Eisenstein, Roee R. Vidavski, Denise Ronen, Alexander D. Bershadsky, and Yehiel Zick. It depends on the hinge: a structure-functional analysis of galectin-8, a tandem-repeat type lectin. *Glycobiology*, 16(6):463–476, Jun 2006.

[105] C. J. Barnstable, W. F. Bodmer, G. Brown, G. Galfre, C. Milstein, A. F. Williams, and A. Ziegler. Production of monoclonal antibodies to group a erythrocytes, hla and other human cell surface antigens-new tools for genetic analysis. *Cell*, 14(1):9–20, May 1978.

[106] Zsuzsanna Pál, Péter Antal, Sanjeev Kumar Srivastava, Gábor Hullám, Agnes F. Semsei, János Gál, Mihály Svébis, Györgyi Soós, Csaba Szalai, Sabine André, Elena Gordeeva, György Nagy, Herbert Kaltner, Nicolai V. Bovin, Mária Judit Molnár, András Falus, Hans-Joachim Gabius, and Edit Irén Buzás. Non-synonymous single nucleotide polymorphisms in genes for immunoregulatory galectins: association of galectin-8 (f19y) occurrence with autoimmune diseases in a caucasian population. *Biochim Biophys Acta*, 1820(10):1512–1518, Oct 2012.

[107] Dirk Hose, Thierry Rème, Thomas Hielscher, Jérôme Moreaux, Tobias Messner, Anja Seckinger, Axel Benner, John D Shaughnessy, Jr, Bart Barlogie, Yiming Zhou, Jens Hillengass, Uta Bertsch, Kai Neben, Thomas Möhler, Jean François Rossi, Anna Jauch, Bernard Klein, and Hartmut Goldschmidt.

Proliferation is a central independent prognostic factor and target for personalized and risk-adapted treatment in multiple myeloma. *Haematologica*, 96(1):87–95, Jan 2011.

[108] Dirk Hose, Jérôme Moreaux, Tobias Meissner, Anja Seckinger, Hartmut Goldschmidt, Axel Benner, Karène Mahtouk, Jens Hillengass, Thierry Rème, John De Vos, Michael Hundemer, Maud Condomines, Uta Bertsch, Jean-François Rossi, Anna Jauch, Bernard Klein, and Thomas Möhler. Induction of angiogenesis by normal and malignant plasma cells. *Blood*, 114(1):128–143, Jul 2009.

[109] Tobias Meissner, Anja Seckinger, Thierry Rème, Thomas Hielscher, Thomas Möhler, Kai Neben, Hartmut Goldschmidt, Bernard Klein, and Dirk Hose. Gene expression profiling in multiple myeloma–reporting of entities, risk, and targets in clinical routine. *Clin Cancer Res*, 17(23):7240–7247, Dec 2011.

[110] A. Seckinger, T. Meissner, J. Moreaux, H. Goldschmidt, G. M. Fuhler, A. Benner, M. Hundemer, T. Rème, JD Shaughnessy, Jr, B. Barlogie, U. Bertsch, J. Hillengass, A. D. Ho, V. Pantesco, A. Jauch, J. De Vos, J. F. Rossi, T. Möhler, B. Klein, and D. Hose. Bone morphogenic protein 6: a member of a novel class of prognostic factors expressed by normal and malignant plasma cells inhibiting proliferation and angiogenesis. *Oncogene*, 28(44):3866–3879, Nov 2009.

[111] Ursula Pieper, Narayanan Eswar, Hannes Braberg, M. S. Madhusudhan, Fred P. Davis, Ashley C. Stuart, Nebojsa Mirkovic, Andrea Rossi, Marc A. Marti-Renom, Andras Fiser, Ben Webb, Daniel Greenblatt, Conrad C. Huang, Thomas E. Ferrin, and Andrej Sali. Modbase, a database of annotated comparative protein structure models, and associated resources. *Nucleic Acids Res*, 32(Database issue):D217–D222, Jan 2004.

[112] Hiromi Yoshida, Satoshi Yamashita, Misa Teraoka, Aiko Itoh, Shin-ichi Nakakita, Nozomu Nishi, and Shigehiro Kamitori. X-ray structure of a protease-resistant mutant form of human galectin-8 with two carbohydrate recognition domains. *FEBS J*, 279(20):3937–3951, Oct 2012.

[113] Byeong-Won Kim, Seung Beom Hong, Jun Hoe Kim, Do Hoon Kwon, and Hyun Kyu Song. Structural basis for recognition of autophagic receptor ndp52 by the sugar receptor galectin-8. *Nat Commun*, 4:1613, 2013.

[114] Viktor Hornak, Robert Abel, Asim Okur, Bentley Strockbine, Adrian Roitberg, and Carlos Simmerling. Comparison of multiple amber force fields and development of improved protein backbone parameters. *Proteins*, 65(3):712–725, Nov 2006.

[115] Bart Barlogie, Guido Tricot, Elias Anaissie, John Shaughnessy, Erik Rasmussen, Frits van Rhee, Athanasios Fassas, Maurizio Zangari, Klaus Hollmig, Mauricio Pineda-Roman, Choon Lee, Giampaolo Talamo, Raymond Thertulien, Elias Kiwan, Somashekar Krishna, Michele Fox, and John Crowley. Thalidomide and hematopoietic-cell transplantation for multiple myeloma. *N Engl J Med*, 354(10):1021–1030, Mar 2006.

[116] Bart Barlogie, Elias Anaissie, Frits van Rhee, Jeffrey Haessler, Klaus Hollmig, Mauricio Pineda-Roman, Michele Cottler-Fox, Abid Mohiuddin, Yazan Alsayed, Guido Tricot, Vanessa Bolejack, Maurizio Zangari, Joshua Epstein, Nathan Petty, Douglas Steward, Bonnie Jenkins, Jennifer Gurley, Ellen Sullivan, John Crowley, and John D Shaughnessy, Jr. Incorporating bortezomib into upfront treatment for multiple myeloma: early results of total therapy 3. *Br J Haematol*, 138(2):176–185, Jul 2007.

[117] Jérôme Moreaux, Bernard Klein, Régis Bataille, Géraldine Descamps, Sophie Maïga, Dirk Hose, Hartmut Goldschmidt, Anna Jauch, Thierry Rème, Michel Jourdan, Martine Amiot, and Catherine Pellat-Deceunynck. A high-risk signature for patients with multiple myeloma established from the molecular classification of human myeloma cell lines. *Haematologica*, 96(4):574–582, Apr 2011.

[118] Roman Hajek, Samuel A. Okubote, and Hana Svachova. Myeloma stem cell concepts, heterogeneity and plasticity of multiple myeloma. *Br J Haematol*, 163(5):551–564, Dec 2013.

[119] Luca Agnelli, Pierfrancesco Tassone, and Antonino Neri. Molecular profiling of multiple myeloma: from gene expression analysis to next-generation sequencing. *Expert Opin Biol Ther*, 13 Suppl 1:S55–S68, Jun 2013.

[120] Andrew C. Newman, Martin N. Nakatsu, Wayne Chou, Paul D. Gershon, and Christopher C W. Hughes. The requirement for fibroblasts in angiogenesis: fibroblast-derived matrix proteins are essential for endothelial cell lumen formation. *Mol Biol Cell*, 22(20):3791–3800, Oct 2011.

[121] Joji Ando and Kimiko Yamamoto. Vascular mechanobiology: endothelial cell responses to fluid shear stress. *Circ J*, 73(11):1983–1992, Nov 2009.

[122] Norihiko Ohura, Kimiko Yamamoto, Sigeru Ichioka, Takaaki Sokabe, Hideki Nakatsuka, Atsushi Baba, Masahiro Shibata, Takashi Nakatsuka, Kiyonori Harii, Youichiro Wada, Takahide Kohro, Tatsuhiko Kodama, and Joji Ando. Global analysis of shear stress-responsive genes in vascular endothelial cells. *J Atheroscler Thromb*, 10(5):304–313, 2003.

[123] Stuart Egginton. In vivo shear stress response. *Biochem Soc Trans*, 39(6):1633–1638, Dec 2011.

[124] Martina Willhauck-Fleckenstein, Thomas M. Moehler, Anette Merling, Susann Pusunc, Hartmut Goldschmidt, and Reinhard Schwartz-Albiez. Transcriptional regulation of the vascular endothelial glycome by angiogenic and inflammatory signalling. *Angiogenesis*, 13(1):25–42, Mar 2010.

[125] Cecile Boscher, James W. Dennis, and Ivan R. Nabi. Glycosylation, galectins and cellular signaling. *Curr Opin Cell Biol*, 23(4):383–392, Aug 2011.

[126] Omai B. Garner and Linda G. Baum. Galectin-glycan lattices regulate cell-surface glycoprotein organization and signalling. *Biochem Soc Trans*, 36(Pt 6):1472–1477, Dec 2008.

[127] Moran Jerabek-Willemsen, Chistoph J. Wienken, Dieter Braun, Philipp Baaske, and Stefan Duhr. Molecular interaction studies using microscale thermophoresis. *Assay Drug Dev Technol*, 9(4):342–353, Aug 2011.

[128] Roy Heusschen, Iris A. Schulkens, Judy van Beijnum, Arjan W. Griffioen, and Victor L. Thijssen. Endothelial lgals9 splice variant expression in endothelial cell biology and angiogenesis. *Biochim Biophys Acta*, 1842(2):284–292, Feb 2014.

[129] Feng Zhang, Minhua Zheng, Ying Qu, Jianfang Li, Jun Ji, Bo Feng, Aiguo Lu, Jianwen Li, Mingliang Wang, and Bingya Liu. Different roles of galectin-9 isoforms in modulating e-selectin expression and adhesion function in lovo colon carcinoma cells. *Mol Biol Rep*, 36(5):823–830, May 2009.

[130] Yifat Levy, Denise Ronen, Alexander D. Bershadsky, and Yehiel Zick. Sustained induction of erk, protein kinase b, and p70 s6 kinase regulates cell spreading and formation of f-actin microspikes upon ligation of integrins by galectin-8, a mammalian lectin. *J Biol Chem*, 278(16):14533–14542, Apr 2003.

[131] Adriana Lepur, Emma Salomonsson, Ulf J. Nilsson, and Hakon Leffler. Ligand induced galectin-3 protein self-association. *J Biol Chem*, 287(26):21751–21756, Jun 2012.

[132] Laurent Ingrassia, Isabelle Camby, Florence Lefranc, Véronique Mathieu, Prosper Nshimyumukiza, Francis Darro, and Robert Kiss. Anti-galectin compounds as potential anti-cancer drugs. *Curr Med Chem*, 13(29):3513–3527, 2006.

[133] Ruud P M. Dings, Nigam Kumar, Michelle C. Miller, Melissa Loren, Huzaifa Rangwala, Thomas R. Hoye, and Kevin H. Mayo. Structure-based optimization of angiostatic agent 6dbf7, an allosteric antagonist of galectin-1. *J Pharmacol Exp Ther*, 344(3):589–599, Mar 2013.

[134] Kimberley A. Stannard, Patrick M. Collins, Koichi Ito, Emily M. Sullivan, Stacy A. Scott, Elwyn Gabutero, I. Darren Grice, Pauline Low, Ulf J. Nilsson, Hakon Leffler, Helen Blanchard, and Stephen J. Ralph. Galectin inhibitory

disaccharides promote tumour immunity in a breast cancer model. *Cancer Lett*, 299(2):95–110, Dec 2010.

[135] Peter G. Traber, Hsin Chou, Eliezer Zomer, Feng Hong, Anatole Klyosov, Maria-Isabel Fiel, and Scott L. Friedman. Regression of fibrosis and reversal of cirrhosis in rats by galectin inhibitors in thioacetamide-induced liver disease. *PLoS One*, 8(10):e75361, 2013.

[136] Peter G. Traber and Eliezer Zomer. Therapy of experimental nash and fibrosis with galectin inhibitors. *PLoS One*, 8(12):e83481, 2013.

[137] Hitomi Yamamoto, Nozomu Nishi, Hiroki Shoji, Aiko Itoh, Liang-Hao Lu, Mitsuomi Hirashima, and Takanori Nakamura. Induction of cell adhesion by galectin-8 and its target molecules in jurkat t-cells. *J Biochem*, 143(3):311–324, Mar 2008.